



Universiteit
Leiden
The Netherlands

Hereditary paraganglioma : genetics and tumor biology

Hoekstra, A.S.

Citation

Hoekstra, A. S. (2017, February 2). *Hereditary paraganglioma : genetics and tumor biology*. Retrieved from <https://hdl.handle.net/1887/45622>

Version: Not Applicable (or Unknown)

License: [Licence agreement concerning inclusion of doctoral thesis in the Institutional Repository of the University of Leiden](#)

Downloaded from: <https://hdl.handle.net/1887/45622>

Note: To cite this publication please use the final published version (if applicable).

Cover Page



Universiteit Leiden



The handle <http://hdl.handle.net/1887/45622> holds various files of this Leiden University dissertation.

Author: Hoekstra, A.S.

Title: Hereditary paraganglioma : genetics and tumor biology

Issue Date: 2017-02-02

Hereditary Paraganglioma

Genetics and tumor biology

Attje Sietske Hoekstra

Cover design: Attje S. Hoekstra and GVO Drukkers & vormgevers B.V.

Hereditary Paraganglioma – Genetics and Tumor Biology.

Thesis, University of Leiden, The Netherlands.

Layout by Attje S. Hoekstra and GVO Drukkers & vormgevers B.V.

Print by GVO Drukkers & vormgevers B.V., Ede, The Netherlands.

© 2017 Attje S. Hoekstra

ISBN: 978-94-6332-134-1

Hereditary Paraganglioma

Genetics and tumor biology

Proefschrift

ter verkrijging van

de graad van Doctor aan de Universiteit Leiden,

op gezag van Rector Magnificus prof.mr. C.J.J.M. Stolker,

volgens besluit van het College voor Promoties

te verdedigen op donderdag 2 februari 2017

klokke 15.00 uur

door

Attje Sietske Hoekstra

geboren te Makkum

in 1986

Promotor: Prof. Dr. P. Devilee

Copromotor: Dr. JP. Bayley

Leden promotiecommissie:

Prof. Dr. J.V.M.G. Bovée
Leiden University Medical Center
Leiden, The Netherlands

Dr. E.F. Hensen
University of Amsterdam (UvA)
Amsterdam, The Netherlands

Prof. Dr. R. de Krijger
Erasmus Medical Center
Rotterdam, The Netherlands

Dr. M. Robledo
Centro Nacional de Investigaciones Oncológicas (CNIO)
Madrid, Spain

Contents

CHAPTER 1	7
General introduction	
1.1 The paraganglion system	8
1.2 Paragangliomas and pheochromocytomas.....	9
1.3 Genetics of paragangliomas.....	11
1.4 Molecular biology of paragangliomas.....	20
1.5 Outline of this thesis	24
 CHAPTER 2	 31
Inactivation of SDH and FH cause loss of 5hmC and increased H3K9me3 in paraganglioma/pheochromocytoma and smooth muscle tumors	
<i>Oncotarget. 6 (2015) 38777-88</i>	
 CHAPTER 3	 49
Parent-of-origin tumorigenesis is mediated by an essential imprinted modifier in SDHD-linked paragangliomas: SLC22A18 and CDKN1C are candidate tumor modifiers	
<i>Accepted in Human Molecular Genetics</i>	
 CHAPTER 4	 75
Loss of maternal chromosome 11 is a signature event in SDHAF2, SDHD, and VHL-related paragangliomas, but less significant in SDHB-related paragangliomas	
<i>Submitted</i>	
 CHAPTER 5	 97
Simple and rapid characterization of novel large germline deletions in SDHB, SDHC and SDHD-related paraganglioma	
<i>Accepted in Clinical Genetics</i>	
 CHAPTER 6	 115
Summary and Discussion	
 CHAPTER 7	 125
Nederlandse samenvatting	

DANKWOORD.....	134
CURRICULUM VITAE.....	136
PUBLICATIONS.....	137

CHAPTER 1

General introduction

Partly published in:

Hoekstra AS, Bayley JP. The role of complex II in disease. (2013) Biochim Biophys Acta. 1827:543-51

Hoekstra AS, Devilee P, Bayley JP. Models of parent-of-origin tumorigenesis in hereditary paraganglioma. (2015) Semin Cell Dev Biol. 43:117-24

1.1 The paraganglion system

Paraganglia are small clusters of chromaffin cells that originate from neuroectodermal tissue of the neural crest. The paraganglion system encompasses the sympathetic paraganglia and the parasympathetic paraganglia (1). The sympathetic paraganglia are found from the level of the superior cervical ganglion, descending the sympathetic trunk to the pelvis (Figure 1A), and include the organs of Zuckerkandl and the celiac, renal, suprarenal and hypogastric plexuses. The organs of Zuckerkandl are the main source of catecholamines in the early gestational period and they normally start to regress in the third trimester, being subsequently replaced by the largest paraganglion in the body, the adrenal medulla, which is the main source of catecholamines in adults (2). The parasympathetic paraganglia are localized almost exclusively in the head and neck along the branches of the glossopharyngeal and vagus nerves (Figure 1B). The most prominent parasympathetic paraganglia are the carotid bodies, found at the carotid bifurcation, which function as sensitive chemoreceptors of arterial carbon dioxide and oxygen levels, and of arterial pH. The carotid bodies respond by rapidly increasing breathing and blood pressure, thus maintaining normal oxygen tension (3).

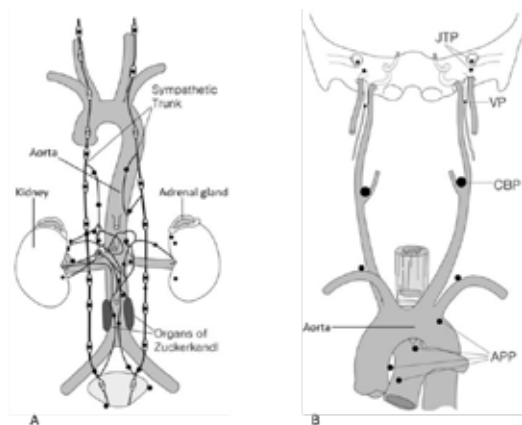


Figure 1. Paraganglion system (adapted from (4)). Paraganglia associated with the (A) sympathetic nervous system and the (B) parasympathetic nervous system. APP: aorticopulmonary paraganglia, CBP: carotid body paraganglion, VP: vagal paraganglia, JTP: jugulotympanic paraganglia.

Histology

Microscopically, the normal paraganglion is organized into typical cell nests (“Zellballen”), characterized by clusters of neuroendocrine cells, referred to as ‘chief’ or ‘type 1’ cells, that are partially or completely surrounded by ‘sustentacular’ or ‘type 2’ cells, a glial-like cell (Figure 2). These cell nests are separated by fibrovascular stroma. The chief cells are polygonal cells with abundant cytoplasm and have numerous membrane-bound, electron-dense granules that contain catecholamines. Chief cells can be distinguished immunohistochemically by expression of chromogranin A, neuron specific enolase and synaptophysin, whereas sustentacular cells express the

S-100 and glial fibrillary acidic proteins (GFAP). Sustentacular cells have a more flattened, elongated morphology, with less cytoplasm and an absence of granules (5).

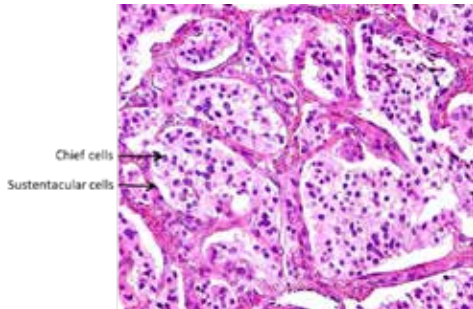


Figure 2. Hematoxylin and eosin (HE) stained carotid body paraganglioma tissue displaying the characteristic Zellballen pattern, with the sustentacular cells surrounding the chief cells.

1.2 Paragangliomas and pheochromocytomas

Paragangliomas (PGLs) and pheochromocytomas (PCCs) are neuroendocrine tumors that originate from both the sympathetic and parasympathetic branches of the autonomic nervous system. Parasympathetic PGLs usually occur in the head and neck region, most commonly in the carotid body at the bifurcation of the carotid artery. PGLs of the head and neck are highly vascular, with generally very slow growth and only rarely develop metastases (6). Strikingly, the architecture of the normal paraganglia, the characteristic Zellballen pattern, is usually maintained in the tumor (Figure 2). The chief cells have been demonstrated to be the tumorigenic component, apparently driving the expansion of other non-transformed cell populations such as the sustentacular cells, resulting in a very heterogeneous tumor (7).

Extra-adrenal (EA) PGLs and PCCs are tumors associated with the sympathetic nervous system. EA PGLs can develop from the neck to the pelvic floor in any of the sympathetic paraganglia, occurring most frequently in the abdomen and pelvis and less frequently in the thorax. PCCs are derived from the chromaffin cells of the adrenal medulla (8). In contrast to head and neck PGLs, abdominal PGLs show relatively frequent malignancy and patients with malignant tumors have an estimated 5-year survival of 34–60% (9). PCCs of the adrenal medulla rarely metastasize but are clinically important due to the potentially life-threatening hypertensive crises that may result from the excessive production and secretion of catecholamines.

Incidence

Both parasympathetic and sympathetic paragangliomas are rare. Estimates of the overall incidence of head and neck PGLs range from 1 in 30,000 to 1 in 100,000, with carotid body tumors making up nearly 60% of cases, followed by jugular PGLs (23%), vagal PGLs (13%), and tympanicum PGLs (6%)

(10). However, as obtaining reliable figures for paraganglioma incidence has received little attention, it is likely that current estimates underrate true incidences. In necropsy studies, incidences of 1:3.860 to 1:13.400 were reported for carotid body PGLs (11). The population-based clinical incidence of PCCs per year has been estimated to be 1:200.000 (5;12;13). Although tumors may occur in all age groups, age-related incidence is highest between 40 and 50 years, with an approximately equal sex distribution (14;15).

Clinical presentation

Head and neck PGLs range in spectrum from small lesions to large unresectable masses and may remain clinically silent for years due to the slow growth rate (6). Their location in close proximity to nerves and vascular structures can lead to compression or infiltration of the adjacent structures, causing symptoms such as dysphagia, hearing loss, tinnitus, and cranial nerve palsies. Carotid body tumors usually present as a painless cervical mass. The majority of head and neck PGLs do not secrete catecholamines (up to 70%–95%) and are therefore mostly discovered by anatomical and functional imaging (16). Patients with sympathetic PGLs present with symptoms and signs of catecholamine excess including headache, palpitation, perspiration, pallor, and hypertension. Catecholamine secreting tumors can be distinguished from head and neck PGLs through the evaluation of the urine or plasma concentrations of metanephrine and normetanephrine, metabolites of catecholamines, which are rarely elevated in head and neck PGLs (17).

Treatment

Treatment strategies for head and neck PGLs include watchful waiting, surgery and radiotherapy. As most tumors grow slowly, a wait-and-scan option is often advised. No intervention is performed and tumor growth is monitored regularly with repeated MRI. However, the obvious benefits of surgery include the reduction or removal of the tumor mass and the prevention of tumor progression to malignancy. Due to the highly vascularized nature of head and neck PGLs and the characteristic involvement with the carotid artery, the jugular vein, multiple cranial nerves, and/or the skull base, there is a real risk of surgical complications. Moreover, the rate of surgical complications increases with the size of the tumor (18). Preoperative embolization may simplify the surgical procedure and reduce blood loss but does not decrease rates of cranial nerve damage (19). While most head and neck PGLs are benign, some PGLs can metastasize to cervical lymph nodes or systemic regions including bone, lung and liver (20). Complete surgical resection of the primary tumor and the regional lymph nodes is the strategy of choice for malignant head and neck PGLs. Postoperative radiation may be beneficial in slowing the progression of residual disease (20). The third treatment option is radiotherapy, which can result in local tumor control of head and neck PGLs and sometimes regression through the generation of fibrosis and vascular sclerosis (21). Stereotactic radiosurgery, the most spatially precise form of therapeutic radiation, has been shown to be highly effective in terms of tumor control and symptom relief (22;23). However, long-term negative effects of radiotherapy include possible recurrences and potential induction of malignancy.

Surgical treatment is the primary strategy for EA PGLs and PCCs, where adequate peri-operative treatment is mandatory to minimize surgical complications (hypertensive crisis and arrhythmias) (24). There is currently no effective treatment for malignant EA PGLs and PCCs, and different treatment strategies result in quite variable and site-specific outcomes (24). Therefore, the optimal choice of treatment for both parasympathetic and sympathetic PGLs and PCCs often unclear and must be evaluated in relation to tumor growth velocity, biological activity of the tumor, patient age, tumor size and site, malignancy, and potential for treatment-related morbidity.

1.3 Genetics of paragangliomas

Paragangliomas and pheochromocytomas can occur both sporadically and in the context of hereditary syndromes. Historically, PCCs were considered to have a syndromic presentation in about 10% of cases, as part of the neurofibromatosis type 1 (caused by mutations in the *NF1* gene), multiple endocrine neoplasia type 2 (due to activating *RET* mutations) or von Hippel Lindau (associated with mutations in *VHL* gene) syndromes (25). Today, approximately 40% of PGLs and PCCs are associated with a germline mutation in one of at least 15 genes (Table 1) (26). These genes belong to a wide range of functional categories that include kinase receptors (*RET*), regulators of signaling (*NF1*), hypoxia-related factors (*VHL*, *HIF2A*; also known as *EPAS1*, *PHD2*), enzymes involved in energy metabolism (*SDHA*, *SDHB*, *SDHC*, *SDHD*, *SDHAF2*, *FH*, *MDH2*), endosomal signaling factors (*TMEM127*), vesicle transport/apoptosis (*KIF1B*), and transcription factors (*MAX*).

Major advances in genomic analyses have allowed studies that identified somatic mutations in the *RET*, *VHL*, *NF1*, *MAX*, *HIF2A* and *HRAS* genes (Table 1) in up to 30% of PGLs/PCCs (26). Recently, somatic mutations of *ATRX*, *TP53*, *CDKN2A*, *MET*, *CDH1*, *GNAS*, and *FHIT* have been identified in a subset of PGL/PCC patients by whole exome sequencing (27;28). However, the precise role of these genes in PGL/PCC tumor development has yet to be established.

Table 1. Summary of PGL/PCC susceptibility genes and the clinical presentation

Gene	Locus	Mutation type	Localization							Related conditions
			Malignant PGL/PCC	HNPGL	EA-PGL	Multiple PGL	PCC	Bilateral PCC		
<i>SDHA</i>	5p15	Germline	-	+	+	-	-	-	Leigh syndrome, GIST, PA	
<i>SDHB</i>	1p36	Germline	+++	++	+++	++	++	+	GIST, RCC, PA	
<i>SDHC</i>	1q23	Germline	+	++	+	+	+	-	GIST, RCC	
<i>SDHD</i>	11q23	Germline	+	+++	++	+++	+	-	GIST, PA	
<i>SDHAF2</i>	11q12	Germline	-	+++	-	++	-	-	-	
<i>VHL</i>	3p25	Germline, somatic	+	Rare	+	+	++	+++	VHL	
<i>NF1</i>	17q11	Germline, somatic	+	-	+	-	+	-	NF1	
<i>RET</i>	10q11	Germline, somatic	+	Very rare	-	-	++	++	MEN2	
<i>TMEM127</i>	2q11	Germline	+/-	Very rare	+/-	+/-	+++	++	-	
<i>MAX</i>	14q23	Germline, somatic	+	-	-	-	++	++	-	
<i>FH</i>	1q43	Germline	+	+	+	+	+	-	Uterine leiomyoma	
<i>HIF2A</i>	2p21	Germline, somatic	-	-	+	+	+	-	Polycythemia and somatostatinoma	
<i>PHD2</i>	1q42	Germline	+	-	+	+	+	-	Polycythemia and erythrocytosis	
<i>MDH2</i>	7q11	Germline	+	-	+	+	-	-	-	
<i>KIF1B</i>	1p36	Germline, somatic	-	-	-	-	++	+	Neuroblastoma, ganglioglioma, ganglioglioma	
<i>HRAS</i>	11p15	Somatic	-	-	+	-	++	-	-	

+ present, - absent

PGL: paraganglioma, PCC: pheochromocytoma, HNPGL: head and neck paraganglioma, EA PGL: extra-adrenal paraganglioma, AD: autosomal dominant, ADPI: autosomal dominant paternal inheritance, GIST: gastrointestinal stromal tumor, RCC: renal cell carcinoma, PA: pituitary adenoma, VHL: von Hippel Lindau, NF1: neurofibromatosis type 1, MEN2: multiple endocrine neoplasia type 2

The succinate dehydrogenase genes

Hereditary paraganglioma-pheochromocytoma syndromes are associated with germline mutations in succinate dehydrogenase (SDH) complex genes, including *SDHD* (PGL1), *SDHAF2* (PGL2), *SDHC*

(PGL3), and *SDHB* (PGL4) (29-32). SDH is a heterotetramer consisting of two soluble proteins, a flavoprotein (encoded by *SDHA*) and an iron-sulfur protein (*SDHB*), which together form the catalytic subunit, while subunits encoded by *SDHC* and *SDHD* anchor the complex in the inner mitochondrial membrane and bind ubiquinone. Succinate dehydrogenase complex assembly factor 2 (*SDHAF2*) encodes a protein involved in complex assembly. Biochemical analyses have demonstrated that mutations in each of these subunits or assembly factor results in the loss of a functional enzyme complex (26).

SDHD

The identification of *SDHD* (located on chromosome 11q23) demonstrated for the first time that mitochondrial proteins involved in intermediary metabolism could act as tumor suppressors (30). Germline mutations in *SDHD* generally result in benign head and neck PGLs but are also associated with EA PGLs and PCCs (Table 1) (33). Metastatic disease is rare (0-10%). PGL1 is the autosomal dominant syndrome caused by mutation in the *SDHD* gene. Carriers of *SDHD* mutations have a very high propensity for tumor development (penetrance) upon paternal transmission, variously estimated at 87–100%, although not all carriers will develop overt clinical symptoms or even be aware of their tumor (34-36). In the Netherlands, the majority of mutation-positive patients with head and neck PGL are explained by the Dutch *SDHD* founder mutations p.Asp92Tyr and p.Leu139Pro (37;38).

SDHB

The *SDHB* gene (located on chromosome 1p36) is the most commonly mutated of all the *SDH*-related genes and *SDHB* mutation carriers may develop EA PGLs, PCCs or head and neck PGLs (Table 1) (15;29). Mutations in the *SDHB* gene cause an autosomal dominant syndrome with incomplete penetrance (PGL4). Around 20% of *SDHB* mutation carriers will develop metastatic disease (15;34). *SDHB* mutations tend to show low penetrance and only 25–40% of all carriers will eventually develop a tumor (39;40), suggesting that many carriers go undetected. This is reflected in the apparently sporadic presentation of many patients, with further investigation of family members often revealing germline mutations in asymptomatic carriers, many of whom remain tumor-free to advanced age. Two founder mutations in *SDHB* have been identified in Dutch PGL families, the *SDHB* exon 3 deletion and the c.423+1G>A splice site mutation (41;42).

SDHC

Despite the close physical interaction of the *SDHC* and *SDHD* proteins, PGLs due to *SDHC* mutations are far less common than *SDHD*-related PGLs. Although the number of *SDHC*-related patients is still insufficient to allow firm conclusions to be drawn, the penetrance of *SDHC* mutations appears to be low, more closely reflecting that of *SDHB* than *SDHD*. Similar to *SDHB*, *SDHC* is located on chromosome 1 (1q23). The clinical expression of *SDHC* mutations appears to be comparable to that of *SDHD*, with most patients showing primarily head and neck PGLs, although some EA PGLs have been reported (Table 1) (43). The average age at diagnosis is 38-46 years (44). In the Netherlands, *SDHC* mutations represent only 0.3% of all mutations found in *SDH*-related genes (37).

SDHA

Mutations in *SDHA* were originally described as a cause of Leigh syndrome, a rare mitochondrial deficiency resulting in encephalopathy, myopathy, developmental retardation, loss of vision, loss of hearing, and a limited life expectancy (45). The identification of mutations of complex II in hereditary paraganglioma–pheochromocytoma syndrome immediately implied a role for the major catalytic subunit, SDHA, located on chromosome 5p15. In 2010, a heterozygous *SDHA* germline mutation was identified in a patient with abdominal PGL (46). *SDHA* germline mutations have been convincingly associated with disease through biochemical analysis, and found in at least 3% of patients affected by apparently sporadic head and neck PGLs and PCCs (Table 1), but the same mutations have been found at a relatively high frequency in healthy controls (0.5%) (47). This suggests that *SDHA* mutations may show extremely low penetrance, with most mutation carriers escaping the development of clinical symptoms (47). SDHA is the most stable of the SDH proteins when soluble and also appears to be a component of a mitochondrial ATP-sensitive potassium channel (48). This additional function could be an explanation for the rarity of mutations if maintenance of this complex is essential for cell viability, although this supposition is challenged by the existence of Leigh syndrome patients with homozygous *SDHA* mutations. However, in patients with Leigh syndrome, considerable residual cytoplasmic SDHA immunostaining and activity can still be detected, indicating that SDHA stability is affected but SDHA functionality is not completely lost (45). So another explanation might be that mutations that eliminate all SDHA activity are incompatible with life. An alternative, genetic explanation might be that the ‘second hit’, usually occurring via complete or partial chromosomal loss, would result in the concomitant loss of essential genes in the proximity of *SDHA* (46). If these genes are essential to cell viability, only very specific and rare molecular events may be tolerated.

SDHAF2

SDHAF2, located on chromosome 11q13, encodes a gene for a novel protein that acts as an assembly factor for the SDH complex, adding a flavin-adenine dinucleotide (FAD) prosthetic group to form a catalytically active SDHA flavoprotein. SDHAF2 was shown to be essential for the correct flavination of SDHA and function of the SDH complex (31). The first mutation identified in *SDHAF2*, a missense variant c.232G>A (p.Gly78Arg), was identified in a large Dutch head and neck PGL kindred and was shown to result in the loss of SDHA flavination and activity of the SDH complex (31). A follow-up study in 443 PGL and PCC patients found no further mutations and demonstrated that *SDHAF2* mutations make a very modest contribution to the overall genetic burden in these syndromes (49). A notable characteristic of *SDHAF2* mutations is the very high penetrance (50). Head and neck PGLs occur in 70–91% carriers of paternally inherited mutations, occurring from a relatively young age (earliest affected aged 22 years) and often multifocal, but with no reported cases of malignancy to date (Table 1) (50). This high level of penetrance is reminiscent of *SDHD*, which also shows very high penetrance compared to other *SDH*-related genes.

Other PGL/PCC-associated genes

VHL

VHL is a tumor suppressor gene located on chromosome 3p25 and tumor formation occurs upon loss of the wild type allele. Germline mutations in *VHL* predispose to von Hippel Lindau disease, a cancer syndrome characterized by clear cell renal cell carcinomas, PCCs, PGLs and hemangioblastomas, as well as cysts of the retina, cerebellum, kidney and pancreas (51). The incidence of the syndrome is 1 in 36.000 births (51;52). PCCs occur in approximately 20% of *VHL* mutant patients and may be one of the earliest manifestations of the disease. The mean age of PCC presentation in *VHL*-related patients is around 30 years-of-age and most PCCs are bilateral and multiple (Table 1). The rate of malignant PCC in *VHL* disease is approximately 5% (51;52). *VHL* mutations in head and neck PGLs are rare and are found in less than 1% of *VHL* cases (53).

NF1

The *NF1* gene, located on 17q11, acts as a tumor suppressor gene and its main function is to suppress cell proliferation by converting the RAS protein to an inactive form, thereby inhibiting the oncogenic RAS/RAF/MAPK and the PI3Kinase/AKT/mTOR signaling pathways (54;55). Mutations in *NF1* lead to neurofibromatosis type 1, the most common tumor syndrome of the peripheral nervous system, with an estimated prevalence of 1:3000 (56). This syndrome may also present with other tumors such as gastrointestinal tumors, gliomas and myeloid leukemia. PCC arises in 0.1% to 5.7% of *NF1* mutant patients, although this tumor has been found at autopsy in 3.3–13.0% of *NF1* mutant patients (57). The mean age at presentation for PCC is 42 years, similar to the general population. *NF1*-associated PCCs have a predominantly unilateral, intra-adrenal location, and *NF1*-associated tumors are seldom PGLs (Table 1) (53). The malignancy rate for *NF1*-associated PCCs is approximately 3% to 12% (58).

RET

Activating mutations in the *RET* proto-oncogene (located on 10q11) cause multiple endocrine neoplasia type 2 (MEN2), subtype A (MEN2A) and MEN2B. *RET* encodes a transmembrane receptor tyrosine kinase predominantly expressed in neural crest cells and urogenital cells. The *RET* protein is involved in the initiation of PI3Kinase/AKT/mTOR and RAS/RAF/MAPK intracellular pathways and therefore drives cell growth, differentiation and survival (59). MEN2A is characterized by medullary thyroid carcinoma, PCC and hyperparathyroidism, while MEN2B is associated with medullary thyroid carcinoma, PCC, mucosal neuroma, and marfanoid habitus. The incidence of *RET*-associated MEN2 syndrome is 1:35.000 in the general population (51). About 30% to 50% of patients with MEN2 develop PCCs, and *RET*-associated PCCs are mostly bilateral (50% to 80%) and multifocal, though the risk of malignancy is low (Table 1) (60;61). In MEN2, patients with PCCs usually present between the ages of 30 and 40 years. PGL is reported to be rare in MEN2 (53).

TMEM127

Transmembrane protein 127 (TMEM127), located on chromosome 2q11, has been identified as a PGL/PCC susceptibility gene. Truncating germline *TMEM127* mutations comprised 30% of the 103 tested familial tumors (negative for all other PCC/PGL-related gene mutations) and about 3% of apparently sporadic PCCs, with the wild type allele consistently deleted in tumor DNA (62).

TMEM127 functions as a negative regulator of mTOR and in this way can modulate cellular growth, angiogenesis and cell survival (62). Neumann *et al.* reported germline mutations of *TMEM127* in 4% (2/48) of patients with multiple PGLs and one patient had a bilateral carotid body tumor (Table 1) (63). The prevalence of *TMEM127* mutations in the overall PCC and PGL population seems to be low (1-2%) (64;65). The mean age at presentation of *TMEM127*-related PCCs is 42-45 years and these tumors have a low risk of malignancy (65;66).

MAX

MAX (chromosome 14q23) is a basic helix-loop-helix transcription factor that forms a complex with the important oncogene MYC. MAX is also found in repressor complexes with other transcription factors, which effectively oppose the function of the MYC-MAX heterodimer. Germline loss-of-function *MAX* mutations were identified by sequencing the entire exome of 3 unrelated patients with a family history of PCC (Table 1) (67). Intriguingly, these patients exhibited a loss of heterozygosity of the wild type allele that was shown to be dependent on uniparental disomy (in this case duplication of the paternal chromosome). An additional 5 cases were identified in a follow-up study (67), and in a study of 1694 PGLs and PCCs negative for mutations in other known genes Burnichon *et al.* showed that germline mutations in *MAX* were responsible for 1.1% of cases (68). Although the total number of patients identified is still limited, these studies showed exclusively paternal transmission of *MAX* mutations in affected patients, with tumor formation absent in individuals with maternally inherited mutations. In addition, it was shown that *MAX* is not imprinted (67). These studies indicate that *MAX* mutations show a paternal bias, a pattern of transmission analogous to that observed in the *SDHD* and *SDHAF2* paraganglioma–pheochromocytoma syndromes.

Inheritance

Paraganglioma–pheochromocytoma syndrome, with some notable exceptions, shows a classic Mendelian pattern of dominant inheritance in families. However, as with other tumors associated with tumor suppressor genes, at the cellular level tumor occurrence resembles a recessive disease with predominantly adult onset. Mechanistically, an inherited mutation is initially functionally silent and carriers are phenotypically normal at birth, but at some point a chance second mutation or loss of the remaining normal allele occurs, and this so-called ‘second hit’ leads to the initiation and growth of a tumor (26).

Although germline mutations in most of the PGL/PCC susceptibility genes lead to autosomal dominant inheritance patterns of the disease in families, there are several prominent exceptions: *SDHD*, *SDHAF2* and *MAX* (Table 1). Gene mutations in *SDHD*, *SDHAF2* and *MAX* show a parent-of-origin effect whereby tumor formation occurs almost exclusively following paternal transmission of the mutation (31;67;69). The failure of maternally transmitted mutations to initiate tumorigenesis initially suggested that a maternally imprinted gene could be the underlying cause of the tumor (70). However, biallelic expression of *SDHD* in multiple tissues and no imprinting of *MAX* has been demonstrated (67;71). Although at present there is no explanation for the pattern of inheritance, it is worth noting that chromosome 11 (*SDHD* and *SDHAF2*) and chromosome 14 (*MAX*) harbors several imprinted genes.

To date, three different models have sought to explain the striking inheritance pattern seen in *SDHD* and *SDHAF2*-linked families. The ‘threshold model’ hypothesized by Muller assumes a “partial inactivation” of the maternally derived copies of either *SDHD* or *SDHAF2* and requires the existence of an as yet purely theoretical mechanism of partial imprinting (72). The model proposes that partial inactivation of the maternal allele, together with an inactivating mutation on the paternal allele, results in a state in which some residual activity of SDH is maintained in cells with a paternally derived mutation. This residual activity is sufficient to maintain normal function in paraganglia cells over long periods (decades). Functionally, the model goes on to postulate that ongoing exposure to elevated levels of ROS and succinate (both known to be elevated by *SDH* gene mutations), together with chronic hypoxia, favor pathogenic processes and chromosomal nondisjunction. This results in loss of maternal chromosome 11 and causes SDH activity to dip below a permissive threshold, triggering the adult-onset of PGL tumorigenesis. Conversely, a maternally derived mutation does not have a similarly deleterious effect because sufficient SDH activity and normal function is maintained due to the activity of the paternally derived wild type *SDHD* allele (72).

Recently, two cases of maternal transmission of *SDHD* mutation resulting in head and neck PGL have been described. Both cases showed somatic recombination of chromosome 11 in the tumor, resulting in loss of the paternal wild type *SDHD* gene and the maternal 11p15 region (73;74), which can’t be accommodated by Muller’s model.

An alternative model has been advanced by Baysal and colleagues (71). They focus on the idea that tissue-specific hypermethylation at or near the *SDHD* locus determines the pattern of inheritance (71). They identified several factors which collectively support imprinting within an alternative promoter of a non-coding RNA sequence located at the boundary between the *SDHD* locus and a flanking gene desert. However, RT-PCR and sequencing analyses to estimate allelic expression of the non-coding RNA gene in seven fetuses showed biallelic expression in the adrenal gland, lung, kidney, skin and brain tissues in six out of seven fetuses. In addition, no allelic imbalance was found for *SDHD*. The authors also observed biallelic *SDHD* expression in non-paraganglioma tissues. These data, together with the two PGL cases caused by maternal transmission of *SDHD* mutation, appear to argue against the mechanism proposed by Baysal and colleagues (71). A further issue with the Baysal model is that this elaborate genetic mechanism would need to be replicated at the *SDHAF2* locus in order to explain the close similarities to *SDHD* in terms of inheritance, phenotype and penetrance.

Hensen model

Against a background of theoretical models of direct maternal imprinting, an unexpected finding in *SDHD*-linked PGLs was the frequent loss of the maternal copy of chromosome 11 (69). Although this conforms to the Knudson two-hit model for tumor suppressor genes in which the remaining wild type allele is lost early in tumorigenesis, it is counterintuitive if one assumes that imprinting inactivates the maternal allele. The presence of a paternal parent-of-origin effect in *SDHAF2*-associated PGL families, together with its absence in families caused by other *SDH* genes, again argues that their physical location on chromosome 11 is an important factor in *SDHD* and *SDHAF2*-related tumorigenesis. The role of chromosomal location, with the main cluster of human imprinted genes located on the short arm of chromosome 11 (11p15), led to the development of an alternative

hypothesis, now known as the ‘Hensen model’ (69). The Hensen model implies that loss of the maternal copy of chromosome 11 in paraganglionic cells of individuals carrying a paternally-derived mutation in *SDHD* or *SDHAF2* not only completely inactivated wild type activity at these loci, but also inactivated a critical maternally expressed, paternally imprinted gene in the 11p15 region (Figure 3).

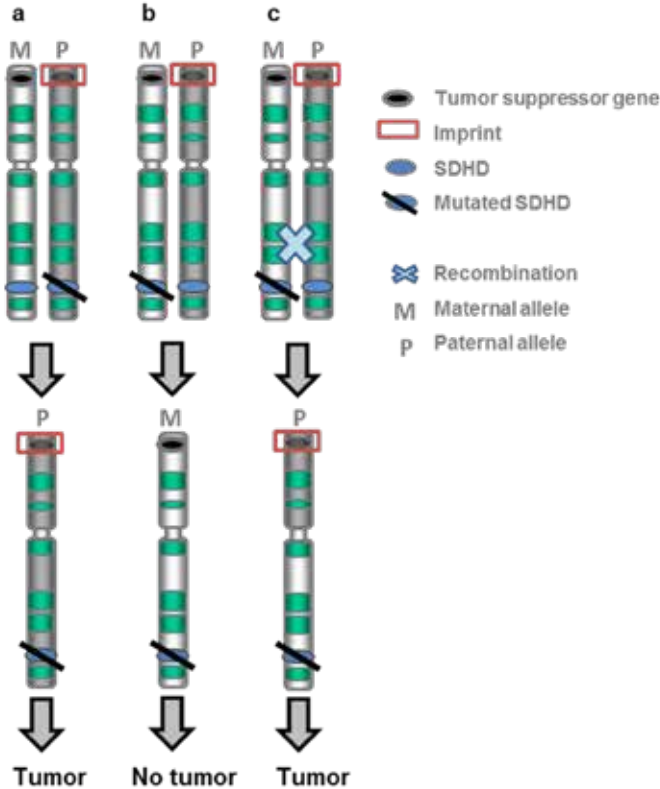


Fig. 3. Hensen model explaining parent-of-origin transmission in *SDHD*-linked PGL/PCC. Maternal (white) and paternal (gray) chromosomes 11 are depicted. (a) Paternal transmission of a *SDHD* mutation together with loss of maternal chromosome 11 targets both the wild type maternal *SDHD* allele and a second tumor suppressor gene, tumor formation is initiated. (b) In the case of transmission of a maternal *SDHD* mutation, followed by loss of paternal chromosome 11, a second tumor suppressor gene is still present on the maternal chromosome and tumor formation is suppressed. (c) Upon maternal transmission of a mutated *SDHD* gene, two events are required for tumor development: mitotic recombination of the paternal wild type *SDHD* allele with a section of the maternal chromosome containing a second tumor suppressor gene, followed by loss of the recombined chromosome.

It is conceivable that the loss of an as yet unidentified locus (or loci) in 11p15 provides the necessary conditions in which *SDHD*-null cells can foster tumor development. Several genes on chromosome 11 are known to be exclusively maternally expressed, including *CDKN1C*, *KCNQ1*, *KCNQ1DN*, *ZNF215*, *SLC22A18*, *PHLDA2*, *OSBP15*, and *H19*. Two particularly well-described genes in the chromosome 11p15.5 region are *CDKN1C* and *H19*, the expression of which is frequently deregulated in imprinting disorders such as Beckwith–Wiedemann Syndrome and Silver–Russell Syndrome (75). Although it

has been shown that the loss of chromosome 11p does not occur in all *SDH*-related PGL/PCC, other genetic and epigenetic mechanisms may result in functional loss of one or more genes in the 11p region. It is interesting to note that chromosome 11p loss is also a prominent feature in *VHL*-related PGL/PCC (27). If the loss of chromosome 11 is important for the development of all *SDH*-related tumors, one prediction of the Hensen model is that mutations in *SDHD* and *SDHAF2* will display higher penetrance than mutations in *SDHA*, *SDHB*, or *SDHC*. Tumorigenesis in *SDHD* and *SDHAF2* mutation carriers requires only a single somatic genetic event (chromosome 11 loss), as opposed to the two events required in *SDHA*, *SDHB*, and *SDHC* mutation carriers (loss of the respective wild type allele, together with independent loss of chromosome 11). This prediction appears to be borne out by the wide difference in lifetime penetrance between mutations in *SDHD* (~90%) (35) and *SDHAF2* (>95%) (50), compared to *SDHB* (~30%) (39;40;42), and *SDHA* and *SDHC* (both with unknown, but probably very low, penetrance). Particularly striking is the contrast in penetrance between germline mutations of *SDHA*, in which carriers appear to be sporadic cases, and its assembly factor, *SDHAF2*, in which germline mutations have a clearly familial presentation and display almost full penetrance in known pedigrees. As the role of *SDHAF2* mutations in tumorigenesis is thought to be mediated through the loss of *SDHA*, *SDHA* mutations could reasonably be expected to show a similar or even higher penetrance.

However, the rarity of *SDHA*-related PGLs may be due to the relatively low frequency of the loss of the chromosomal region containing the *SDHA* locus (5p15), compared with the 1p36 (*SDHB*), 11q13 (*SDHAF2*) and 11q23 (*SDHD*) loci that often show loss in tumor tissues (46). The role of haploinsufficiency for individual components of SDH may also play a role, as a 50% reduction in genetic content for the *SDHB*, *SDHC*, or *SDHD* genes results in no noticeable physiological phenotype, while heterozygous mutations of *SDHA*, accompanied by reduced enzymatic activity, can give rise to late-onset neurodegenerative diseases (76).

The Hensen model is also relevant to the rare cases in which maternal inheritance leads to tumor development. Hensen and colleagues predicted that “when the *SDHD* mutation is maternally transmitted, at least two events caused by different chromosomal mechanisms will be required. . . namely loss of the paternal wild type *SDHD* allele by, for example, mitotic recombination, followed by loss of the recombined paternal chromosome containing the paternal 11q23 region and the maternal 11p15 region” (69). This phenomenon has indeed been observed in at least two cases of maternal inheritance (73;74). Both cases were patients with PCC, caused by a mutation in *SDHD*, both inherited via the maternal line. Analysis of microsatellite markers revealed only partial loss of the paternal chromosome, with loss of a significant proportion of the maternal chromosome 11 including the p arm and centromeric q arm. Both cases showed somatic recombination of chromosome 11 in the tumor, resulting in loss of the paternal wild type *SDHD* gene and the maternal 11p15 region (73;74).

1.4 Molecular biology of paragangliomas

PGLs and PCCs of various genetic backgrounds can be segregated by their transcriptional profile into two main clusters: cluster 1 and cluster 2. Cluster 1 contains tumors with mutations in *SDHx* and *FH*, *VHL* and *HIF2A* and is enriched for genes that are associated with angiogenesis and the hypoxic response (Figure 4). Cluster 1 can be further subdivided into clusters 1A and 1B. Cluster 1A consists of PGL/PCC related to *SDHx* and *FH* while Cluster 1B includes tumors with *VHL* and *HIF2A* gene mutations (27;77). Cluster 2 comprises *RET*, *NFI*, *TMEM127* and *MAX* mutant tumors that are associated with abnormal activation of kinase signaling pathways such as PI3Kinase/AKT/mTOR, and the RAS/RAF/ERK pathway (78).

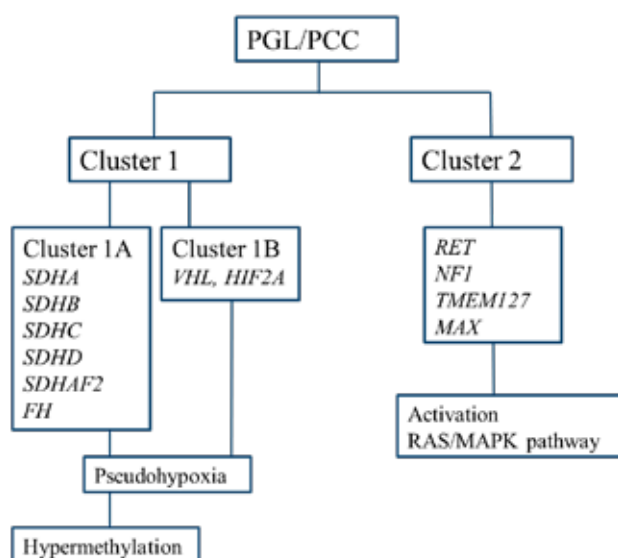


Fig. 4. The cluster 1 and 2 subdivisions of molecular pathways in PGL/PCC. Cluster 1 genes induce the activation of HIF and can be further divided into 2 groups based on methylation profiles. Cluster 1A contains PGL/PCC related to *SDHx* and *FH* which show a hypermethylation phenotype, while Cluster 1B contains tumors with *VHL* and *HIF2A* mutations. Cluster 2 comprises *RET*, *NFI*, *TMEM127* and *MAX* mutated tumors which show activation of PI3Kinase/AKT/mTOR, and/or the RAS/RAF/ERK pathway.

Pseudohypoxia

SDH, also known as succinate–coenzyme Q reductase, has a dual function as an enzyme of the mitochondrial tricarboxylic acid (TCA) cycle and as complex II of the electron transport chain. Combining these functions places SDH at the center of the two essential energy producing processes of the cell. In the TCA cycle, SDH oxidizes succinate to fumarate, while in its latter role SDH reduces ubiquinone to ubiquinol, contributing to the generation of ATP by oxidative phosphorylation. SDH inactivation leads to an accumulation of its substrate, succinate, (Figure 5) (79) and to the

generation of reactive oxygen species owing to frustrated electron transport through the respiratory chain (80). Accumulation of succinate leads to the inhibition of α -ketoglutarate-dependent HIF prolyl hydroxylases and the activation of hypoxia inducible factor (HIF) (79).

HIFs are transcription factors that respond to changes in tissue oxygen concentration. These proteins are composed of α and β subunits. The HIF- β subunit is constitutively expressed whereas HIF- α levels increase exponentially as oxygen levels decrease (81). Under normoxic conditions, HIF-1 α and HIF-2 α levels are reduced, primarily by the activity of prolyl hydroxylases (PHD) 1, 2, and 3. PHDs are α -ketoglutarate-dependent dioxygenases, using molecular oxygen, iron, and ascorbate to hydroxylate their substrate HIF- α so that it can be ubiquitinated by VHL-E3 ubiquitin-protein ligase complex, after which it is targeted for proteasomal degradation (82). Under hypoxic conditions, HIF-1 α degradation is inhibited and HIF-1 α is translocated to the nucleus where it dimerizes with the HIF-1 β subunit, leading to HIF stabilization. This in turn results in transcription of HIF target genes involved in cell proliferation, glucose transport and metabolism, glycolysis, apoptosis and angiogenesis. Pseudohypoxia occurs when HIF pathways are constitutively activated, regardless of oxygen levels, which has been shown for *SDH*-related tumors, but also for *VHL* and *HIF2A* mutant tumors (26). Inactivating mutations of *VHL* result in reduction of HIF- α degradation, leading to stabilization of HIF and the activation of hypoxia-inducible target genes (77;83). *HIF2A* mutations affect the conformation of HIF-2 α , which disrupts binding to PHDs and VHL, and, consequently, increased stabilization of HIF-2 α with induction of its downstream targets (84).

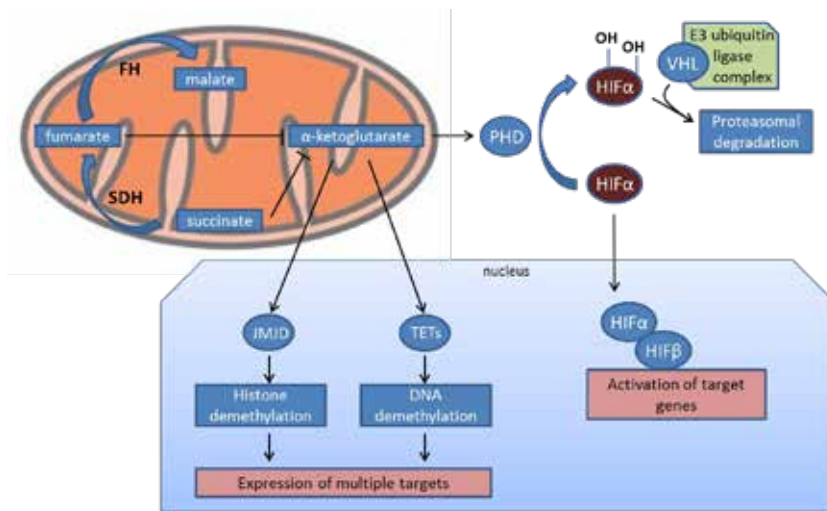


Fig. 5. Schematic representation of the consequences of succinate dehydrogenase (SDH) inactivation. Inactivation of SDH or fumarate hydratase (FH) leads to accumulation of its substrate succinate or fumarate, respectively, which inhibits α -ketoglutarate-dependent prolyl hydroxylases (PHD). Defects in SDH, the von Hippel-Lindau (VHL) protein, HIF2A, and FH all inhibit the degradation of hypoxia-inducible factor HIF α , and HIF α is subsequently transported to the nucleus where it binds HIF β forming the transcription factor HIF and activates hypoxia-inducible target genes. Other dioxygenases, including Jumonji (JM)-related histone demethylases (JMJDs) and the ten-eleven translocation (TET) family of DNA hydroxylases, are also inhibited by succinate and fumarate accumulation, resulting in global hypermethylation of target genes.

Hypermethylation

In addition to the α -ketoglutarate-dependent prolyl hydroxylases, other enzymes use α -ketoglutarate as a substrate, with succinate as a product, and are inhibited in *SDH*-related PGLs. These include the histone demethylases and the ten-eleven translocation (TET) family of DNA hydroxylases (Figure 5) (85). Human histone demethylases are defined by a catalytic jumonji (JMJ) domain, and the JMJ histone demethylases (JMJD) remove methyl groups from the histones H3 and H4. Histone methylation affects gene activity by altering chromatin structure, which is amongst others, dependent on both the exact nature and degree of methylation (86). TET enzymes have been shown to demethylate DNA, by converting 5-methylcytosine to 5-hydroxymethylcytosine, and regulate gene expression (87). Global hypermethylation of target genes has been reported for *SDH* mutant PGLs/PCCs (88).

A second enzyme of the TCA cycle was shown to be a tumor suppressor with the identification of fumarate hydratase (FH) (89). Germline mutations in *FH* predispose to dominantly inherited uterine fibroids, skin leiomyomata and papillary renal cell cancer (89). The link between *SDH* and *FH* inactivation was strengthened by the recent identification of *FH* gene mutations in PCCs that displayed transcriptional and methylation similarities to *SDH* mutant tumors (88;90). *FH* catalyses the reaction that follows *SDH* in the TCA cycle, converting fumarate to malate (Figure 5). Deficiency in *FH* activity results in the accumulation of its substrate fumarate, which shares structural similarities with succinate and similarly affects the same classes of α -ketoglutarate-dependent enzymes (85;90). Very recently, a germline mutation in *MDH2*, coding for another enzyme of the TCA cycle, was found in two family members with paraganglioma (91). This study also reported that *MDH2* mutations are associated with a methylator phenotype and showed a transcriptional profile similar to *SDH* gene mutated tumors.

Insights from *SDH*-deficient mouse models

Elucidating the primary link between loss of *SDH* and disease is an important clinical aim that could open the way to new treatments. A major barrier to further progress is the current lack of relevant animal and cell models. Several mouse lines carrying knockouts of *SDH* genes have been described, and homozygous knockout is lethal (92). Heterozygous *SDHD* inactivation in mice induced a slight increase in the percentage of glomus cells in the carotid body and a significant increase of spontaneous carotid body activity under normoxic conditions but did not lead to carotid body PGL nor PCC (92). In order to mimic the parent-of-origin inheritance pattern of *SDHD* tumorigenesis observed in human (see paragraph 1.3; inheritance), a *SDHD/H19* double knockout mouse model was created but also did not show increased PGL or PCC susceptibility, which might indicate that *H19* is not a modifier gene in tumor development, at least in mice (93). Conditional and tissue-specific *SDH*-deficient models also failed to develop disease (88;94). TH promoter is expected to drive Cre recombinase expression in all catecholaminergic cells, while PSA, although supposedly specific to the prostate, can also drive expression in the adrenal medulla of mice (95). Furthermore, *PTEN*⁺/mice are reported to be predisposed to PCC (96). Consequently, a *SDHB/PTEN* double conditional knockout model expressing Cre recombinase under the control of PSA promoter was generated and these mice developed only half as many tumors compared to *PTEN* knockout mice (97). The carotid bodies and adrenal glands of these mice were smaller, with few chromaffin cells when *SDHB* was

completely eliminated. Major cell death was caused by the complete deletion of *SDHB* and the tumors that did arise showed no accumulation of succinate, demonstrating normal SDH activity. This widespread cell death due to complete *SDHB* deletion suggested that mouse cells respond poorly to loss of SDH subunits and as such will be unlikely to survive when loss occurs in many cells concurrently (97). It is understandable that a cell that loses a protein central to energy generation would have poor survival chances, suggesting that a subtle approach might succeed where blunt force fails.

1.5 Outline of this thesis

The aim of this thesis is to gain insight in the genetics, inheritance and tumor biology of head and neck paragangliomas with a focus on *SDHD* and *SDHAF2*-related tumors and the Hensen model.

In **chapter one**, an overview of current knowledge of causative genes and inheritance patterns in paraganglioma and pheochromocytoma is given. Although germline mutations in most of these genes lead to autosomal dominant inheritance patterns of the disease in families, there are prominent exceptions: *SDHD* and *SDHAF2*. Mutations in *SDHD* and *SDHAF2* show a remarkable parent-of-origin dependent tumorigenesis in which tumor formation almost exclusively occurs following paternal transmission of the mutation. Several models are discussed that attempt to explain the striking inheritance pattern seen in *SDHD* and *SDHAF2*-linked families.

In **chapter two**, the epigenetic consequences of the accumulation of succinate and fumarate caused by germline mutations in succinate dehydrogenase (SDH) and fumarate hydratase (FH), respectively, were assessed. Since the accumulation of succinate and fumarate can inhibit α -ketoglutarate dependent dioxygenases, including histone demethylases and the ten-eleven translocation (TET) family of DNA hydroxylases, histone and DNA modifications were evaluated in *SDH*-linked paragangliomas/pheochromocytomas and *FH*-related smooth muscle tumors in comparison to their normal counterparts using immunohistochemistry.

In **chapter three**, the parent-of-origin dependent tumorigenesis in *SDHD*-linked patients is studied. The hypothesis that a second target gene(s) on chromosome 11p15, a region known to harbor an imprinted gene cluster, is involved in tumor formation is further investigated by creating an *in vitro* model. Two potential tumor modifier genes involved in tumor formation of *SDHD*-mutated PGL were identified and expression of these genes was evaluated in *SDHD*-linked tumors.

In **chapter four**, loss of the maternal copy of chromosome 11 is studied in *SDHD*, *SDHAF2*, *SDHB* and *VHL* mutant paragangliomas and pheochromocytomas using highly polymorphic microsatellite markers. In addition, genome-wide copy number changes and loss of heterozygosity were investigated in these tumors by SNP array analysis.

Chapter five describes the characterization of large deletions in *SDHB*, *SDHC* or *SDHD*-related PGL/PCC patients who tested negative for point mutations by Sanger sequencing of the *SDH* genes. A long-range PCR 'chromosome walking' approach was used and the advantages and limitations of this long-range PCR method were evaluated. The detection of collateral deletion of neighboring genes may be of phenotypic significance and are discussed here.

Chapter six provides a summary and discussion of the thesis, with an emphasis on the Hensen model, and the striking differences between *SDH*-related tumors.

References

- (1) Wasserman PG, Savargaonkar P. Paragangliomas: classification, pathology, and differential diagnosis. *Otolaryngol Clin North Am* 2001 October;34(5):845-vi.
- (2) Subramanian A, Maker VK. Organs of Zuckermandl: their surgical significance and a review of a century of literature. *Am J Surg* 2006 August;192(2):224-34.
- (3) Carlsoo B, Dahlqvist A, Domeij S, Hellstrom S, Dedo HH, Izdebski K. Carotid-body-like tissue within the recurrent laryngeal nerve: an endoneural chemosensitive micro-organ? *Am J Otolaryngol* 1983 September;4(5):334-41.
- (4) Lee KY, Oh YW, Noh HJ, Lee YJ, Yong HS, Kang EY, Kim KA, Lee NJ. Extraadrenal paragangliomas of the body: imaging features. *AJR Am J Roentgenol* 2006 August;187(2):492-504.
- (5) Lack EE, Cubilla AL, Woodruff JM. Paragangliomas of the head and neck region. A pathologic study of tumors from 71 patients. *Hum Pathol* 1979 March;10(2):191-218.
- (6) Jansen JC, van den BR, Kuiper A, Van Der Mey AG, Zwinderman AH, Cornelisse CJ. Estimation of growth rate in patients with head and neck paragangliomas influences the treatment proposal. *Cancer* 2000 June 15;88(12):2811-6.
- (7) Douwes Dekker PB, Corver WE, Hogendoorn PC, Van Der Mey AG, Cornelisse CJ. Multiparameter DNA flow-sorting demonstrates diploidy and SDHD wild-type gene retention in the sustentacular cell compartment of head and neck paragangliomas: chief cells are the only neoplastic component. *J Pathol* 2004 April;202(4):456-62.
- (8) Petri BJ, van Eijck CH, de Herder WW, Wagner A, de Krijger RR. Pheochromocytomas and sympathetic paragangliomas. *Br J Surg* 2009 December;96(12):1381-92.
- (9) Pacak K, Eisenhofer G, Ahlman H, Bornstein SR, Gimenez-Roqueplo AP, Grossman AB, Kimura N, Mannelli M, McNicol AM, Tischler AS. Pheochromocytoma: recommendations for clinical practice from the First International Symposium. October 2005. *Nat Clin Pract Endocrinol Metab* 2007 February;3(2):92-102.
- (10) Erickson D, Kudva YC, Ebersold MJ, Thompson GB, Grant CS, van Heerden JA, Young WF, Jr. Benign paragangliomas: clinical presentation and treatment outcomes in 236 patients. *J Clin Endocrinol Metab* 2001 November;86(11):5210-6.
- (11) Baysal BE. Hereditary paraganglioma targets diverse paraganglia. *J Med Genet* 2002 September;39(9):617-22.
- (12) Beard CM, Sheps SG, Kurland LT, Carney JA, Lie JT. Occurrence of pheochromocytoma in Rochester, Minnesota, 1950 through 1979. *Mayo Clin Proc* 1983 December;58(12):802-4.
- (13) Stenstrom G, Svarsdudd K. Pheochromocytoma in Sweden 1958-1981. An analysis of the National Cancer Registry Data. *Acta Med Scand* 1986;220(3):225-32.
- (14) Cascon A, Pita G, Burnichon N, Landa I, Lopez-Jimenez E, Montero-Conde C, Leskela S, Leandro-Garcia LJ, Leton R, Rodriguez-Antona C, Diaz JA, Lopez-Vidriero E, Gonzalez-Neira A, Velasco A, Matias-Guiu X, Gimenez-Roqueplo AP, Robledo M. Genetics of pheochromocytoma and paraganglioma in Spanish patients. *J Clin Endocrinol Metab* 2009 May;94(5):1701-5.
- (15) Mannelli M, Castellano M, Schiavi F, Filetti S, Giacche M, Mori L, Pignataro V, Bernini G, Giache V, Bacca A, Biondi B, Corona G, Di TG, Grossrubatscher E, Reimondo G, Arnaldi G, Giacchetti G, Veglio F, Loli P, Colao A, Ambrosio MR, Terzolo M, Letizia C, Ercolino T, Opocher G. Clinically guided genetic screening in a large cohort of italian patients with pheochromocytomas and/or functional or nonfunctional paragangliomas. *J Clin Endocrinol Metab* 2009 May;94(5):1541-7.
- (16) Taieb D, Varoquaux A, Chen CC, Pacak K. Current and future trends in the anatomical and functional imaging of head and neck paragangliomas. *Semin Nucl Med* 2013 November;43(6):462-73.
- (17) van DN, Steenvoorden D, Kema IP, Jansen JC, Vriends AH, Bayley JP, Smit JW, Romijn JA, Corssmit EP. Increased Urinary Excretion of 3-Methoxytyramine in Patients with Head and Neck Paragangliomas. *J Clin Endocrinol Metab* 2009 November 6.
- (18) Lim JY, Kim J, Kim SH, Lee S, Lim YC, Kim JW, Choi EC. Surgical treatment of carotid body paragangliomas: outcomes and complications according to the shamblin classification. *Clin Exp Otorhinolaryngol* 2010 June;3(2):91-5.
- (19) Power AH, Bower TC, Kasperbauer J, Link MJ, Oderich G, Cloft H, Young WF, Jr., Gloviczki P. Impact of preoperative embolization on outcomes of carotid body tumor resections. *J Vasc Surg* 2012 October;56(4):979-89.
- (20) Lee JH, Barich F, Karnell LH, Robinson RA, Zhen WK, Gantz BJ, Hoffman HT. National Cancer Data Base report on malignant paragangliomas of the head and neck. *Cancer* 2002 February 1;94(3):730-7.

- (21) van Hulsteijn LT, Corssmit EP, Coremans IE, Smit JW, Jansen JC, Dekkers OM. Regression and local control rates after radiotherapy for jugulotympanic paragangliomas: systematic review and meta-analysis. *Radiother Oncol* 2013 February;106(2):161-8.
- (22) Bianchi LC, Marchetti M, Brait L, Bergantin A, Milanesi I, Broggi G, Fariselli L. Paragangliomas of head and neck: a treatment option with CyberKnife radiosurgery. *Neurol Sci* 2009 December;30(6):479-85.
- (23) Navarro MA, Maitz A, Grills IS, Bojrab D, Kartush J, Chen PY, Hahn J, Pieper D. Successful treatment of glomus jugulare tumours with gamma knife radiosurgery: clinical and physical aspects of management and review of the literature. *Clin Transl Oncol* 2010 January;12(1):55-62.
- (24) Chen H, Sippel RS, O'Dorisio MS, Vinik AI, Lloyd RV, Pacak K. The North American Neuroendocrine Tumor Society consensus guideline for the diagnosis and management of neuroendocrine tumors: pheochromocytoma, paraganglioma, and medullary thyroid cancer. *Pancreas* 2010 August;39(6):775-83.
- (25) Tischler AS. Pheochromocytoma and extra-adrenal paraganglioma: updates. *Arch Pathol Lab Med* 2008 August;132(8):1272-84.
- (26) Dahia PL. Pheochromocytoma and paraganglioma pathogenesis: learning from genetic heterogeneity. *Nat Rev Cancer* 2014 February;14(2):108-19.
- (27) Castro-Vega LJ, Letouze E, Burnichon N, Buffet A, Disderot PH, Khalifa E, Lorient C, Elarouci N, Morin A, Menara M, Lepoutre-Lussey C, Badoual C, Sibony M, Dousset B, Libe R, Zinzindohoue F, Plouin PF, Bertherat J, Amar L, De RA, Favier J, Gimenez-Roqueplo AP. Multi-omics analysis defines core genomic alterations in pheochromocytomas and paragangliomas. *Nat Commun* 2015;6:6044.
- (28) Fishbein L, Khare S, Wubbenhorst B, DeSloover D, D'Andrea K, Merrill S, Cho NW, Greenberg RA, Else T, Montone K, LiVolsi V, Fraker D, Daber R, Cohen DL, Nathanson KL. Whole-exome sequencing identifies somatic ATRX mutations in pheochromocytomas and paragangliomas. *Nat Commun* 2015;6:6140.
- (29) Astuti D, Latif F, Dallol A, Dahia PL, Douglas F, George E, Skoldberg F, Husebye ES, Eng C, Maher ER. Gene mutations in the succinate dehydrogenase subunit SDHB cause susceptibility to familial pheochromocytoma and to familial paraganglioma. *Am J Hum Genet* 2001 July;69(1):49-54.
- (30) Baysal BE, Ferrell RE, Willett-Brozick JE, Lawrence EC, Myssiorek D, Bosch A, van der MA, Taschner PE, Rubinstein WS, Myers EN, Richard CW, III, Cornelisse CJ, Devilee P, Devlin B. Mutations in SDHD, a mitochondrial complex II gene, in hereditary paraganglioma. *Science* 2000 February 4;287(5454):848-51.
- (31) Hao HX, Khalimonchuk O, Schraders M, Dephoure N, Bayley JP, Kunst H, Devilee P, Cremers CW, Schiffman JD, Bentz BG, Gygi SP, Winge DR, Kremer H, Rutter J. SDH5, a gene required for flavination of succinate dehydrogenase, is mutated in paraganglioma. *Science* 2009 August 28;325(5944):1139-42.
- (32) Niemann S, Muller U. Mutations in SDHC cause autosomal dominant paraganglioma, type 3. *Nat Genet* 2000 November;26(3):268-70.
- (33) Erlic Z, Rybicki L, Peczkowska M, Golcher H, Kann PH, Brauckhoff M, Mussig K, Muresan M, Schaffler A, Reisch N, Schott M, Fassnacht M, Opocher G, Klose S, Fottner C, Forrer F, Plockinger U, Petersenn S, Zabolotny D, Kollukch O, Yaremchuk S, Januszewicz A, Walz MK, Eng C, Neumann HP. Clinical predictors and algorithm for the genetic diagnosis of pheochromocytoma patients. *Clin Cancer Res* 2009 October 15;15(20):6378-85.
- (34) Benn DE, Gimenez-Roqueplo AP, Reilly JR, Bertherat J, Burgess J, Byth K, Croxson M, Dahia PL, Elston M, Gimm O, Henley D, Herman P, Murday V, Niccoli-Sire P, Pasiaka JL, Rohmer V, Tucker K, Jeunemaitre X, Marsh DJ, Plouin PF, Robinson BG. Clinical presentation and penetrance of pheochromocytoma/paraganglioma syndromes. *J Clin Endocrinol Metab* 2006 March;91(3):827-36.
- (35) Hensen EF, Jansen JC, Siemers MD, Oosterwijk JC, Vriends AH, Corssmit EP, Bayley JP, Van Der Mey AG, Cornelisse CJ, Devilee P. The Dutch founder mutation SDHD.D92Y shows a reduced penetrance for the development of paragangliomas in a large multigenerational family. *Eur J Hum Genet* 2010 January;18(1):62-6.
- (36) Neumann HP, Pawlu C, Peczkowska M, Bausch B, McWhinney SR, Muresan M, Buchta M, Franke G, Klisch J, Bley TA, Hoegerle S, Boedeker CC, Opocher G, Schipper J, Januszewicz A, Eng C. Distinct clinical features of paraganglioma syndromes associated with SDHB and SDHD gene mutations. *JAMA* 2004 August 25;292(8):943-51.
- (37) Hensen EF, van DN, Jansen JC, Corssmit EP, Tops CM, Romijn JA, Vriends AH, Van Der Mey AG, Cornelisse CJ, Devilee P, Bayley JP. High prevalence of founder mutations of the succinate dehydrogenase genes in the Netherlands. *Clin Genet* 2012 March;81(3):284-8.

- (38) Taschner PE, Jansen JC, Baysal BE, Bosch A, Rosenberg EH, Brocker-Vriends AH, Der Mey AG, van Ommen GJ, Cornelisse CJ, Devilee P. Nearly all hereditary paragangliomas in the Netherlands are caused by two founder mutations in the SDHD gene. *Genes Chromosomes Cancer* 2001 July;31(3):274-81.
- (39) Schiavi F, Milne RL, Anda E, Blay P, Castellano M, Opocher G, Robledo M, Cascon A. Are we overestimating the penetrance of mutations in SDHB? *Hum Mutat* 2010 June;31(6):761-2.
- (40) Solis DC, Burnichon N, Timmers HJ, Raygada MJ, Kozupa A, Merino MJ, Makey D, Adams KT, Venisse A, Gimenez-Roqueplo AP, Pacak K. Penetrance and clinical consequences of a gross SDHB deletion in a large family. *Clin Genet* 2009 April;75(4):354-63.
- (41) Bayley JP, Grimbergen AE, van Bunderen PA, van der WM, Kunst HP, Lenders JW, Jansen JC, Dullaart RP, Devilee P, Corssmit EP, Vriends AH, Losekoot M, Weiss MM. The first Dutch SDHB founder deletion in paraganglioma-pheochromocytoma patients. *BMC Med Genet* 2009;10:34.
- (42) Hes FJ, Weiss MM, Woortman SA, de Miranda NF, van Bunderen PA, Bonsing BA, Stokkel MP, Morreau H, Romijn JA, Jansen JC, Vriends AH, Bayley JP, Corssmit EP. Low penetrance of a SDHB mutation in a large Dutch paraganglioma family. *BMC Med Genet* 2010;11:92.
- (43) Peczkowska M, Cascon A, Prejbisz A, Kubaszek A, Cwikla BJ, Furmanek M, Eric S, Eng C, Januszewicz A, Neumann HP. Extra-adrenal and adrenal pheochromocytomas associated with a germline SDHC mutation. *Nat Clin Pract Endocrinol Metab* 2008 February;4(2):111-5.
- (44) Schiavi F, Boedeker CC, Bausch B, Peczkowska M, Gomez CF, Strassburg T, Pawlu C, Buchta M, Salzman M, Hoffmann MM, Berlis A, Brink I, Cybulla M, Muresan M, Walter MA, Forrer F, Valimaki M, Kaweck A, Szutkowski Z, Schipper J, Walz MK, Pigny P, Bateurs C, Willet-Brozick JE, Baysal BE et al. Predictors and prevalence of paraganglioma syndrome associated with mutations of the SDHC gene. *JAMA* 2005 October 26;294(16):2057-63.
- (45) Pagnamenta AT, Hargreaves IP, Duncan AJ, Taanman JW, Heales SJ, Land JM, Bitner-Glindzic M, Leonard JV, Rahman S. Phenotypic variability of mitochondrial disease caused by a nuclear mutation in complex II. *Mol Genet Metab* 2006 November;89(3):214-21.
- (46) Burnichon N, Briere JJ, Libe R, Vescovo L, Riviere J, Tissier F, Jouanno E, Jeunemaitre X, Benit P, Tzagoloff A, Rustin P, Bertherat J, Favier J, Gimenez-Roqueplo AP. SDHA is a tumor suppressor gene causing paraganglioma. *Hum Mol Genet* 2010 August 1;19(15):3011-20.
- (47) Korpershoek E, Favier J, Gaal J, Burnichon N, van GB, Oudijk L, Badoual C, Gadessaud N, Venisse A, Bayley JP, van Dooren MF, de Herder WW, Tissier F, Plouin PF, van Nederveen FH, Dinjens WN, Gimenez-Roqueplo AP, de Krijger RR. SDHA immunohistochemistry detects germline SDHA gene mutations in apparently sporadic paragangliomas and pheochromocytomas. *J Clin Endocrinol Metab* 2011 September;96(9):E1472-E1476.
- (48) Ardehali H, Chen Z, Ko Y, Mejia-Alvarez R, Marban E. Multiprotein complex containing succinate dehydrogenase confers mitochondrial ATP-sensitive K⁺ channel activity. *Proc Natl Acad Sci U S A* 2004 August 10;101(32):11880-5.
- (49) Bayley JP, Kunst HP, Cascon A, Sampietro ML, Gaal J, Korpershoek E, Hinojar-Gutierrez A, Timmers HJ, Hoefsloot LH, Hermsen MA, Suarez C, Hussain AK, Vriends AH, Hes FJ, Jansen JC, Tops CM, Corssmit EP, de KP, Lenders JW, Cremers CW, Devilee P, Dinjens WN, de Krijger RR, Robledo M. SDHAF2 mutations in familial and sporadic paraganglioma and pheochromocytoma. *Lancet Oncol* 2010 April;11(4):366-72.
- (50) Kunst HP, Rutten MH, De Monnik JP, Hoefsloot LH, Timmers HJ, Marres HA, Jansen JC, Kremer H, Bayley JP, Cremers CW. SDHAF2 (PGL2-SDH5) and Hereditary Head and Neck Paraganglioma. *Clin Cancer Res* 2011 January 15;17(2):247-54.
- (51) Santos P, Pimenta T, Taveira-Gomes A. Hereditary Pheochromocytoma. *Int J Surg Pathol* 2014 August;22(5):393-400.
- (52) Barontini M, Dahia PL. VHL disease. *Best Pract Res Clin Endocrinol Metab* 2010 June;24(3):401-13
- (53) Curras-Freixes M, Inglada-Perez L, Mancikova V, Montero-Conde C, Leton R, Comino-Mendez I, Apellaniz-Ruiz M, Sanchez-Barroso L, Aguirre Sanchez-Covisa M, Alcazar V, Aller J, Alvarez-Escola C, Andia-Melero VM, Azriel-Mira S, Calatayud-Gutierrez M, Diaz JA, Diez-Hernandez A, Lamas-Oliveira C, Marazuela M, Matias-Guiu X, Meoro-Aviles A, Patino-Garcia A, Pedrinaci S, Riesco-Eizaguirre G, Sabado-Alvarez C et al. Recommendations for somatic and germline genetic testing of single pheochromocytoma and paraganglioma based on findings from a series of 329 patients. *J Med Genet* 2015 October;52(10):647-56.
- (54) Johannessen CM, Reczek EE, James MF, Brems H, Legius E, Cichowski K. The NF1 tumor suppressor critically regulates TSC2 and mTOR. *Proc Natl Acad Sci U S A* 2005 June 14;102(24):8573-8.

- 1
- (55) Johannessen CM, Johnson BW, Williams SM, Chan AW, Reczek EE, Lynch RC, Rieth MJ, McClatchey A, Ryeom S, Cichowski K. TORC1 is essential for NF1-associated malignancies. *Curr Biol* 2008 January 8;18(1):56-62.
 - (56) Opocher G, Schiavi F. Genetics of pheochromocytomas and paragangliomas. *Best Pract Res Clin Endocrinol Metab* 2010 December;24(6):943-56.
 - (57) Walther MM, Herring J, Enquist E, Keiser HR, Linehan WM. von Recklinghausen's disease and pheochromocytomas. *J Urol* 1999 November;162(5):1582-6.
 - (58) Bausch B, Borozdin W, Mautner VF, Hoffmann MM, Boehm D, Robledo M, Cascon A, Harenberg T, Schiavi F, Pawlu C, Peczkowska M, Letizia C, Calvieri S, Arnaldi G, Klingenberg-Noftz RD, Reisch N, Fassina A, Brunaud L, Walter MA, Mannelli M, MacGregor G, Palazzo FF, Barontini M, Walz MK, Kremens B et al. Germline NF1 mutational spectra and loss-of-heterozygosity analyses in patients with pheochromocytoma and neurofibromatosis type 1. *J Clin Endocrinol Metab* 2007 July;92(7):2784-92.
 - (59) Besset V, Scott RP, Ibanez CF. Signaling complexes and protein-protein interactions involved in the activation of the Ras and phosphatidylinositol 3-kinase pathways by the c-Ret receptor tyrosine kinase. *J Biol Chem* 2000 December 15;275(50):39159-66.
 - (60) Machens A, Brauckhoff M, Holzhausen HJ, Thanh PN, Lehnert H, Dralle H. Codon-specific development of pheochromocytoma in multiple endocrine neoplasia type 2. *J Clin Endocrinol Metab* 2005 July;90(7):3999-4003.
 - (61) Wohllk N, Schweizer H, Erlic Z, Schmid KW, Walz MK, Raue F, Neumann HP. Multiple endocrine neoplasia type 2. *Best Pract Res Clin Endocrinol Metab* 2010 June;24(3):371-87.
 - (62) Qin Y, Yao L, King EE, Buddavarapu K, Lenci RE, Chocron ES, Lechleiter JD, Sass M, Aronin N, Schiavi F, Boaretto F, Opocher G, Toledo RA, Toledo SP, Stiles C, Aguiar RC, Dahia PL. Germline mutations in TMEM127 confer susceptibility to pheochromocytoma. *Nat Genet* 2010 March;42(3):229-33.
 - (63) Neumann HP, Sullivan M, Winter A, Malinoc A, Hoffmann MM, Boedeker CC, Bertz H, Walz MK, Moeller LC, Schmid KW, Eng C. Germline mutations of the TMEM127 gene in patients with paraganglioma of head and neck and extraadrenal abdominal sites. *J Clin Endocrinol Metab* 2011 August;96(8):E1279-E1282.
 - (64) Abermil N, Guillaud-Bataille M, Burnichon N, Venisse A, Manivet P, Guignat L, Drui D, Chupin M, Josseume C, Affres H, Plouin PF, Bertherat J, Jeunemaitre X, Gimenez-Roqueplo AP. TMEM127 screening in a large cohort of patients with pheochromocytoma and/or paraganglioma. *J Clin Endocrinol Metab* 2012 May;97(5):E805-E809.
 - (65) Yao L, Schiavi F, Cascon A, Qin Y, Inglada-Perez L, King EE, Toledo RA, Ercolino T, Rapizzi E, Ricketts CJ, Mori L, Giacche M, Mendola A, Taschin E, Boaretto F, Loli P, Iacobone M, Rossi GP, Biondi B, Lima-Junior JV, Kater CE, Bex M, Vikkula M, Grossman AB, Gruber SB et al. Spectrum and prevalence of FP/TMEM127 gene mutations in pheochromocytomas and paragangliomas. *JAMA* 2010 December 15;304(23):2611-9.
 - (66) Qin Y, Yao L, King EE, Buddavarapu K, Lenci RE, Chocron ES, Lechleiter JD, Sass M, Aronin N, Schiavi F, Boaretto F, Opocher G, Toledo RA, Toledo SP, Stiles C, Aguiar RC, Dahia PL. Germline mutations in TMEM127 confer susceptibility to pheochromocytoma. *Nat Genet* 2010 March;42(3):229-33.
 - (67) Comino-Mendez I, Gracia-Aznarez FJ, Schiavi F, Landa I, Leandro-Garcia LJ, Leton R, Honrado E, Ramos-Medina R, Caronia D, Pita G, Gomez-Grana A, De Cubas AA, Inglada-Perez L, Maliszewska A, Taschin E, Bobisse S, Pica G, Loli P, Hernandez-Lavado R, Diaz JA, Gomez-Morales M, Gonzalez-Neira A, Roncador G, Rodriguez-Antona C, Benitez J et al. Exome sequencing identifies MAX mutations as a cause of hereditary pheochromocytoma. *Nat Genet* 2011 July;43(7):663-7.
 - (68) Burnichon N, Cascon A, Schiavi F, Morales NP, Comino-Mendez I, Abermil N, Inglada-Perez L, De Cubas AA, Amar L, Barontini M, de Quiros SB, Bertherat J, Bignon YJ, Blok MJ, Bobisse S, Borrego S, Castellano M, Chanson P, Chiara MD, Corssmit EP, Giacche M, de Krijger RR, Ercolino T, Girerd X, Gomez-Garcia EB et al. MAX mutations cause hereditary and sporadic pheochromocytoma and paraganglioma. *Clin Cancer Res* 2012 May 15;18(10):2828-37.
 - (69) Hensen EF, Jordanova ES, van Minderhout IJHM, Hogendoorn PCW, Taschner PEM, van der Mey AGL, Devilee P, Cornelisse CJ. Somatic loss of maternal chromosome 11 causes parent-of-origin-dependent inheritance in SDHD-linked paraganglioma and pheochromocytoma families. *Oncogene* 2004 May 20;23(23):4076-83.
 - (70) Van Der Mey AG, Maaswinkel-Mooy PD, Cornelisse CJ, Schmidt PH, van de Kamp JJ. Genomic imprinting in hereditary glomus tumours: evidence for new genetic theory. *Lancet* 1989 December 2;2(8675):1291-4.

- (71) Baysal BE, McKay S, Kim YJ, Zhang Z, Alila L, Willett-Brozick JE, Pacak K, Kim TH, Shadel GS. Genomic imprinting at a boundary element flanking the SDHD locus. *Hum Mol Genet* 2011 August 23.
- (72) Muller U. Pathological mechanisms and parent-of-origin effects in hereditary paraganglioma/pheochromocytoma (PGL/PCC). *Neurogenetics* 2011 August;12(3):175-81.
- (73) Bayley JP, Oldenburg RA, Nuk J, Hoekstra AS, van der Meer CA, Korpershoek E, McGillivray B, Corssmit EP, Dinjens WN, de Krijger RR, Devilee P, Jansen JC, Hes FJ. Paraganglioma and pheochromocytoma upon maternal transmission of SDHD mutations. *BMC Med Genet* 2014;15:111.
- (74) Yeap PM, Tobias ES, Mavraki E, Fletcher A, Bradshaw N, Freel EM, Cooke A, Murday VA, Davidson HR, Perry CG, Lindsay RS. Molecular Analysis of Pheochromocytoma after Maternal Transmission of SDHD Mutation Elucidates Mechanism of Parent-of-Origin Effect. *J Clin Endocrinol Metab* 2011 September 21.
- (75) Mussa A, Russo S, Larizza L, Riccio A, Ferrero GB. (Epi)genotype-phenotype correlations in Beckwith-Wiedemann syndrome: a paradigm for genomic medicine. *Clin Genet* 2015 July 3.
- (76) Birch-Machin MA, Taylor RW, Cochran B, Ackrell BA, Turnbull DM. Late-onset optic atrophy, ataxia, and myopathy associated with a mutation of a complex II gene. *Ann Neurol* 2000 September;48(3):330-5.
- (77) Lopez-Jimenez E, Gomez-Lopez G, Leandro-Garcia LJ, Munoz I, Schiavi F, Montero-Conde C, De Cubas AA, Ramires R, Landa I, Leskela S, Maliszewska A, Inglada-Perez L, de I, V, Rodriguez-Antona C, Leton R, Bernal C, de Campos JM, Diez-Tascon C, Fraga MF, Boullosa C, Pisano DG, Opocher G, Robledo M, Cascon A. Research resource: Transcriptional profiling reveals different pseudohypoxic signatures in SDHB and VHL-related pheochromocytomas. *Mol Endocrinol* 2010 December;24(12):2382-91.
- (78) Dahia PL, Ross KN, Wright ME, Hayashida CY, Santagata S, Barontini M, Kung AL, Sanso G, Powers JF, Tischler AS, Hodin R, Heitritter S, Moore F, Dluhy R, Sosa JA, Ocal IT, Benn DE, Marsh DJ, Robinson BG, Schneider K, Garber J, Arum SM, Korbonits M, Grossman A, Pigny P et al. A HIF1alpha regulatory loop links hypoxia and mitochondrial signals in pheochromocytomas. *PLoS Genet* 2005 July;1(1):72-80.
- (79) Selak MA, Armour SM, MacKenzie ED, Boulahbel H, Watson DG, Mansfield KD, Pan Y, Simon MC, Thompson CB, Gottlieb E. Succinate links TCA cycle dysfunction to oncogenesis by inhibiting HIF-alpha prolyl hydroxylase. *Cancer Cell* 2005 January;7(1):77-85.
- (80) Ishii T, Yasuda K, Akatsuka A, Hino O, Hartman PS, Ishii N. A mutation in the SDHC gene of complex II increases oxidative stress, resulting in apoptosis and tumorigenesis. *Cancer Res* 2005 January 1;65(1):203-9.
- (81) Keith B, Johnson RS, Simon MC. HIF1alpha and HIF2alpha: sibling rivalry in hypoxic tumour growth and progression. *Nat Rev Cancer* 2012 January;12(1):9-22.
- (82) Willam C, Nicholls LG, Ratcliffe PJ, Pugh CW, Maxwell PH. The prolyl hydroxylase enzymes that act as oxygen sensors regulating destruction of hypoxia-inducible factor alpha. *Adv Enzyme Regul* 2004;44:75-92.
- (83) Dahia PL. Transcription association of VHL and SDH mutations link hypoxia and oxidoreductase signals in pheochromocytomas. *Ann N Y Acad Sci* 2006 August;1073:208-20.
- (84) Jochmanova I, Zelinka T, Widimsky J, Jr., Pacak K. HIF signaling pathway in pheochromocytoma and other neuroendocrine tumors. *Physiol Res* 2014;63 Suppl 2:S251-S262.
- (85) Xiao M, Yang H, Xu W, Ma S, Lin H, Zhu H, Liu L, Liu Y, Yang C, Xu Y, Zhao S, Ye D, Xiong Y, Guan KL. Inhibition of alpha-KG-dependent histone and DNA demethylases by fumarate and succinate that are accumulated in mutations of FH and SDH tumor suppressors. *Genes Dev* 2012 June 15;26(12):1326-38.
- (86) Agger K, Christensen J, Cloos PA, Helin K. The emerging functions of histone demethylases. *Curr Opin Genet Dev* 2008 April;18(2):159-68.
- (87) Wu H, Zhang Y. Mechanisms and functions of Tet protein-mediated 5-methylcytosine oxidation. *Genes Dev* 2011 December 1;25(23):2436-52.
- (88) Letouze E, Martinelli C, Loriot C, Burnichon N, Abermil N, Ottolenghi C, Janin M, Menara M, Nguyen AT, Benit P, Buffet A, Marcaillou C, Bertherat J, Amar L, Rustin P, De RA, Gimenez-Roqueplo AP, Favier J. SDH mutations establish a hypermethylator phenotype in paraganglioma. *Cancer Cell* 2013 June 10;23(6):739-52.
- (89) Tomlinson IPM, Alam NA, Rowan AJ, Barclay E, Jaeger EEM, Kelsell D, Leigh I, Gorman P, Lamlum H, Rahman S, Roylance RR, Olpin S, Bevan S, Barker K, Hearle N, Houlston RS, Kiuru M, Lehtonen R, Karhu A, Vilkki S, Laiho P, Eklund C, Vierimaa O, Aittomaki K, Hietala M et al. Germline mutations in FH predispose to dominantly inherited uterine fibroids, skin leiomyomata and papillary renal cell cancer. *Nature Genetics* 2002 April;30(4):406-10.

- (90) Castro-Vega LJ, Buffet A, De Cubas AA, Cascon A, Menara M, Khalifa E, Amar L, Azriel S, Bourdeau I, Chabre O, Curras-Freixes M, Franco-Vidal V, Guillaud-Bataille M, Simian C, Morin A, Leton R, Gomez-Grana A, Pollard PJ, Rustin P, Robledo M, Favier J, Gimenez-Roqueplo AP. Germline mutations in FH confer predisposition to malignant pheochromocytomas and paragangliomas. *Hum Mol Genet* 2014 May 1;23(9):2440-6.
- (91) Cascon A, Comino-Mendez I, Curras-Freixes M, De Cubas AA, Contreras L, Richter S, Peitzsch M, Mancikova V, Inglada-Perez L, Perez-Barrios A, Calatayud M, Azriel S, Villar-Vicente R, Aller J, Setien F, Moran S, Garcia JF, Rio-Machin A, Leton R, Gomez-Grana A, Apellaniz-Ruiz M, Roncador G, Esteller M, Rodriguez-Antona C, Satrustegui J et al. Whole-exome sequencing identifies MDH2 as a new familial paraganglioma gene. *J Natl Cancer Inst* 2015 May;107(5).
- (92) Piruat JJ, Pintado CO, Ortega-Saenz P, Roche M, Lopez-Barneo J. The mitochondrial SDHD gene is required for early embryogenesis, and its partial deficiency results in persistent carotid body glomus cell activation with full responsiveness to hypoxia. *Mol Cell Biol* 2004 December;24(24):10933-40.
- (93) Bayley JP, van M, I, Hogendoorn PC, Cornelisse CJ, van der WA, Prins FA, Teppema L, Dahan A, Devilee P, Taschner PE. Sdhb and SDHD/H19 knockout mice do not develop paraganglioma or pheochromocytoma. *PLoS One* 2009;4(11):e7987.
- (94) Diaz-Castro B, Pintado CO, Garcia-Flores P, Lopez-Barneo J, Piruat JJ. Differential impairment of catecholaminergic cell maturation and survival by genetic mitochondrial complex II dysfunction. *Mol Cell Biol* 2012 August;32(16):3347-57.
- (95) Korpershoek E, Loonen AJ, Corvers S, van Nederveen FH, Jonkers J, Ma X, Ziel-van der Made A, Korsten H, Trapman J, Dinjens WN, de Krijger RR. Conditional Pten knock-out mice: a model for metastatic pheochromocytoma. *J Pathol* 2009 March;217(4):597-604.
- (96) You MJ, Castrillon DH, Bastian BC, O'Hagan RC, Bosenberg MW, Parsons R, Chin L, DePinho RA. Genetic analysis of Pten and Ink4a/Arf interactions in the suppression of tumorigenesis in mice. *Proc Natl Acad Sci U S A* 2002 February 5;99(3):1455-60.
- (97) Lepoutre-Lussey C, Thibault C, Buffet A, Morin A, Badoual C, Benit P, Rustin P, Ottolenghi C, Janin M, Castro-Vega LJ, Trapman J, Gimenez-Roqueplo AP, Favier J. From Nf1 to Sdhb knockout: Successes and failures in the quest for animal models of pheochromocytoma. *Mol Cell Endocrinol* 2016 February 5;421:40-8.

CHAPTER 2

Inactivation of SDH and FH cause loss of 5hmC and increased H3K9me3 in paraganglioma/pheochromocytoma and smooth muscle tumors

Attje S Hoekstra¹, Marieke A de Graaff², Inge H Briaire-de Bruijn², Cor Ras³, Reza Maleki Seifar³, Ivonne van Minderhout⁴, Cees J Cornelisse², Pancras CW Hogendoorn², Martijn H Breuning⁴, Johnny Suijker², Esther Korpershoek⁵, Henricus PM Kunst⁶, Norma Frizzell⁷, Peter Devilee^{1,2}, Jean-Pierre Bayley¹, Judith VMG Bovée²

¹ Department of Human Genetics, Leiden University Medical Center, Leiden, The Netherlands

² Department of Pathology, Leiden University Medical Center, Leiden, The Netherlands

³ Department of Biotechnology, Delft University of Technology, Delft, The Netherlands

⁴ Department of Clinical Genetics, Leiden University Medical Center, Leiden, The Netherlands

⁵ Department of Pathology, Josephine Nefkens Institute, Erasmus Medical Center Rotterdam, Rotterdam, The Netherlands

⁶ Department of Otorhinolaryngology, Head and Neck Surgery, Radboud University Nijmegen Medical Center, Nijmegen, The Netherlands

⁷ Department of Pharmacology, Physiology & Neuroscience, School of Medicine, University of South Carolina, Columbia, SC, USA

Oncotarget. 6 (2015) 38777-88

Abstract

Succinate dehydrogenase (SDH) and fumarate hydratase (FH) are tricarboxylic acid (TCA) cycle enzymes and tumor suppressors. Loss-of-function mutations give rise to hereditary paragangliomas/pheochromocytomas and hereditary leiomyomatosis and renal cell carcinoma. Inactivation of SDH and FH results in an abnormal accumulation of their substrates succinate and fumarate, leading to inhibition of numerous α -ketoglutarate dependent dioxygenases, including histone demethylases and the ten-eleven-translocation (TET) family of 5-methylcytosine (5mC) hydroxylases.

To evaluate the distribution of DNA and histone methylation, we used immunohistochemistry to analyze the expression of 5mC, 5-hydroxymethylcytosine (5hmC), TET1, H3K4me3, H3K9me3, and H3K27me3 on tissue microarrays containing paragangliomas/pheochromocytomas (n = 134) and hereditary and sporadic smooth muscle tumors (n = 56) in comparison to their normal counterparts.

Our results demonstrate distinct loss of 5hmC in tumor cells in SDH- and FH-deficient tumors. Loss of 5hmC in SDH-deficient tumors was associated with nuclear exclusion of TET1, a known regulator of 5hmC levels. Moreover, increased methylation of H3K9me3 occurred predominantly in the chief cell component of SDH mutant tumors, while no changes were seen in H3K4me3 and H3K27me3, data supported by in vitro knockdown of SDH genes. We also show for the first time that FH-deficient smooth muscle tumors exhibit increased H3K9me3 methylation compared to wildtype tumors.

Our findings reveal broadly similar patterns of epigenetic deregulation in both FH- and SDH-deficient tumors, suggesting that defects in genes of the TCA cycle result in common mechanisms of inhibition of histone and DNA demethylases.

Introduction

The tricarboxylic acid (TCA) cycle enzymes isocitrate dehydrogenase (IDH), succinate dehydrogenase (SDH) and fumarate hydratase (FH) are mutated in a subset of human cancers, leading to alterations in cell metabolism. In the TCA cycle, the SDH complex converts succinate to fumarate, while FH catalyzes the hydroxylation of fumarate to L-malate. Germline mutations in *SDHA* (46), *SDHB* (29), *SDHC* (98), *SDHD* (30), and *SDHAF2* (31) cause paraganglioma/pheochromocytoma (PGL/PCC). PGL of the head and neck arise most commonly in the carotid body, a chemoreceptor organ with two predominant cell types: the chief (type I) cells, which represent the neoplastic population in paragangliomas (99), and the surrounding supportive sustentacular (type II) cells. Inactivating germline mutations of *FH* result in hereditary leiomyomatosis and renal cell carcinoma (HLRCC), which is inherited in an autosomal dominant manner (100;101). Leiomyomas, benign smooth muscle tumors predominantly found in the skin and uterus, are the most common tumor type in HLRCC, but papillary type 2 renal cell carcinomas may also occur, although less frequently. Rare germline mutations in *FH* were recently reported in patients with PGL/PCC (88;90;102).

Although the mechanisms by which mutations in metabolic enzymes promote tumor formation are still poorly understood, the stabilization of hypoxia inducible factor (HIF) under conditions of normoxia is the most widely studied mechanism. Inactivation of SDH and FH leads to accumulation of the respective substrates succinate and fumarate, which inhibit α -ketoglutarate (α -KG) dependent HIF prolyl hydroxylases, leading to HIF activation (79;103). Other dioxygenases, including histone demethylases and the TET (ten-eleven translocation) family of 5-methylcytosine (5mC) hydroxylases, are also inhibited by succinate and fumarate accumulation (85;104;105). The JmjC domain-containing histone demethylases and the TET family of DNA hydroxylases play central roles in epigenetic control of genomic information. While the JmjC domain-containing histone demethylases catalyze the oxidation of methyl groups on the lysine residues of histones H3 and H4 (106), TET1 and TET2 are responsible for the oxidation of 5mC to 5-hydroxymethylcytosine (5hmC), a process requiring α -KG and oxygen (107). TET3 is mainly involved in the oxidation of 5mC to 5hmC in zygotic paternal DNA after fertilization (108).

Mutations in *SDH* are also found in gastrointestinal stromal tumors, in addition to the more commonly occurring mutations in *KIT* or *PDGFRA*. In these tumors, *SDH* mutations were shown to be associated with global hypermethylation and loss of 5hmC (109). Furthermore, a PGL/PCC cohort showed a hypermethylation phenotype in *SDH* mutant tumors, reminiscent of the methylation signature of gliomas with *IDH* mutations (88;109).

Enchondromas carrying an *IDH1* mutation also display a hypermethylation profile (110). The common *IDH1* and *IDH2* mutations cause a gain-of-function and confer a neomorphic catalytic activity that allows the synthesis and accumulation of the oncometabolite 2-hydroxyglutaric acid (2HG). Due to the structural similarity to α -KG, 2HG competitively inhibits α -KG-dependent TET and histone demethylase enzyme families (111).

Intriguingly, a study by Letouzé *et al.* (88) included a hypermethylated PGL/PCC subgroup in which the only tumor sample without *SDH* mutations was shown to harbor germline inactivating *FH* mutations. A study in five patients with *FH*-deficient PGL/PCC reported loss of hydroxylation of 5mC in tumor cells (90). This was also seen in *SDH*-deficient PGL/PCC and *IDH* mutant gliomas, suggesting that a common pathophysiological mechanism leads to alterations in DNA methylation.

Furthermore, increased expression of the repressive trimethylation of H3K9 (H3K9me3) and a trend

towards an increase in trimethylation of H3K27 (H3K27me3) was reported in *IDH1* mutant gliomas, while no differences were observed in the active trimethylation of H3K4 (112). To date, DNA and histone methylation profiles have not been reported for *FH*-deficient smooth muscle tumors. In addition, the role of TET1 has not yet been explored in *SDH* mutant PGL/PCC or in *FH*-deficient tumors.

Using immunohistochemistry, we investigated the distribution of 5mC, 5hmC, TET1, and histone methylation in *SDH*-mutant PGL/PCC and in *FH*-deficient smooth muscle tumors in comparison to non-*SDH* or *FH*-mutated PGL/PCC and smooth muscle tumors, respectively. Interestingly, we found a similar pattern of epigenetic deregulation in *FH*-deficient smooth muscle tumors compared to *SDH*-deficient PGL/PCC, both in terms of loss of 5hmC expression and increased trimethylation of H3K9 in tumor cells.

Material and Methods

Tissue samples

Formalin-fixed paraffin-embedded (FFPE) tissue samples of head and neck paragangliomas (PGL), pheochromocytomas (PCC), leiomyomas (LM) and leiomyosarcomas (LMS) were retrieved from the archives of the Department of Pathology. The histological appearances of all cases and controls were reviewed (JVMGB, JPB, PCWH, MAdG). For all PGL/PCC tumors and normal carotid bodies, the diagnosis was confirmed by routine S-100 immunohistochemical staining detecting sustentacular cells and chromogranin A detecting chief cells (Supplemental Figure 1A, B). In the smooth muscle tumors, at least one of the smooth muscle markers h-caldesmon or desmin was positive. PGL/PCC tumors were benign. The tissue samples were arrayed in tissue microarray (TMA) format resulting in a TMA including 100 PGL and 17 PCC samples in triplicate as previously described (113). The TMAs were constructed using 0.5mm diameter punch (Beecher Instruments, Silver Spring, MD) to transfer tumor punches to the recipient block. Cores from human adrenal medulla, adrenal cortex, kidney, and liver were included for control and orientation purposes. TMAs with LM and LMS tumor samples were constructed from a panel of FFPE tumors including 7 uterine LM and 44 LMS as described previously (114). Cores from colon, liver, placenta, prostate, skin, and tonsil were included for control and orientation purposes. As normal controls, we used whole sections of 6 normal carotid bodies, obtained from patients at autopsy within 24 hours after death, and 13 whole sections of normal smooth muscle of uterus, carotid artery, oesophagus, bowel wall, and aorta. In addition, we included whole sections from 9 *SDHAF2* PGL tumors obtained from Radboud UMC, Nijmegen, Netherlands, 8 *VHL* (Von Hippel-Lindau) PCC tumors obtained from Erasmus MC, Rotterdam, Netherlands, 2 uterine LM, and 2 cutaneous LM from two patients; 1 HLRCC patient with a germline *FH* mutation (115), and 1 suspected HLRCC patient (based on clinical data) with a *FH* mutation as detected by 2SC staining. The mutation status for most tumors was known (Table 1) and nonfamilial tumors with an unknown mutation status were excluded for analysis. All samples were handled according to the Dutch code of proper secondary use of human material approved by the Dutch society of pathology (www.federa.org), and samples were handled in a coded (pseudonymised) fashion according to procedures agreed with the LUMC ethical board.

Immunohistochemistry and scoring

The primary antibodies used in immunohistochemistry analysis are described in supplemental Table 1, with tonsil, colon and liver acting as positive controls. After antigen retrieval by microwave heating in Tris-EDTA buffer, pH 9.0 or citrate buffer, pH 6.0 at 100°C for 10 min, sections were blocked for 30 min with 10% goat serum and incubated overnight at 4°C with primary antibodies. Signal detection was performed with Envision+ (DAKO K3468, Agilent Technologies, Belgium) and the chromogen 3,3'-diaminobenzidine according to manufacturer's instructions.

The results of the immunohistochemical labeling were scored semi-quantitatively: the intensity of labeling was assessed on a scale of 0 to 3 (0 = none; 1 = weak; 2 = moderate; 3 = strong), and the percentage of positive cells was assessed on a scale of 0 to 4 (0 = 0% positive; 1 = 1-24% positive; 2 = 25-49% positive; 3 = 50-74%; 4 = 75-100% positive cells). The two scores were then added to find a total sum score ranging from 0-7, as described previously (116). Chief cells and sustentacular cells were scored separately, if possible. For TET1, only subcellular localization was scored, as described (117). In addition, TET1 expression was only scored in chief cells in PGL/PCC tumors.

A tumor was scored negative only when a positive internal control was present. Tumor samples were excluded from the analysis when substantial tissue was lost during sectioning. The scoring was performed independently by two observers blinded for clinicopathological data (ASH and JVMGB) and discrepancies were discussed. Immunohistochemistry images were taken using a Leica DFC550 camera with LAS software version 4.5 (Heerbrugg, Switzerland).

Cell culture

HEK293 cells were obtained from DSMZ (ACC 305, Braunschweig, Germany) and grown in Dulbecco's Modified Eagle Medium (DMEM, Life Technologies, Paisley, UK) supplemented with 10% fetal bovine serum (Life Technologies) and penicillin/streptomycin (Life Technologies). HEK293 cells were maintained at 37°C in a humidified atmosphere of 5% CO₂ in air.

Lentiviral vector-based silencing of SDHD, SDHB and SDHAF2

To silence *SDHD*, *SDHB* and *SDHAF2*, three validated MISSION® shRNA constructs (TRCN0000231553 -236398, -159253 respectively) targeting human *SDHD* (NM_003002.1), *SDHB* (NM_003000.2), and *SDHAF2* (NM_017841.2) (Sigma Aldrich, St. Louis, USA) or scramble shRNA encoding plasmid (SHC002 Sigma Aldrich) were used to produce infectious virus particles (LV). To evaluate the transduction efficiency, the MISSION TurboGFP control plasmid (SHC003 Sigma Aldrich) was used. HEK293T cells were transfected with the shRNA constructs together with helper plasmids encoding HIV-1 gag-pol, HIV-1 rev, and the VSV-G envelope as described (118). Viral supernatants were added to HEK293 cells in fresh medium supplemented with 8 µg/ml Polybrene (Sigma Aldrich) and the cells were incubated overnight. The next day, the medium was replaced with fresh medium. Transduction efficiency was analysed 3 to 6 days post transduction by evaluating GFP labelled cells. Experiments were performed 2-3 and 4-5 weeks after transduction of HEK293 cells with shRNAs.

Western blotting

For preparation of total protein extracts, cells were extracted in RIPA buffer (Sigma Aldrich) supplemented with "complete" protease inhibitor cocktail (Roche, Germany). Total histone fractions were prepared using sodium dodecyl sulfate (sds) buffer containing 1% SDS, 10mM EDTA, and 10mM Tris pH 7.4, supplemented with "complete" protease inhibitor cocktail (Roche) and phosSTOP (Roche). The concentration of protein was determined by bicinchoninic acid protein assay (Thermo

Scientific Pierce, Rockford, USA). Equal amounts of protein (30 µg) were separated by SDS-PAGE and transferred onto polyvinylidene fluoride (PVDF) membranes (Millipore). After blocking with 5% (w/v) non-fat milk powder, membranes were incubated overnight at 4 °C with the following antibodies: SDHB 1:500 (Sigma Aldrich), α-tubulin 1:2000 (Sigma Aldrich), H3 and H3K9me3 1:2000 (Abcam, Cambridge, UK), H3K4me3 1:1000 and H3K27me3 1:2000 (Millipore, Billerica, USA). Visualization and quantification was carried out with the LI-COR Odyssey® scanner (Bad Homburg, Germany) and software (LI-COR Biosciences).

Succinate and fumarate quantification by LC-MS/MS

Sample preparation for biochemical analysis of HEK293 cells with knockdown of *SDHD*, *SDHB* or *SDHAF2* and scrambled cells was performed according to (119), using ice cold 90% MeOH: CHCl₃ as extraction solvent containing ¹³C-labeled isotopes of nucleotides as internal standards. Dried samples were reconstituted in 100µl H₂O for compatibility with the liquid chromatography-tandem mass spectrometry (LC-MS/MS) method (120) and the concentrations of succinate and fumarate were determined by anion-exchange LC-MS/MS [44].

Statistical analysis

IBM SPSS Statistics 20.0 for Windows software package (SPSS, Armonk, NY: IBM Corp) was used to analyze the results. The statistical significance of differences between 2 groups was assessed by the Mann-Whitney U test, and the 1-way analysis of variance test was used for comparisons of more than 2 groups. Statistical significance was determined by Pearson chi-square test to evaluate TET1 correlation with loss of 5hmC. P<0.05 was considered statistically significant.

Results

Low prevalence of FH mutations in smooth muscle tumors and absence in PGL

To estimate the prevalence of *FH* mutations in smooth muscle tumors and to exclude *FH* mutations in *SDH* wildtype PGL, we performed immunohistochemistry for 2-succinocysteine (2SC), a robust biomarker for *FH* mutations (90;121-123). Of all hereditary and sporadic smooth muscle tumors (n=56), 1 uterine LM and 1 cutaneous LM from a patient with suspected HLRCC, and 2 LMS tumors were positive for 2SC, indicating the presence of an *FH* mutation (Table 1). Of the LM/leiomyosarcoma (LMS) tumors with an unknown *FH* mutation status, 1 uterine LM and 1 cutaneous LM (from a patient with suspected HLRCC), and 2 LMS tumors were positive for 2SC (Table 1). All PGL/PCC tumors were negative for 2SC. In addition, negative SDHB staining and positive SDHA staining correlated exactly with the known mutation status in all *SDHB*, *SDHC*, *SDHD* and *SDHAF2* mutant tumors.

Table 1. Genomic characteristics of tumor specimens

Mutation status	Paraganglioma (n=109)	Pheochromocytoma (n=25)	Uterine Leiomyoma (n=9)	Cutaneous Leiomyoma (n=3)	Leiomyosarcoma (n=44)
SDHB	2				
SDHC	1				
SDHD	59	1			
SDHAF2	12				
VHL		9			
NF1		2			
MEN1		1			
RET		3			
Nonfamilial ¹	35	9	7	1	42
FH	0	0	2	2	2*

Mutation status is indicated for each tumor sample, in absolute numbers of each group size. Abbreviations: SDH, succinate dehydrogenase; VHL, von hippel landau; NF1, neurofibromatosis type 1; MEN1, multiple endocrine neoplasia type 1; RET, rearranged during transfection (mutation gives rise to multiple endocrine neoplasia type 2); FH, fumarate hydratase.¹No *SDHA/B/C/D/AF2/VHL* or *FH* mutation. **FH* mutation detected by 2SC staining.

Loss of 5hmC in SDH and FH mutant tumors

Since elevated intracellular succinate and fumarate competitively inhibit TET-catalyzed oxidation of 5mC to 5hmC (85), we analyzed expression of 5hmC and 5mC in *SDH/FH*-deficient and non-*SDH/FH* mutant tumors. In PGL/PCC, the expression of 5hmC differed markedly between chief cells and sustentacular cells within the same tumor (Figure 1A,C,D). Of the *SDH* mutant PGLs, 95% showed no or low expression (score 0-2) of 5hmC in chief cells, whereas 90% of the sustentacular cells in the same tumors showed high expression levels (score 4-7). When compared with chief cells in normal carotid bodies (Figure 1A, B), the chief cells in the tumor showed significantly lower expression of 5hmC ($p=0.0001$). Similarly, 5hmC was significantly lower or even absent in *FH*-deficient tumors compared to normal smooth muscle tissue and *FH* wildtype tumors (Figure 1A, F-G) ($p=0.0001$). In PCC, the difference between tumor cells and sustentacular cells was less pronounced, but significant ($p=0.001$) (Figure 1E). Likewise, the ratio of 5hmC expression in the chief cells and the sustentacular cells per tumor sample differed significantly between *SDH*-deficient tumors, normal carotid bodies, and non-*SDH* mutant tumors (Supplemental Fig. 3). We also analyzed 5mC, which is present at up to 40-fold greater levels in cells than 5hmC (124). Perhaps unsurprisingly, the large shifts seen in the small 5hmC pool were not reflected in a detectable shift in the far larger 5mC pool, and 5mC was found to be highly expressed in all *SDH*- and *FH*-deficient tumors and controls (Figure 2A,D).

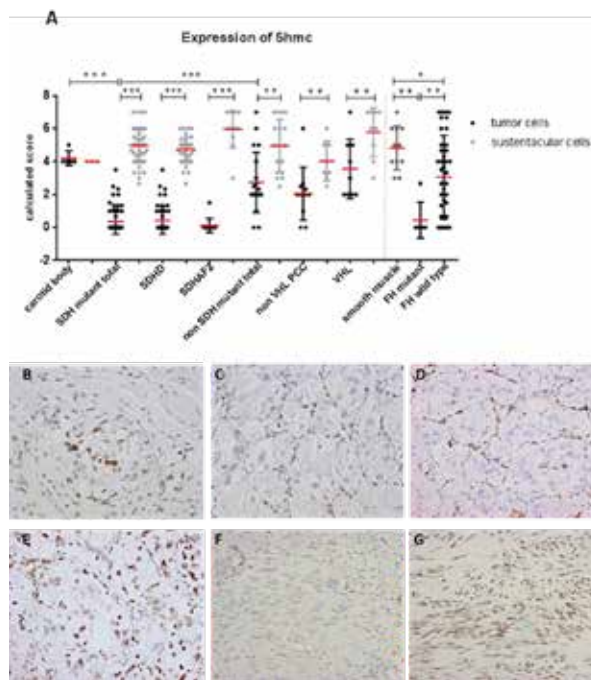


Figure 1. Loss of 5hmC expression in tumor cells of *SDH* and *FH* mutant tumors. (A) Dot plot presenting results of immunohistochemical 5hmC expression in tissues. Data are represented as calculated mean score \pm standard deviation. * $p < 0.05$; ** $p < 0.001$; *** $p < 0.0001$. (B) Micrographs of representative staining (40x magnification) show strong immunostaining of sustentacular cell nuclei in normal carotid body and in (C-E) all *SDH*-related tumor types, whereas tumor cell staining (chief cell) was weaker or absent in *SDH*-mutated tumors compared to (E) *VHL* mutant PCC. (F) Loss of 5hmC in tumor cells of *FH* mutant compared to (G) *FH* wildtype.

Nuclear exclusion of TET1 is associated with loss of 5hmC in SDH mutant tumors

Since TET1 is responsible for the oxidation of 5mC to 5hmC and gliomas with loss of 5hmC expression have been reported to show nuclear exclusion of TET1 expression (117), we investigated this correlation in *SDH* and *FH* mutant tumors. Indeed, absence of nuclear staining for TET1 was more common in *SDH* mutant PGL/PCC (38 of 52, 73%) compared to either non-*SDH* mutated PGL/PCC (5/19, 26%) ($p = 0.002$) or normal carotid bodies (1/5, 20%) ($p = 0.03$) (Figure 2B,E). *SDH*-deficient tumors with cytoplasmic TET1 expression more frequently showed loss of 5hmC (Figure 2C, $p = 0.01$). Absence of nuclear staining was also more frequent in *FH*-deficient smooth muscle tumors (2 of 5, 40%), compared to *FH* wildtype tumors (9/45, 20%) or smooth muscle tissue (0/8). However, this difference was not significant ($p = 0.5$) and was not correlated to loss of 5hmC expression ($p = 1.0$).

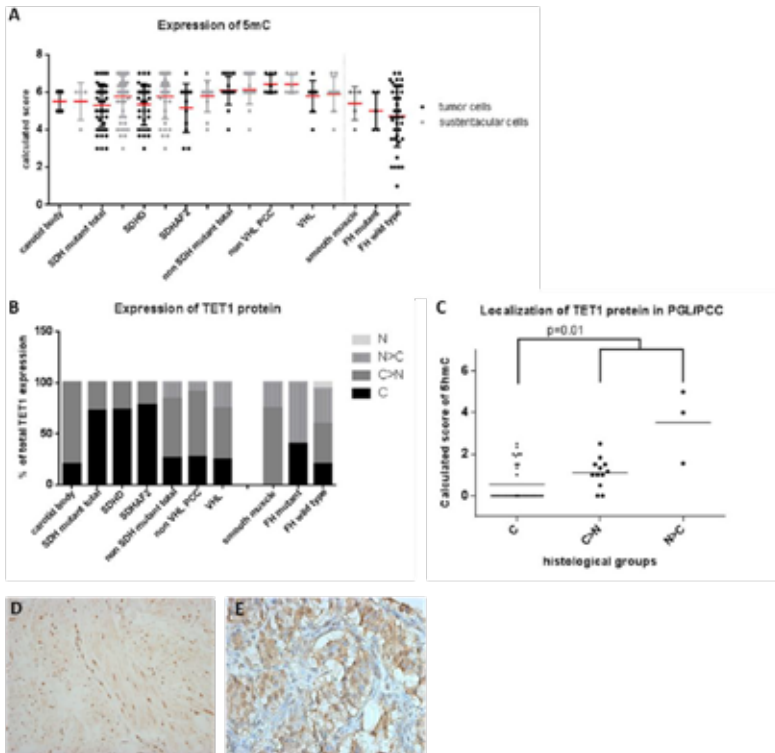


Figure 2. 5mC and TET1 protein expression in *SDH* and *FH* mutant tumors. (A) Dot plot presenting results of immunohistochemical 5mC expression demonstrating a high expression in all tumors. Data are represented as calculated mean score \pm standard deviation. (B) TET1 expression and its subcellular localization, demonstrating nuclear exclusion in *SDHx* related tumors (C) which is associated with low 5hmC expression levels ($p=0.01$). (D) Micrographs of representative staining (40x magnification) of TET1 are shown for *FH* mutant LM with predominantly nuclear staining and (E) *SDHD* mutant tumor with cytoplasmic staining. Subcellular localization of the protein: C, exclusively cytoplasmic; C > N, predominantly cytoplasmic; N, exclusively nuclear; N > C, predominantly nuclear.

Increased H3K9me3 in *SDH* and *FH* mutant tumors

Succinate and fumarate have been shown to directly inhibit α -KG dependent histone demethylase activity in a manner similar to 2HG, resulting in increased methylation of various lysine residues of histone H3 (85;112). We therefore evaluated H3K4me3, H3K9me3, and H3K27me3 expression in *SDH* and *FH* mutant tumors by immunohistochemistry. Expression of trimethylated H3K4 was significantly increased in chief cells of *SDH* mutant tumors compared to sustentacular cells (Figure 3A,B) ($p=0.01$). However, expression levels of H3K4me3 were also high in chief cells of normal carotid bodies and in non-*SDH* mutant tumors. No differences were seen in H3K4me3 expression between smooth muscle cells, *FH*-deficient, and *FH* wildtype tumors (Figure 3A,C).

The expression of H3K9me3 was significantly increased in chief cells compared to sustentacular cells in *SDH*-deficient tumors ($p=0.0001$), but again, this was not significantly different from the

expression in normal carotid bodies or non-*SDH* mutant tumors (Figure 3D,F). However, when we plotted the ratio of H3K9me3 expression per tumor sample by dividing the expression in the chief cells by the expression in the sustentacular cells within the same tumor, thus co-opting sustentacular cells as an inter-tumor control, expression levels of H3K9me3 were significantly increased in *SDH*-deficient tumors compared to non-*SDH* mutant tumors (Figure 3E) ($p=0.01$). Regarding PCCs, H3K4me3 and H3K9me3 levels were increased in *VHL*-deficient tumors compared to non-*VHL* mutant PCC. Interestingly, *FH*-deficient smooth muscle tumors showed significantly elevated levels of H3K9me3 compared to smooth muscle cells ($p=0.027$) and *FH* wildtype tumors (Figure 3D,G) ($p=0.004$). In contrast, no expression differences were seen for H3K27me3, with high expression in all tumors and controls, regardless of the manner of analysis (Figure 3H).

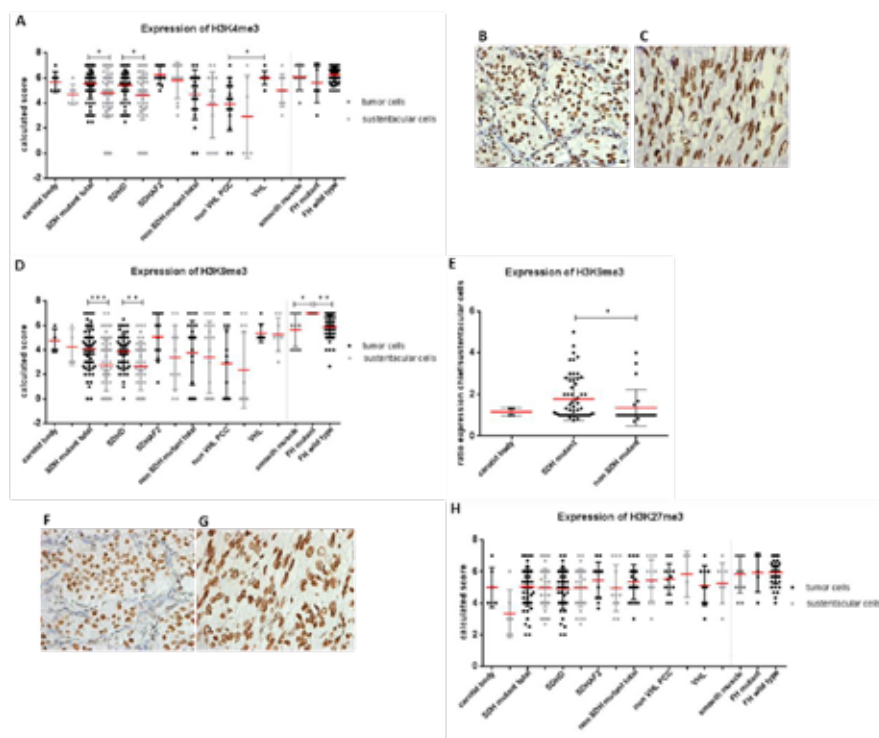


Figure 3. Expression of histone markers in *SDH* and *FH* mutant tumors. (A) Dot plot presenting results of immunohistochemical H3K4me3 levels in *SDHx* and *FH* mutant tumors. Micrographs of representative staining (40x magnification) are shown for (B) *SDHD* mutant and (C) *FH* mutant tumors. (D) H3K9me3 expression levels are significantly increased in chief cells compared to sustentacular cells in *SDH* mutant tumors and in tumor cells of *FH*-deficient tumors compared to smooth muscle cells and *FH* wildtype tumors. (E) Increased ratio of H3K9me3 expression observed in *SDH* mutant compared to non-*SDH* mutant tumors. Micrographs of representative staining (40x magnification) are shown for (F) *SDHD* mutant and (G) *FH* mutant tumors. (H) No differences observed in H3K27me3 expression. Data are represented as calculated mean score ± standard deviation. * $p < 0.05$; ** $p < 0.001$; *** $p < 0.0001$.

Increased H3K9me3 upon inhibition of SDHD, SDHB or SDHAF2 in vitro

In order to establish a direct causal link between histone methylation and loss of SDH, we derived subclones of HEK293 cells with stable knockdown of *SDHD*, *SDHB* and *SDHAF2*. Stable knockdown was confirmed by RT-PCR analysis of RNA expression levels and by immunoblotting, with decreased SDHB protein levels under all three conditions taken as a marker for *SDH* deficiency (125) (Figure 4A). Analysis of nuclear histones in these subclones revealed an increase in steady-state levels of H3K9me3 upon silencing of *SDHD* (by 1.7-fold), *SDHB* (by 1.7-fold), and *SDHAF2* (by 1.9-fold) (Figure 4B). Furthermore, silencing of *SDHD*, *SDHB*, and *SDHAF2* did not lead to increased trimethylation of H3K4 or H3K27 in HEK293 cells. To further validate the level of *SDHD*, *SDHB* and *SDHAF2* silencing in HEK293 cells, succinate and fumarate levels were quantified by LC-MS/MS. Succinate levels were increased in cells with knockdown of *SDHD*, *SDHB* or *SDHAF2* compared to scrambled cells. Likewise, the succinate-to-fumarate ratio was increased in the silenced cells compared to scrambled cells (Figure 4C), results which accord with those reported by Lendvai *et al.* (126).

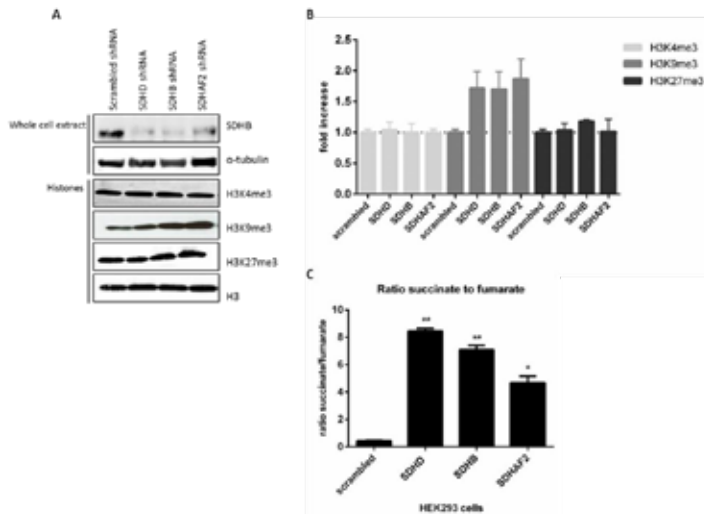


Figure 4. Increased H3K9me3 protein by succinate dehydrogenase gene inhibition. (A) HEK293 cells with stable knockdown of *SDHD*, *SDHB* and *SDHAF2* demonstrate decreased SDHB protein levels in total protein extract. α -Tubulin was used as a loading control. Histone lysine methylation levels were assessed in total histone fractions by western blotting with specific antibodies. Total H3 was used as a loading control. (B) Quantification of western blotting demonstrates only H3K9me3 levels were increased by silencing of *SDHD* (by 1.72-fold), *SDHB* (by 1.7-fold) and *SDHAF2* (by 1.9-fold) in HEK293 cells compared to scrambled shRNA. (C) HEK293 cells with stable knockdown of *SDHD*, *SDHB* and *SDHAF2* demonstrate a significant increased ratio of succinate to fumarate compared to scrambled cells, measured by LC-MS/MS. * $p < 0.05$; ** $p < 0.001$.

Discussion

Loss-of-function mutations in *SDH* and *FH* leading to the accumulation of succinate and fumarate indirectly act as inhibitors of α -KG dependent dioxygenases. Here, we demonstrate that *SDH* and *FH* mutations can inhibit DNA and histone demethylases, leading to loss of 5hmC and increased H3K9me3 levels. We convincingly showed loss of 5hmC in chief cells in almost all (95%) *SDH*-

deficient PGL/PCC. Moreover, *FH*-deficient smooth muscle tumors (83%) showed loss of 5hmC expression in tumor cells as compared to normal smooth muscle or *FH* wildtype smooth muscle tumors. Loss of 5hmC in *SDH*-deficient tumors correlated significantly with nuclear exclusion of TET1 protein.

Our results agree with findings reported by Müller *et al.* (117), who demonstrated that nuclear exclusion of TET1 is associated with loss of 5hmC in gliomas. In contrast, *FH*-deficient smooth muscle tumors showed nuclear exclusion of TET1 in only 40% of cases and exclusion was not correlated with loss of 5hmC. Given that that oxidation of 5mC to 5hmC is considered to be a nuclear event, these results suggests TET1 is not the main player in the hydroxylation of 5mC in *FH*-deficient smooth muscle tumors. Thus far, little information is available on post-translational modifications of TET enzymes that may determine their subcellular localization. TET1 has three nuclear localization signals, suggesting a mainly nuclear localization of the protein. In addition, Xiao *et al.* (85) showed in HEK293 cells that stable knockdown of *SDHA/B* or *FH* reduced both TET1- and TET2-induced 5hmC levels as compared to control cells with normal *SDH* and *FH* expression. Therefore, in addition to TET1, the TET2 protein may also be associated with loss of 5hmC in *SDH*- and *FH*-deficient tumors, especially in *FH*-deficient HLRCC. Future studies should explore the role of TET2, principally in a much larger cohort of *FH*-deficient tumors than presently available. Also of note, we confirmed that 2-succinocysteine (2SC) immunohistochemistry is a robust biomarker for *FH* mutation status, consistent with earlier reports (121;123). In addition to the correct identification of two tumors from a HLRCC patient with a previously determined *FH* mutation, two sporadic LMS tumors were also positive for 2SC. However, insufficient paraffin-embedded tissue was available to allow *FH* germline mutation analysis and therefore the mutation might be somatic. Our results are consistent with earlier reports of very low *FH* mutation rates in LMS, including those of Kiuru *et al.* (127) who found germline *FH* mutations in 1–2% of apparently sporadic early-onset LMS, and Barker *et al.* (128), who observed no *FH* mutations in 26 sporadic LMS.

Besides the inhibition of the TET family of DNA hydroxylases, accumulation of succinate and fumarate negatively affects the enzyme activity of histone demethylases (85;104;105;111). We found an increased expression of H3K4me3 and H3K9me3 in chief cells compared to sustentacular cells in *SDH*-deficient tumors. However, we also found that H3K4me3 and H3K9me3 were highly expressed in the chief cell compartment of normal carotid bodies. Previous studies have used *SDH* wildtype PGL/PCC or adrenal glands with low expression levels of different histone methylation markers as a control group (88;109). This might explain differences with earlier results, since in our study chief cell expression levels of H3K4me3 and H3K9me3 are higher in *SDH*-deficient tumors compared to non-*SDH* mutant tumors, but did not differ significantly from the levels present in normal carotid bodies.

Regarding PCCs, we separated tumors into *VHL* mutant and non-mutant groups, as Letouzé *et al.* previously reported three stable DNA methylation clusters for PGLs and PCCs, including *SDHx* tumors, *VHL* tumors, and *NF1-RET*. The group differences in DNA and/or histone methylation suggested in this previous study were supported by our data, which showed increased H3K4me3 and H3K9me3 levels in *VHL* mutant PCC tumor cells compared to non *VHL* mutant PCC. This finding lends support to the idea that changes in histone methylation may not be due to a direct effect of succinate accumulation, but may relate to the stabilization of HIF1, as HIF1 can directly regulate the activity of some JmjC domain-containing histone demethylases (129).

Of note, our study supports the concept of the chief cell compartment as the sole source of tumor cells in PGL, in agreement with previous reports (7;104), and also underlines the curious heterogeneity of cells found in these tumors. Plotting sustentacular-chief cell ratios of H3K9me3 expression per tumor sample showed that expression levels of H3K9me3 were significantly increased in *SDH*-deficient tumors compared to non-*SDH* mutant tumors. This finding suggests that intra-tumor heterogeneity can mask differences in H3K9me3 levels. Furthermore, the involvement of SDH in modulating H3K9me3 levels was confirmed by *in vitro* silencing of *SDHB*, *SDHD* or *SDHAF2*, supporting the immunohistochemistry results in tumors. Despite small numbers, our results showed significantly elevated H3K9me3 levels in *FH*-deficient smooth muscle tumors, supporting the hypothesis that fumarate inhibits histone demethylation.

In contrast to H3K9me3, neither *SDH* nor *FH* mutant tumors displayed elevated H3K27me3 expression levels compared to control groups. These data contrast with other reports in which *SDH* mutant tumors reportedly showed an increased expression of H3K27me3 compared to *SDH* wildtype tumors (88). A possible explanation for this difference might be the inclusion of predominantly *SDHB* mutated tumors in the earlier study, whereas our cohort consisted of mostly *SDHD* and *SDHAF2*-related tumors, which are known to have similar gene-expression profiles (130). Letouzé *et al.* (88) reported a significantly higher mean level of hypermethylation in *SDHB*-mutated PGL/PCC compared to other SDH PGL/PCC, which might explain the difference in outcomes.

Overall, we found a similar pattern of epigenetic deregulation in *FH*-deficient smooth muscle tumors and *SDH*-deficient HPGL, with loss of 5hmC proving a robust marker of deregulated DNA methylation. Like DNA methylation, H3K9me3 is often associated with regulatory elements of transcriptionally repressed genes and constitutive heterochromatic regions of the genome, and was also increased in both *SDH*- and *FH*-deficient tumors. Although not directly targetable, loss of SDH and FH do afford clinical opportunities such as synthetic lethal interactions. The DNA methyltransferase inhibitors 5-azacytidine and decitabine are of particular interest, where 5-azacytidine has been shown to reduce the proliferative index in an *in vivo* IDH1 glioma model (131) and decitabine repressed the migration capacities of *Sdhb*^{-/-} cells (88). This could lead to clinical opportunities of epigenetic targeting in tumors caused by TCA cycle defects.

References

- (1) Burnichon N, Briere JJ, Libe R, Vescovo L, Riviere J, Tissier F, Jouanno E, Jeunemaitre X, Benit P, Tzagoloff A, Rustin P, Bertherat J, Favier J, Gimenez-Roqueplo AP. SDHA is a tumor suppressor gene causing paraganglioma. *Hum Mol Genet* 2010 August 1;19(15):3011-20.
- (2) Astuti D, Latif F, Dallol A, Dahia PL, Douglas F, George E, Skoldberg F, Husebye ES, Eng C, Maher ER. Gene mutations in the succinate dehydrogenase subunit SDHB cause susceptibility to familial pheochromocytoma and to familial paraganglioma. *Am J Hum Genet* 2001 July;69(1):49-54.
- (3) Niemann S, Muller U. Mutations in SDHC cause autosomal dominant paraganglioma, type 3. *Nature Genetics* 2000 November;26(3):268-70.
- (4) Baysal BE, Ferrell RE, Willett-Brozick JE, Lawrence EC, Myssiorek D, Bosch A, van der MA, Taschner PE, Rubinstein WS, Myers EN, Richard CW, III, Cornelisse CJ, Devilee P, Devlin B. Mutations in SDHD, a mitochondrial complex II gene, in hereditary paraganglioma. *Science* 2000 February 4;287(5454):848-51.
- (5) Hao HX, Khalimonchuk O, Schraders M, Dephoure N, Bayley JP, Kunst H, Devilee P, Cremers CW, Schiffman JD, Bentz BG, Gygi SP, Winge DR, Kremer H, Rutter J. SDH5, a gene required for flavination of succinate dehydrogenase, is mutated in paraganglioma. *Science* 2009 August 28;325(5944):1139-42.
- (6) van Schothorst EM, Beekman M, Torremans P, Kuipers-Dijkshoorn NJ, Wessels HW, Bardoel AF, Van Der Mey AG, van der Vijver MJ, van Ommen GJ, Devilee P, Cornelisse CJ. Paragangliomas of the head and neck region show complete loss of heterozygosity at 11q22-q23 in chief cells and the flow-sorted DNA aneuploid fraction. *Hum Pathol* 1998 October;29(10):1045-9.
- (7) Tomlinson IP, Alam NA, Rowan AJ, Barclay E, Jaeger EE, Kelsell D, Leigh I, Gorman P, Lamlum H, Rahman S, Roylance RR, Olpin S, Bevan S, Barker K, Hearle N, Houlston RS, Kiuru M, Lehtonen R, Karhu A, Vilkki S, Laiho P, Eklund C, Vierimaa O, Aittomaki K, Hietala M et al. Germline mutations in FH predispose to dominantly inherited uterine fibroids, skin leiomyomata and papillary renal cell cancer. *Nat Genet* 2002 April;30(4):406-10.
- (8) Launonen V, Vierimaa O, Kiuru M, Isola J, Roth S, Pukkala E, Sistonen P, Herva R, Aaltonen LA. Inherited susceptibility to uterine leiomyomas and renal cell cancer. *Proc Natl Acad Sci U S A* 2001 March 13;98(6):3387-92.
- (9) Castro-Vega LJ, Buffet A, De Cubas AA, Cascon A, Menara M, Khalifa E, Amar L, Azriel S, Bourdeau I, Chabre O, Curras-Freixes M, Franco-Vidal V, Guillaud-Bataille M, Simian C, Morin A, Leton R, Gomez-Grana A, Pollard PJ, Rustin P, Robledo M, Favier J, Gimenez-Roqueplo AP. Germline mutations in FH confer predisposition to malignant pheochromocytomas and paragangliomas. *Hum Mol Genet* 2014 May 1;23(9):2440-6.
- (10) Clark GR, Sciacovelli M, Gaude E, Walsh DM, Kirby G, Simpson MA, Trembath RC, Berg JN, Woodward ER, Kinning E, Morrison PJ, Frezza C, Maher ER. Germline FH mutations presenting with pheochromocytoma. *J Clin Endocrinol Metab* 2014 October;99(10):E2046-E2050.
- (11) Letouze E, Martinelli C, Loriot C, Burnichon N, Abermil N, Ottolenghi C, Janin M, Menara M, Nguyen AT, Benit P, Buffet A, Marcaillou C, Bertherat J, Amar L, Rustin P, De RA, Gimenez-Roqueplo AP, Favier J. SDH mutations establish a hypermethylator phenotype in paraganglioma. *Cancer Cell* 2013 June 10;23(6):739-52.
- (12) Pollard PJ, Briere JJ, Alam NA, Barwell J, Barclay E, Wortham NC, Hunt T, Mitchell M, Olpin S, Moat SJ, Hargreaves IP, Heales SJ, Chung YL, Griffiths JR, Dalgleish A, McGrath JA, Gleeson MJ, Hodgson SV, Poulson R, Rustin P, Tomlinson IP. Accumulation of Krebs cycle intermediates and over-expression of HIF1alpha in tumours which result from germline FH and SDH mutations. *Hum Mol Genet* 2005 August 1;14(15):2231-9.
- (13) Selak MA, Armour SM, MacKenzie ED, Boulahbel H, Watson DG, Mansfield KD, Pan Y, Simon MC, Thompson CB, Gottlieb E. Succinate links TCA cycle dysfunction to oncogenesis by inhibiting HIF-alpha prolyl hydroxylase. *Cancer Cell* 2005 January;7(1):77-85.
- (14) Cervera AM, Bayley JP, Devilee P, McCreath KJ. Inhibition of succinate dehydrogenase dysregulates histone modification in mammalian cells. *Mol Cancer* 2009;8:89.
- (15) Smith EH, Janknecht R, Maher LJ, III. Succinate inhibition of alpha-ketoglutarate-dependent enzymes in a yeast model of paraganglioma. *Hum Mol Genet* 2007 December 15;16(24):3136-48.
- (16) Xiao M, Yang H, Xu W, Ma S, Lin H, Zhu H, Liu L, Liu Y, Yang C, Xu Y, Zhao S, Ye D, Xiong Y, Guan KL. Inhibition of alpha-KG-dependent histone and DNA demethylases by fumarate and succinate that are

- accumulated in mutations of FH and SDH tumor suppressors. *Genes Dev* 2012 June 15;26(12):1326-38.
- (17) Tsukada Y, Fang J, Erdjument-Bromage H, Warren ME, Borchers CH, Tempst P, Zhang Y. Histone demethylation by a family of JmjC domain-containing proteins. *Nature* 2006 February 16;439(7078):811-6.
 - (18) Tahiliani M, Koh KP, Shen Y, Pastor WA, Bandukwala H, Brudno Y, Agarwal S, Iyer LM, Liu DR, Aravind L, Rao A. Conversion of 5-methylcytosine to 5-hydroxymethylcytosine in mammalian DNA by MLL partner TET1. *Science* 2009 May 15;324(5929):930-5.
 - (19) Gu TP, Guo F, Yang H, Wu HP, Xu GF, Liu W, Xie ZG, Shi L, He X, Jin SG, Iqbal K, Shi YG, Deng Z, Szabo PE, Pfeifer GP, Li J, Xu GL. The role of Tet3 DNA dioxygenase in epigenetic reprogramming by oocytes. *Nature* 2011 September 29;477(7366):606-10.
 - (20) Killian JK, Kim SY, Miettinen M, Smith C, Merino M, Tsokos M, Quezado M, Smith WI, Jr., Jahromi MS, Xekouki P, Szarek E, Walker RL, Lasota J, Raffeld M, Klotzle B, Wang Z, Jones L, Zhu Y, Wang Y, Waterfall JJ, O'Sullivan MJ, Bibikova M, Pacak K, Stratakis C, Janeway KA et al. Succinate dehydrogenase mutation underlies global epigenomic divergence in gastrointestinal stromal tumor. *Cancer Discov* 2013 June;3(6):648-57.
 - (21) Pansuriya TC, van ER, d'Adamo P, van Ruler MA, Kuijjer ML, Oosting J, Cleton-Jansen AM, van Oosterwijk JG, Verbeke SL, Meijer D, van WT, Nord KH, Sangiorgi L, Toker B, Liegl-Atzwanger B, San-Julian M, Sciot R, Limaye N, Kindblom LG, Daugaard S, Godfraind C, Boon LM, Vikkula M, Kurek KC, Szuhai K et al. Somatic mosaic IDH1 and IDH2 mutations are associated with enchondroma and spindle cell hemangioma in Ollier disease and Maffucci syndrome. *Nat Genet* 2011 December;43(12):1256-61.
 - (22) Xu W, Yang H, Liu Y, Yang Y, Wang P, Kim SH, Ito S, Yang C, Wang P, Xiao MT, Liu LX, Jiang WQ, Liu J, Zhang JY, Wang B, Frye S, Zhang Y, Xu YH, Lei QY, Guan KL, Zhao SM, Xiong Y. Oncometabolite 2-hydroxyglutarate is a competitive inhibitor of alpha-ketoglutarate-dependent dioxygenases. *Cancer Cell* 2011 January 18;19(1):17-30.
 - (23) Lu C, Ward PS, Kapoor GS, Rohle D, Turcan S, Abdel-Wahab O, Edwards CR, Khanin R, Figueroa ME, Melnick A, Wellen KE, O'Rourke DM, Berger SL, Chan TA, Levine RL, Mellinghoff IK, Thompson CB. IDH mutation impairs histone demethylation and results in a block to cell differentiation. *Nature* 2012 March 22;483(7390):474-8.
 - (24) Bardella C, El-Bahrawy M, Frizzell N, Adam J, Ternette N, Hatipoglu E, Howarth K, O'Flaherty L, Roberts I, Turner G, Taylor J, Giaslakiotis K, Macaulay VM, Harris AL, Chandra A, Lehtonen HJ, Launonen V, Aaltonen LA, Pugh CW, Mihai R, Trudgian D, Kessler B, Baynes JW, Ratcliffe PJ, Tomlinson IP et al. Aberrant succination of proteins in fumarate hydratase-deficient mice and HLRCC patients is a robust biomarker of mutation status. *J Pathol* 2011 September;225(1):4-11.
 - (25) Chen YB, Brannon AR, Toubaji A, Dudas ME, Won HH, Al-Ahmadie HA, Fine SW, Gopalan A, Frizzell N, Voss MH, Russo P, Berger MF, Tickoo SK, Reuter VE. Hereditary leiomyomatosis and renal cell carcinoma syndrome-associated renal cancer: recognition of the syndrome by pathologic features and the utility of detecting aberrant succination by immunohistochemistry. *Am J Surg Pathol* 2014 May;38(5):627-37.
 - (26) Ternette N, Yang M, Laroyia M, Kitagawa M, O'Flaherty L, Wolhuter K, Igarashi K, Saito K, Kato K, Fischer R, Berquand A, Kessler BM, Lappin T, Frizzell N, Soga T, Adam J, Pollard PJ. Inhibition of mitochondrial aconitase by succination in fumarate hydratase deficiency. *Cell Rep* 2013 March 28;3(3):689-700.
 - (27) Globisch D, Munzel M, Muller M, Michalakos S, Wagner M, Koch S, Bruckl T, Biel M, Carell T. Tissue distribution of 5-hydroxymethylcytosine and search for active demethylation intermediates. *PLoS One* 2010;5(12):e15367.
 - (28) Muller T, Gessi M, Waha A, Isselstein LJ, Luxen D, Freihoff D, Freihoff J, Becker A, Simon M, Hammes J, Denkhaus D, zur MA, Pietsch T, Waha A. Nuclear exclusion of TET1 is associated with loss of 5-hydroxymethylcytosine in IDH1 wild-type gliomas. *Am J Pathol* 2012 August;181(2):675-83.
 - (29) van Nederveen FH, Gaal J, Favier J, Korpershoek E, Oldenburg RA, de Bruyn EM, Sleddens HF, Derckx P, Riviere J, Dannenberg H, Petri BJ, Komminoth P, Pacak K, Hop WC, Pollard PJ, Mannelli M, Bayley JP, Perren A, Niemann S, Verhofstad AA, de Bruine AP, Maher ER, Tissier F, Meatchi T, Badoual C et al. An immunohistochemical procedure to detect patients with paraganglioma and pheochromocytoma with germline SDHB, SDHC, or SDHD gene mutations: a retrospective and prospective analysis. *Lancet Oncol* 2009 August;10(8):764-71.

- 2
- (30) Lendvai N, Pawlosky R, Bullova P, Eisenhofer G, Patocs A, Veech RL, Pacak K. Succinate-to-fumarate ratio as a new metabolic marker to detect the presence of SDHB/D-related paraganglioma: initial experimental and ex vivo findings. *Endocrinology* 2014 January;155(1):27-32.
 - (31) Kiuru M, Lehtonen R, Arola J, Salovaara R, Jarvinen H, Aittomaki K, Sjoberg J, Visakorpi T, Knuutila S, Isola J, Delahunt B, Herva R, Launonen V, Karhu A, Aaltonen LA. Few FH mutations in sporadic counterparts of tumor types observed in hereditary leiomyomatosis and renal cell cancer families. *Cancer Res* 2002 August 15;62(16):4554-7.
 - (32) Barker KT, Bevan S, Wang R, Lu YJ, Flanagan AM, Bridge JA, Fisher C, Finlayson CJ, Shipley J, Houlston RS. Low frequency of somatic mutations in the FH/multiple cutaneous leiomyomatosis gene in sporadic leiomyosarcomas and uterine leiomyomas. *Br J Cancer* 2002 August 12;87(4):446-8.
 - (33) Lee HY, Choi K, Oh H, Park YK, Park H. HIF-1-dependent induction of Jumonji domain-containing protein (JMJD) 3 under hypoxic conditions. *Mol Cells* 2014 January;37(1):43-50.
 - (34) Douwes Dekker PB, Corver WE, Hogendoorn PC, Van Der Mey AG, Cornelisse CJ. Multiparameter DNA flow-sorting demonstrates diploidy and SDHD wild-type gene retention in the sustentacular cell compartment of head and neck paragangliomas: chief cells are the only neoplastic component. *J Pathol* 2004 April;202(4):456-62.
 - (35) Hensen EF, Goeman JJ, Oosting J, Van Der Mey AG, Hogendoorn PC, Cremers CW, Devilee P, Cornelisse CJ. Similar gene expression profiles of sporadic, PGL2-, and SDHD-linked paragangliomas suggest a common pathway to tumorigenesis. *BMC Med Genomics* 2009;2:25.
 - (36) Borodovsky A, Salmasi V, Turcan S, Fabius AW, Baia GS, Eberhart CG, Weingart JD, Gallia GL, Baylin SB, Chan TA, Riggins GJ. 5-azacytidine reduces methylation, promotes differentiation and induces tumor regression in a patient-derived IDH1 mutant glioma xenograft. *Oncotarget* 2013 October;4(10):1737-47.
 - (37) Lehtonen HJ, Makinen MJ, Kiuru M, Laiho P, Herva R, van M, I, Hogendoorn PC, Cornelisse C, Devilee P, Launonen V, Aaltonen LA. Increased HIF1 alpha in SDH and FH deficient tumors does not cause microsatellite instability. *Int J Cancer* 2007 September 15;121(6):1386-9.
 - (38) de Graaff MA, Cleton-Jansen AM, Szuhai K, Bovee JV. Mediator complex subunit 12 exon 2 mutation analysis in different subtypes of smooth muscle tumors confirms genetic heterogeneity. *Hum Pathol* 2013 August;44(8):1597-604.
 - (39) Smit DL, Mensenkamp AR, Badeloe S, Breuning MH, Simon ME, van Spaendonck KY, Aalfs CM, Post JG, Shanley S, Krapels IP, Hoefsloot LH, van Moorselaar RJ, Starink TM, Bayley JP, Frank J, van Steensel MA, Menko FH. Hereditary leiomyomatosis and renal cell cancer in families referred for fumarate hydratase germline mutation analysis. *Clin Genet* 2011 January;79(1):49-59.
 - (40) Bovee JV, Cleton-Jansen AM, Kuipers-Dijkshoorn NJ, van den Broek LJ, Taminiou AH, Cornelisse CJ, Hogendoorn PC. Loss of heterozygosity and DNA ploidy point to a diverging genetic mechanism in the origin of peripheral and central chondrosarcoma. *Genes Chromosomes Cancer* 1999 November;26(3):237-46.
 - (41) Carlotti F, Bazuine M, Kekarainen T, Seppen J, Pognonec P, Maassen JA, Hoeben RC. Lentiviral vectors efficiently transduce quiescent mature 3T3-L1 adipocytes. *Mol Ther* 2004 February;9(2):209-17.
 - (42) Lorenz MA, Burant CF, Kennedy RT. Reducing time and increasing sensitivity in sample preparation for adherent mammalian cell metabolomics. *Anal Chem* 2011 May 1;83(9):3406-14.
 - (43) Canelas AB, ten PA, Ras C, Seifar RM, van Dam JC, van Gulik WM, Heijnen JJ. Quantitative evaluation of intracellular metabolite extraction techniques for yeast metabolomics. *Anal Chem* 2009 September 1;81(17):7379-89.

Supplementary data

Table S1. Primary antibodies used for immunohistochemistry analysis.

Primary antibody	Detect	Company	Clone	Dilution	Antigen retrieval buffer
Rabbit polyclonal	Trimethyl-Histone H3, Lys 4	Millipore		1:7000	Tris-EDTA
Rabbit polyclonal	Trimethyl-Histone H3, Lys 27	Millipore		1:7000	Tris-EDTA
Rabbit polyclonal	Trimethyl-Histone H3, Lys 9	Abcam		1:2000	Tris-EDTA
Mouse monoclonal	5-Methylcytosine	Millipore	33D3	1:2000	Tris-EDTA
Rabbit polyclonal	5-Hydroxymethylcytosine	Active motif		1:7000	Citrate
Rabbit polyclonal	Tet oncogene 1	GeneTex		1:800	Citrate
Rabbit polyclonal	2SC*	Eurogentec		1:1000	Citrate
Rabbit polyclonal	SDHB	Atlas		1:4000	Tris-EDTA
Mouse monoclonal	SDHA	Abcam	2E3GC12FB	1:2000	Tris-EDTA

*provided by Norma Frizzell

CHAPTER 3

Parent-of-origin tumorigenesis is mediated by an essential imprinted modifier in SDHD-linked paragangliomas: SLC22A18 and CDKN1C are candidate tumor modifiers

Attje S Hoekstra¹, Ruben D Addie^{2,5}, Cor Ras³, Reza M Seifar³, Claudia A Ruivenkamp⁴, Inge H Briaire-de Bruijn⁵, Frederik J Hes⁴, Jeroen C Jansen⁶, Eleonora PM Corssmit⁷, Willem E Corver⁵, Hans Morreau⁵, Judith VMG Bovée⁵, Jean-Pierre Bayley¹, Peter Devilee^{1,5*}

¹ Department of Human Genetics, Leiden University Medical Center, Leiden, The Netherlands

² Center for Proteomics and Metabolomics, Leiden University Medical Center, Leiden, The Netherlands

³ Department of Biotechnology, Delft University of Technology, Delft, The Netherlands

⁴ Department of Clinical Genetics, Leiden University Medical Center, Leiden, The Netherlands

⁵ Department of Pathology, Leiden University Medical Center, Leiden 2333 ZC, The Netherlands

⁶ Department of Otorhinolaryngology, Leiden University Medical Center, Leiden, The Netherlands

⁷ Department of Endocrinology and Metabolic Diseases, Leiden University Medical Center, Leiden, The Netherlands

Accepted in Human Molecular Genetics

Abstract

Mutations in *SDHD* and *SDHAF2* (both located on chromosome 11) give rise to hereditary paraganglioma almost exclusively after paternal transmission of the mutation, and tumors often show loss of the entire maternal copy of chromosome 11. The 'Hensen' model postulates that a tumor modifier gene located on chromosome 11p15, a region known to harbor a cluster of imprinted genes, is essential to tumor formation. We observed decreased protein expression of the 11p15 candidate genes *CDKN1C*, *SLC22A18* and *ZNF215* evaluated in 60 *SDHD*-mutated tumors compared to normal carotid body tissue and non-*SDH* mutant tumors.

We then created stable knockdown *in vitro* models, reasoning that the simultaneous knockdown of *SDHD* and a maternally expressed 11p15 modifier gene would enhance paraganglioma-related cellular characteristics compared to *SDHD* knockdown alone. Knockdown of *SDHD* in *SNB19* and *SHSY5Y* cells resulted in the accumulation of succinate, the stabilization of HIF1 protein and a reduction in cell proliferation.

Compared to single knockdown of *SDHD*, knockdown of *SDHD* together with *SLC22A18* or with *CDKN1C* led to small but significant increases in cell proliferation and resistance to apoptosis, and to a gene expression profile closely related to the known transcriptional profile of *SDH*-deficient tumors. Of the 60 *SDHD* tumors investigated, 4 tumors showing retention of chromosome 11 showed *SLC22A18* and *CDKN1C* expression levels comparable to levels in tumors showing loss of chromosome 11, suggesting loss of protein expression despite chromosomal retention.

Our data strongly suggest that *SLC22A18* and/or *CDKN1C* are tumor modifier genes involved in the tumorigenesis of *SDHD*-linked paraganglioma.

Introduction

Hereditary paraganglioma–pheochromocytoma syndrome is characterized by neuroendocrine tumors that originate from both the sympathetic and parasympathetic branches of the autonomic nervous system. Pheochromocytomas (PCC) are generally benign catecholamine-secreting tumors of the adrenal medulla (1), whereas extra-adrenal paragangliomas (EA-PGL) are frequently aggressive tumors that arise in the thorax and abdomen. Paragangliomas of the head and neck (HNPGL) arise most commonly in the carotid body, the main sensor of blood oxygenation, and these highly vascular tumors are often characterized by an indolent, non-invasive growth pattern (2).

Although more than 14 different genes have been linked to PGL/PCC, a subgroup of these genes is associated with hereditary PGL/PCC, including *SDHA* (3), *SDHB* (4), *SDHC* (5), *SDHD* (6), and *SDHAF2* (7). These genes encode subunits of the mitochondrial succinate dehydrogenase (SDH) complex, which plays a central role in the tricarboxylic acid (TCA) cycle and the electron transport chain. In the TCA cycle, SDH converts succinate to fumarate while providing electrons for oxidative phosphorylation in the inner mitochondrial membrane. SDH inactivation results in accumulation of its substrate succinate, which can function as competitor of α -ketoglutarate (α -KG) to broadly inhibit α -KG-dependent dioxygenases leading to HIF activation (8-11). Expression profiling of PGL and PCC shows increased hypoxic-angiogenic expression features and reduced oxidoreductase profiles in *SDH*-deficient tumors compared to non-*SDH* mutant tumors (12;13).

Germline mutations of the *SDHD* and *SDHAF2* genes, unlike mutations of the other *SDH* subunit genes, show a parent-of-origin expression phenotype, with tumor development occurring almost exclusively due to mutations inherited via the paternal line (14;15). Carriers of maternally-inherited mutations develop tumors only very rarely. *SDHD* and *SDHAF2* are both located on the long arm of chromosome 11, whereas the *SDHA*, *SDHB* and *SDHC* subunit genes are located on chromosome 5 (*SDHA*) or chromosome 1 (*SDHB* and *SDHC*). The 11p15 region of chromosome 11 harbors the main concentration of imprinted genes in the human genome, with 8 genes (Table 1) expressed exclusively from the maternal allele while the opposite allele is silenced by epigenetic mechanisms. Loss of the entire maternal copy of chromosome 11 is a frequent occurrence in *SDHD*-linked paragangliomas (16-18) and since neither *SDHD* nor *SDHAF2* are imprinted, other gene(s) expressed exclusively from the maternal allele must play a role in tumor formation.

Now known as the Hensen model, in 2004 Hensen and colleagues proposed that selective loss of maternal chromosome 11 results in the simultaneous deletion of the *SDHD* gene and an exclusively maternally expressed gene, leading to a parent-of-origin phenotype (Figure 1A) (17). Based on this model, Hensen and colleagues also predicted that, in order to cause disease, a maternally-transmitted *SDHD* mutation would require “mitotic recombination, followed by loss of the recombined paternal chromosome containing the paternal 11q23 region and the maternal 11p15 region” (Figure 1B) (17). This phenomenon has since been observed in at least two cases of maternal inheritance (19;20), strongly supporting the involvement of still unknown maternal genetic factors in tumor formation.

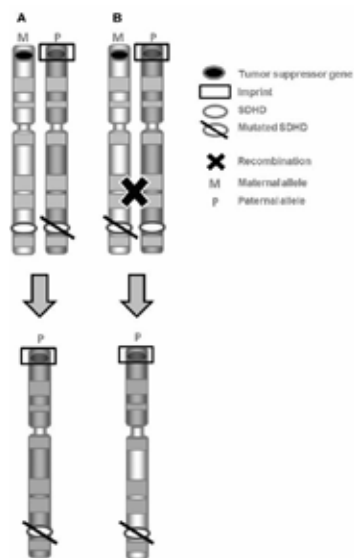


Figure 1. Schematic representation of Hensen model to explain the parent-of-origin effect of *SDHD*-linked paraganglioma. (A) Upon paternal transmission of the *SDHD* mutation and loss of maternal chromosome 11, both the wild type maternal *SDHD* allele and the active tumor suppressor gene located at 11p15 are targeted, thereby initiating tumor formation. (B) In rare cases of maternal transmission of the *SDHD* mutation, at least two events caused by different chromosomal mechanisms will be required to inactivate both the wild type *SDHD* allele and the active maternal tumor suppressor gene, namely loss of the paternal wild type *SDHD* allele by, for example, mitotic recombination, followed by loss of the recombined paternal chromosome containing the paternal 11q23 region and the maternal 11p15 region.

We hypothesized that in a human cell line with two parental copies of chromosome 11, knockdown of *SDHD* together with an additional candidate imprinted gene would lead to a cellular phenotype resembling that of primary paragangliomas. We therefore performed lentiviral stable shRNA knockdown of *SDHD* in SNB19 and SHSY5Y cells, two tumor cell lines of neuroectodermal origin. These cells were then used for additional knockdown of several 11p15 genes, followed by analysis of cell proliferation, apoptosis, TCA cycle metabolites and gene expression profiles. Further (protein/genetics) analysis of candidate tumor modifiers was performed in 60 *SDHD*-mutated tumors. Taken together, our results suggest that *SLC22A18* and *CDKN1C* are potential tumor modifier genes involved in tumor formation of *SDHD*-mutated PGL.

Material and methods

Selection of cell lines

As no human *SDH*-related PGL tumor cell line is currently available, we selected developmentally similar neural crest-derived cell lines. Cell lines carrying somatic mutations in PGL/PCC-linked susceptibility genes, including *VHL* and *MAX* mutations, were excluded based on information from the Catalogue of Somatic Mutations in Cancer (COSMIC) database. SNB19 (glioblastoma) and SHSY5Y (neuroblastoma) cell lines were selected based on a karyotype that demonstrated two copies of chromosome 11. SHSY5Y cells were heterozygous for chromosome 11 as detected by microsatellite markers, while SNB19 cells were homozygous for chromosome 11 (Supplemental Figure 1A). To establish the parental origin of chromosome 11 in the cells, we determined the methylation status of the two imprinted domains at 11p15.5 [H19-differentially methylated region (DMR) and KvDMR]. When both parental copies of chromosome 11 are present, the H19-DMR/KvDMR methylation rate ratio should be around one (39). SHSY5Y cells showed an average methylation rate of 0.75 ± 0.08 for H19-DMR and 0.65 ± 0.1 for KvDMR, resulting in a ratio of 1.1 (Supplemental Figure 1B). The average methylation rate for H19-DMR in SNB19 cells was 0.1 ± 0.1 , while the average methylation rate for

KvDMR 0.005 ± 0.03 , suggesting loss of imprinting. Nonetheless, clear RNA expression of *H19* (expressed from the maternal allele) and absence of expression of *IGF2* (expressed from the paternal allele) indicated that chromosome 11 in SNB19 cells shows a maternal expression pattern. Both cell lines were therefore considered suitable.

Cell culture

SNB19 cells and HEK293 cells were obtained from DSMZ (ACC 305 and ACC 325, Braunschweig, Germany) and cultured in Dulbecco's Modified Eagle Medium (DMEM, Life Technologies, Paisley, UK) supplemented with 10% fetal bovine serum and penicillin/streptomycin (Life Technologies). SHSY5Y cells were obtained from European Collection of Cell Cultures via Sigma Aldrich (St. Louis, USA, Catalogue no. 86012802). SHSY5Y cells were cultured in DMEM-F12 (Life Technologies, Paisley, UK), supplemented with 15% fetal bovine serum and penicillin/streptomycin, and maintained at 37°C in a humidified atmosphere of 5% CO₂ in air.

Patients and samples

A tissue microarray (25) comprising 100 PGL and 17 PCC paraffin-embedded specimens yielded 5 micrometer sections for immunohistochemistry (IHC). All samples were handled according to the Dutch Code for Proper Secondary Use of Human Materials approved by the Dutch Society of Pathology (www.federa.org). *SDHD* mutant FFPE samples were used for DNA extraction. In addition, we included 8 fresh frozen *SDHD* tumor samples and paired blood samples for DNA extraction. The samples were handled in a coded (pseudonymised) fashion according to procedures agreed with the LUMC ethical board (P12.082).

LOH analysis by microsatellite genotyping

DNA from SNB19 and SHSY5Y cells was isolated using the Wizard Genomic DNA purification kit (Promega, Fitchburg, USA) according to the manufacturer's instructions. Representative tumor areas from FFPE samples were selected to punch 3 cores of 0.6 mm in diameter for DNA isolation. FFPE and fresh frozen tumor sections were incubated overnight with proteinase K at 60°C and DNA was isolated using the Qiagen FFPE DNA kit or QIAamp DNA Mini Kit (Qiagen Benelux B.V., Venlo, The Netherlands), respectively, following manufacturer's instructions. All DNA samples were genotyped for microsatellite markers located on chromosome 11 (primer sequences available upon request). For each marker, thirty nanograms of DNA was amplified over 40 cycles using FastStar Taq DNA Polymerase (Roche). Forward primers were labeled with a 6-FAM, HEX or NED fluorophore (Sigma-Aldrich, St. Louis, MO, USA). Amplicons of microsatellite markers were run on an ABI 3730 genetic analyzer and data were analyzed using Gene Marker software (Soft Genetics, State College, PA 16803, USA), with ABI GeneScan Rox 400 as the internal size standards. LOH of markers in tumor samples was calculated using the allelic imbalance ratio: AIR = (Tumor1/Tumor2)/(Normal1/Normal2). Tumors were regarded as positive for LOH when the mean allele ratio between tumor and blood was <0.7 for all informative markers, as described earlier (19). In cases where no matching blood DNA sample was available, allele peak ratios were compared to DNA samples with the same or very similar allele combinations. Some markers were either not informative in the patient or did not perform well enough with tumor DNA to give a reliable result and were therefore excluded.

Karyotyping

Conventional cytogenetic analysis on GTG-banded chromosomes from cultured SNB19, HEK293 and SHSY5Y cells was performed according to standard techniques. Briefly, 17 hours before harvesting the cells, 200 μ l FdU (5 μ M) was added to the cells. Then, the cells were incubated with 200 μ l BrdU (14 mg/ml) for another 5-6 hours. Finally, colcemid was added 15 minutes before harvesting and metaphase spreads were prepared according to standard protocols.

Bisulfite-modified PCR and sequencing

DNA (300 ng) from SNB19 and SHSY5Y cells was bisulfite-treated using the EZ DNA methylation kit (Zymo research, Irvine, USA). Bisulfite-treated DNA was then amplified by PCR using primers specific for modified DNA designed with Meth primer (40). Primer sequences for H19 were 5'-GGTTT TAGTGTGAAATTTTTT-3' (forward) and 5'-CCATAAATATCCTATCCCAAATAAC-3' (reverse), and 5'-TTGAGGAGTTTTTGGAGGTT-3' (forward) 5'-ACCC AACCAATACCTCATAC-3' (reverse) for KvDMR1. The PCR program consisted of an initial denaturation step at 94°C for 15 minutes followed by 44 cycles of 20 seconds at 94°C, 30 seconds at 55°C for KvDMR1 and 52.5°C for H19, followed by 5 minutes at 72°C. Sanger sequencing of PCR products was performed using standard protocols, and methylation rates were evaluated using ESME software (41).

CDKN1C and *SLC22A18* mutation analysis

All exons of the *CDKN1C* and *SLC22A18* genes were amplified by PCR (primer sequences available on request). Twenty nanograms of genomic DNA and matched normal DNA from 6 *SDHD*-linked patients was amplified and primer annealing was performed at 58°C. PCR fragments were purified using the Nucleospin gel and PCR clean-up kit (Macherey-Nagel). Sequencing was performed using standard protocols and data were analyzed using Mutation Surveyor software (Softgenetics).

Tissue samples and immunohistochemistry

FFPE tissue samples used for IHC were as described in 'patients and samples'. As control tissue, whole sections of 4 normal carotid bodies were included, obtained from anonymous patients at autopsy within 24 hours after death. We reviewed the histological appearance of all samples (JVMGB, JPB, ASH) and confirmed diagnoses by routine IHC staining for S-100 (detecting sustentacular cells) and chromogranin A (detecting chief cells). Mutation detection was confirmed by routine SDHA and SDHB immunohistochemical staining, as described previously (30).

Primary antibodies for IHC analysis were used as follows: Rabbit polyclonal antibody for detection of SLC22A18 (1:3200, Proteintech), KCNQ1 (1:100, Sigma Aldrich), PHLDA2 (1:200, Abcam), CDKN1C (1:1600, Sigma Aldrich), ZNF215 (1:200, Sigma Aldrich). Placenta and liver were used as a positive control. After antigen retrieval by exposure to microwave heating in citrate buffer, pH 6.0 at 100°C for 10 min, sections were blocked for 30 min with 10% goat serum and incubated overnight at 4°C with primary antibodies. Signal detection was performed with Envision+ (DAKO, Agilent Technologies, Belgium) and the chromogen 3,3'-diaminobenzidine according to manufacturer's instructions. The results of the immunohistochemical labeling were scored semi-quantitatively: the intensity of labeling was assessed on a scale of 0 to 3 (0 = none; 1 = weak; 2 = moderate; 3 = strong), and the percentage of positive cells was assessed on a scale of 0 to 4 (0 = 0% positive; 1 = 1-24% positive; 2 = 25-49% positive; 3 = 50-74%; 4 = 75-100% positive cells). The two scores were then

added to reach a total sum score ranging from 0-7. The scoring was performed independently by two observers blinded for clinicopathological data (ASH and JVMGB) and discrepancies were discussed. Photos of IHC sections were obtained using a Leica DFC550 camera and the Leica Application Suite, software version 4.5 (Heerbrugg, Switzerland).

Gene knockdown

To create stable cell lines with a single or double knockdown of genes, four validated MISSION® shRNA constructs and one non-validated MISSION® shRNA construct (TRCN0000231553 -237878, -147951, -344525 and -13054) targeting human *SDHD* (NM_003002.1), *CDKN1C* (NM_000076), *OSBPL5* (NM_020896), *SLC22A18* (NM_002555) and *ZNF215* (NM_013250), respectively (Sigma Aldrich, St. Louis, USA) or a scrambled shRNA encoding plasmid (SHC002 Sigma Aldrich) were used to produce infectious virus particles. To evaluate the transduction efficiency, the MISSION TurboGFP control plasmid (SHC003 Sigma Aldrich) was used. HEK293T cells were transfected with the shRNA constructs together with helper plasmids encoding HIV-1 gag-pol, HIV-1 rev, and the VSV-G envelope as described (42). Viral supernatants were added to SNB19, HEK293 and SHSY5Y cells in fresh medium supplemented with 8 µg/ml Polybrene (Sigma Aldrich) and the cells were incubated overnight. The next day, the medium was replaced with fresh medium. Selection was carried out using 2 µg/ml puromycin. Transduction efficiency was analyzed 3 to 6 days post transduction. Experiments were performed 2-3 and 4-5 weeks after transduction of cells with shRNAs.

RT-PCR analysis

Total RNA from cells was isolated using the Nucleospin RNA II kit (Macherey-Nagel, Düren, Germany) according to manufacturer's instructions. cDNA was synthesized from 1µg RNA using the Omniscript RT kit (Qiagen, Venlo, Netherlands). Gene expression was determined using quantitative PCR and was measured in triplicate on the CFX96 Real-Time System (Bio-Rad, USA) using the iQ SYBR Green Supermix (Biorad, California, USA). The relative quantification of target mRNA was performed by the $2^{-\Delta\Delta CT}$ method (43). Results from the housekeeping genes *HNRMP*, *TBP* and *HPRT* were used as references. Target genes were *SDHD*, *CDKN1C*, *SLC22A18*, *OSBPL5*, *ZNF215*, *GLUT1*, *EGLN3*, *BNIP3*, *ENO1* and *VEGF*.

Western blotting

Total protein was isolated using RIPA buffer (Sigma Aldrich) supplemented with "complete" protease inhibitor cocktail (Roche, Germany). The concentration of protein was determined by bicinchoninic acid protein assay (Thermo Scientific Pierce, Rockford, USA). Equal amounts of protein (35 µg) were separated by SDS-PAGE and transferred onto polyvinylidene fluoride (PVDF) membranes (Millipore). After blocking with 5% (w/v) non-fat milk powder, membranes were incubated overnight at 4 °C with the following antibodies: SDHB (Sigma Aldrich) and HIF-1α (Novus Biologicals, Littleton, USA) in a dilution of 1:500 in blocking buffer (Rockland, Gilbertsville, USA). α-tubulin was used as a loading control (1:2000, Sigma Aldrich). Visualization and quantification was carried out using the LI-COR Odyssey® scanner (Bad Homburg, Germany) and software (LI-COR Biosciences).

Microarray expression analysis

Quality control, RNA labeling, hybridization and data extraction were performed at ServiceXS B.V. (Leiden, The Netherlands). RNA concentrations were measured using the Nanodrop ND-1000

spectrophotometer (Nanodrop Technologies, Wilmington, DE, USA). The RNA quality and integrity was determined using Lab-on-a-Chip analysis on the Agilent 2100 Bioanalyzer (Agilent Technologies, Inc., Santa Clara, CA, USA). Biotinylated cRNA was prepared using the Illumina TotalPrep RNA Amplification Kit (Ambion, Inc., Austin, TX, USA) according to the manufacturer's specifications with an input of 200 ng total RNA. Per sample, 750 ng of the obtained biotinylated cRNA samples was hybridized to the Illumina HumanHT-12 v4 BeadChip (Illumina, Inc., San Diego, CA, USA). Hybridization and washing were performed according to the Illumina Manual "Direct Hybridization Assay Guide". Scanning was performed on the Illumina iScan (Illumina, Inc., San Diego, CA, USA). Image analysis and extraction of raw expression data was performed with Illumina GenomeStudio v2011.1 Gene Expression software.

Bioinformatic analysis

3 Normalization and quality control was performed using the Bioconductor "lumi" package of R (lumi) (44). Samples were clustered using an unsupervised hierarchical clustering method to delineate groups with biological distinction. The R package 'Linear Models for Microarray Data' (LIMMA) was used for the assessment of differential expression of individual genes between the different subgroups (45). Overall gene expression differences between scrambled control and *SDHD* knockdown, scrambled control and *SDHD+CDKN1C* knockdown or scrambled control and *SDHD+SLC22A18* knockdown subgroups in SNB19 and SHSY5Y cells were evaluated with the 'global test' designed by J.J. Goeman using the R package 'global test' available on Bioconductor (46). We applied the global test in order to evaluate subtle differences between the different subgroups, as this test has greater power to detect gene sets with small effect sizes (46;47). We performed a pathway-based analysis using the global test on pathways described in the publicly available pathway database Kyoto Encyclopedia of Genes and Genomes (KEGG) annotations (48). KEGG pathway analysis of scrambled control HEK293 cells versus *SDHD* knockdown was not consistent with tumor gene expression profiles of PGL with *SDH* gene mutations (12;49) and was therefore excluded as a relevant model. All tests, both for genes and pathways, were corrected for multiple testing based on the false discovery rate (FDR) criterion, using the Benjamini and Hochberg method (50). Comparison analysis and functional categorization of the different subgroups was performed with Ingenuity Pathway Analysis (IPA; www.ingenuity.com). All data are available at the GEO database (GSE80968).

Cellular DNA content and flow cytometry

Using the Vindelov technique (51), DNA staining was performed as follows: Cells were centrifuged (500g, 5 min) and washed in PBS, then 300 μ l of solution A containing trypsin (0.3 g/L, Sigma) at pH 7.6 was added and incubated for 2 hours at 37°C. Next, 225 μ l of solution B containing RNase (0.5g/L, Sigma) and a trypsin inhibitor (0.1 g/L Sigma) was added, followed by a 10 min incubation at room temperature (RT). Finally, a third incubation at RT was carried out for at least 15 min after the addition of 225 μ l of propidium iodide (PI) (0.42g/L, Sigma) (solution C). Samples were measured using an LSRII (BD Biosciences, Erembodegem, Belgium) flow cytometer. Detector D (BP610/20 nm) was used to collect PI fluorescence. The WinList 8.0 and ModFit 4.0.1 software packages (Verity Software House, Inc., Topsham, ME) were used for data analysis.

xCelligence

The RTCA xCelligence system (Roche Applied Sciences, Almere, the Netherlands), based on cell electrode substrate impedance detection technology, was used for proliferation assays. Cell lines were plated at a density of 10,000 cells per well in a 16-well E-Plate. The plates were loaded into the RTCA station in the cell culture incubator immediately after plating and cell index was acquired every 30 min. Experiments were performed in triplicate.

Assessment of apoptosis

SNB19 and SHSY5Y cells were stimulated with 2, 4 or 8 μM staurosporine (Sigma) or with 10, 20 or 40 μM cisplatin (Sigma). The ApoLive-Glo multiplex Assay (Promega, Madison, USA) was used to measure cell viability and apoptosis in the same sample following the manufacturer's protocol. Briefly, the viability is measured by the activity of a protease marker of cell viability. Apoptosis is measured by the addition of a luminogenic caspase-3/7 substrate (Caspase-Glo 3/7) which is cleaved in apoptotic cells to produce a luminescent signal. Fluorescence at 400 Ex/505 Em (viability) and luminescence (apoptosis) were measured with a Victor 3 machine (PerkinElmer, Massachusetts, USA).

Nuclear fragmentation was determined in SNB19 and SHSY5Y cells stimulated with 4 μM staurosporine. Cells were fixed with 4% paraformaldehyde for 15 min. Then, the cells were washed three times in PBS and stained with 50 $\mu\text{g}/\text{ml}$ 4,6-diamidino-2-phenylindole-2-HCl (DAPI; Sigma) in Vectashield mounting medium under a cover slip. Images of fixed cells were acquired on a Zeiss Axio Imager M2 fluorescence microscope equipped with an HXP 120 metal-halide lamp used for excitation. Fluorescent probes were detected using the following filters: DAPI (excitation filter: 350/50 nm) and GFP (excitation filter: 470/40 nm). Images were recorded using ZEN 2012 software.

TCA cycle metabolite quantification by LC-MS/MS

Sample preparation for biochemical analysis of SNB19 and SHSY5Y cells was performed according to (52), using ice cold 90% MeOH: CHCl_3 as extraction solvent containing ^{13}C -labeled isotopes of nucleotides as internal standards. Dried samples were reconstituted in 100 μl H_2O for compatibility with the liquid chromatography-tandem mass spectrometry (LC-MS/MS) method (53). The concentrations of citric acid, α -ketoglutarate, succinate, fumarate and malate were determined by anion-exchange LC-MS/MS. The concentrations of AMP, ADP and ATP were determined by ion-pair reverse-phase LC-MS/MS (54).

Statistical analysis

IBM SPSS Statistics 20.0 for Windows software package (SPSS, Armonk, NY: IBM Corp) was used to analyze the results. The statistical significance of differences between 2 groups was assessed by the Mann-Whitney U test, and the 1-way analysis of variance test was used for comparisons of more than 2 groups. $P < 0.05$ was considered statistically significant.

Results

Protein expression of chromosome 11p15 candidate genes in SDHD mutant PGL

We selected imprinted 11p15 candidate modifier genes reasoning that a gene of interest would be expressed in normal carotid body tissue and lost in *SDHD* mutant tumors. Using immunohistochemistry (IHC), we analyzed the protein expression of specific 11p15 genes (indicated in bold in Table 1) in normal human post-mortem carotid bodies, *SDHD*-related tumors and non-*SDH* mutant PCCs. Expression of SLC22A18 was significantly decreased in the chief cell, the neoplastic cell population, of *SDHD* mutant tumors, while remaining abundant in all normal carotid bodies and non-*SDH* mutant tumors (Fig. 2A-D). ZNF215 showed no or low expression (score 0-2) in chief cells in 85% of *SDHD*-related tumors, and expression was significantly lower compared to normal carotid bodies (Fig. 2A, E-G). The nuclear expression of CDKN1C was very low in the normal carotid body and absent in *SDHD* mutant PGL (Fig. 2A, 2H-I). However, CDKN1C was expressed in non-*SDH* mutant tumors (Fig. 2A, 2J). By contrast, KCNQ1 and PHLDA2 were expressed in *SDHD* mutant tumors (Fig. 2A, 2K-O), effectively excluding them as candidates.

Table 1. Imprinted genes expressed exclusively from the maternal allele on 11p15

Gene	Chromosome location	Description	Expressed allele	Imprinted allele
KCNQ1DN	11p15.4	non-coding RNA	Maternal	Paternal
ZNF215	11p15.4	zinc finger protein 15	Maternal	Paternal
OSBPL5	11p15.4	member oxysterol-binding protein family	Maternal	Paternal
PHLDA2	11p15.5	pleckstrin homology-like domain family A member 2	Maternal	Paternal
CDKN1C	11p15.5	cyclin-dependent kinase inhibitor 1c	Maternal	Paternal
H19	11p15.5	non-coding RNA	Maternal	Paternal
KCNQ1	11p15.5	encoding voltage-gated potassium channel	Maternal	Paternal
SLC22A18	11p15.5	poly-specific organic cation transporter	Maternal	Paternal

Bold indicates the candidate genes investigated in this study.

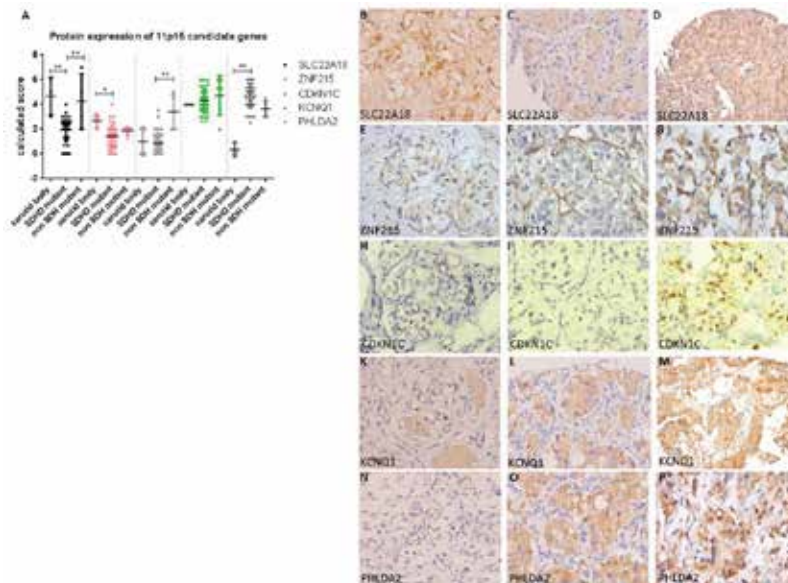


Figure 2. Protein expression in normal human carotid bodies, *SDHD* and non-*SDHD* mutant tumors. (A) Dot plot showing immunohistochemical expression levels of SLC22A18, CDKN1C, ZNF215, KCNQ1, and PHLDA2 in normal carotid bodies, *SDHD* and non-*SDHD* mutant tumors. Data are represented as calculated mean score \pm standard deviation. * $p < 0.05$; ** $p < 0.001$. Representative staining data (40x magnification) show strong nuclear immunostaining of (B) SLC22A18 protein in chief cells in normal carotid bodies, whereas the nuclear tumor cell staining was lost in (C) *SDHD* mutant tumors. (D) SLC22A18 is expressed in non-*SDHD* mutant tumors. (E) Expression of ZNF215 is present in the chief cell compartment of normal carotid body, but is absent in (F) *SDHD*-mutated tumors. (G) Low expression of ZNF215 is observed in non-*SDHD* mutant tumors. (H) Very low nuclear expression of CDKN1C was observed in chief cells of normal carotid bodies and was absent in (I) *SDHD*-mutated tumors. (J) CDKN1C is highly expressed in non-*SDHD* mutant tumors. (K) Cytoplasmic expression of KCNQ1 was observed in normal carotid bodies, (L) *SDHD* mutant tumors, and (M) non-*SDHD* mutant tumors. (N) Cytoplasmic expression of PHLDA2 was present in normal carotid bodies and (O) *SDHD* mutant tumors, and (P) non-*SDHD* mutant tumors.

SDHD knockdown leads to succinate accumulation, reduced ATP levels and HIF activation

In order to evaluate metabolic changes and HIF1 activation induced by loss of *SDHD*, we generated subclones of SNB19 and SHSY5Y cells with stable knockdown of *SDHD*. Knockdown of *SDHD* was confirmed by real-time analysis of RNA expression levels and by immunoblotting (Fig. 3A), with decreased SDHB protein levels taken as a marker for SDH deficiency (21). As expected (11), suppression of *SDHD* resulted in the significant accumulation of succinate in both SNB19 and SHSY5Y cells (Fig. 3B). In addition, ATP levels were also significantly decreased (Fig. 3C). Suppression of *SDHD* expression increased HIF1 α protein levels (Fig. 3D) as well as mRNA expression of HIF1 target genes by at least 2 fold, including glucose transporter 1 (GLUT1), Bcl-2-like 19kDa-interacting protein 3 (BNIP3), prolyl hydroxylase 3 (EGLN3), enolase 1 (ENO1) and vascular endothelial growth factor (VEGF) compared to scrambled control cells (Fig. 3E).

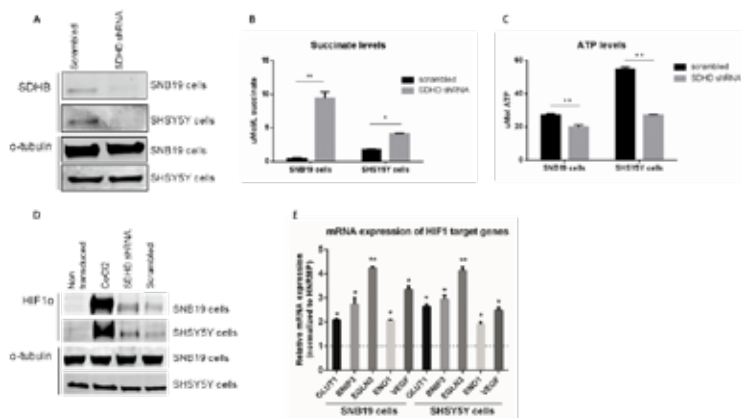


Figure 3. *SDHD* knockdown leads to accumulation of succinate, reduction in ATP levels and HIF1 stabilization. (A) SNB19 and SHSY5Y cells with stable knockdown of *SDHD* demonstrate decreased SDHB protein levels in total protein extract compared to control cells (scrambled shRNA). α -Tubulin was used as a loading control. (B) Succinate levels quantified by LC/MS/MS were increased in SNB19 and SHSY5Y cells with stable knockdown of *SDHD* compared to scrambled control cells. (C) ATP levels as quantified by LC/MS/MS were decreased in SNB19 and SHSY5Y cells with stable knockdown of *SDHD* compared to scrambled control cells. (D,E) HIF1 α levels were assessed in total protein extract by western blotting. α -Tubulin was used as a loading control. Stimulation with 200 μ M CoCl₂ for 24 hours was used to induce HIF1 stabilization. Knockdown of *SDHD* resulted in stabilization of HIF1 α protein and (B) increased mRNA expression of HIF1 target genes, including GLUT1, BNIP3, EGLN3, ENO1 and VEGF, compared to control (dashed line), as measured by RT-PCR. mRNA expression of *SDHD* knockdown cells was normalized to control cells (scrambled shRNA), indicated by the dashed line. HNRMP was used as a housekeeping gene. Error bars represent standard deviation for duplicate experiments. * p <0.05, ** p <0.01.

To study the effects of 11p15 candidate gene loss in *SDHD* knockdown cells, we carried out additional knockdown of *OSBPL5*, *SLC22A18*, *CDKN1C* or *ZNF215* in both SNB19 and SHSY5Y cells. Stable knockdown of each gene was confirmed by real-time analysis of RNA expression levels (Supplementary Fig. 2). Cells with double knockdown of *SDHD* and either *SLC22A18*, *CDKN1C* or *OSBPL5* exhibited succinate levels equivalent to single knockdowns of *SDHD*, while combined knockdown of *SDHD* and *ZNF215* resulted in a small (non-significant) reduction in succinate levels (Figs. 4A and 4B). Consistent with these findings, the ratio of succinate to fumarate was increased in cells with single knockdown of *SDHD* compared to scrambled control cells and did not change significantly following additional knockdown of either *SLC22A18*, *CDKN1C*, *OSBPL5* or *ZNF215* (Fig 4C-D). Furthermore, the elevated succinate/ α -KG ratio following *SDHD* knockdown did not change significantly upon additional knockdown of any candidate gene (Fig. 4E-F).

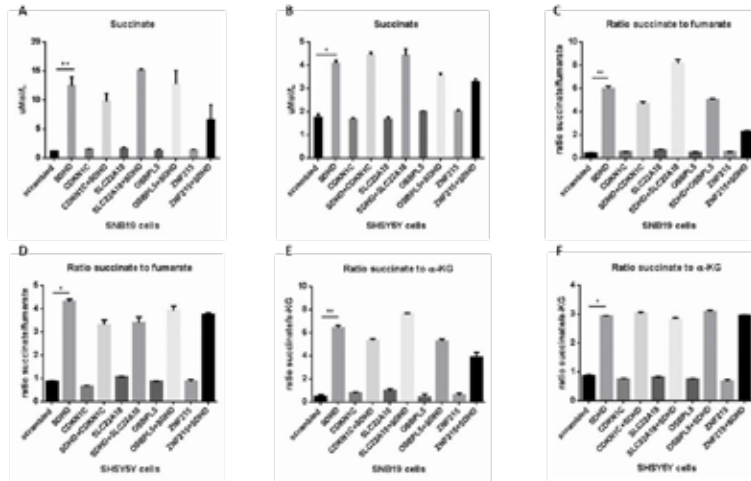


Figure 4. No metabolic changes by stable knockdown of *SDHD* and 11p15 genes. (A,B) Increased succinate levels following stable knockdown of *SDHD* did not change significantly in *CDKN1C*, *SLC22A18* or *OSBP5* double knockdown SNB19 or SHSY5Y cells, as quantified by LC/MS/MS. (C,D) The ratio of succinate to fumarate and (E,F) succinate to α -KG is not increased in cells with double knockdowns of *CDKN1C*, *SLC22A18*, *OSBP5* or *ZNF215* compared to *SDHD* knockdown, as quantified by LC/MS/MS. Error bars represent standard deviation for duplicate experiments. * $p < 0.05$, ** $p < 0.01$.

Increased cell proliferation following SDHD and CDKN1C or SLC22A18 double knockdown

HNPGL is characterized by unusually slow growth, with a reported doubling time of 4 years (2). Using a real-time cell proliferation system, *SDHD* knockdown in SHSY5Y resulted in reduced proliferation (Fig. 5A) and a lower S-phase fraction (Fig. 5B), relative to controls. However, reduced proliferation could not be attributed to cell cycle arrest at G2/M, since no changes were found in the G2/M fraction in *SDHD* knockdown compared to control cells (Fig. 5B).

However, a significantly increased rate of cell proliferation was seen following double knockdown of *SDHD* and *CDKN1C* (Fig. 5C), or of *SDHD* and *SLC22A18* (Fig. 5D), compared to single knockdown of *SDHD*. By contrast, knockdown of *SDHD* together with *OSBP5* (Fig. 5E) or *ZNF215* (Fig. 5F) did not result in enhanced proliferation compared to single knockdown of *SDHD*. Only very minor changes in cell proliferation were observed in SNB19 cells, perhaps because these cells show much faster intrinsic growth compared to SHSY5Y cells.

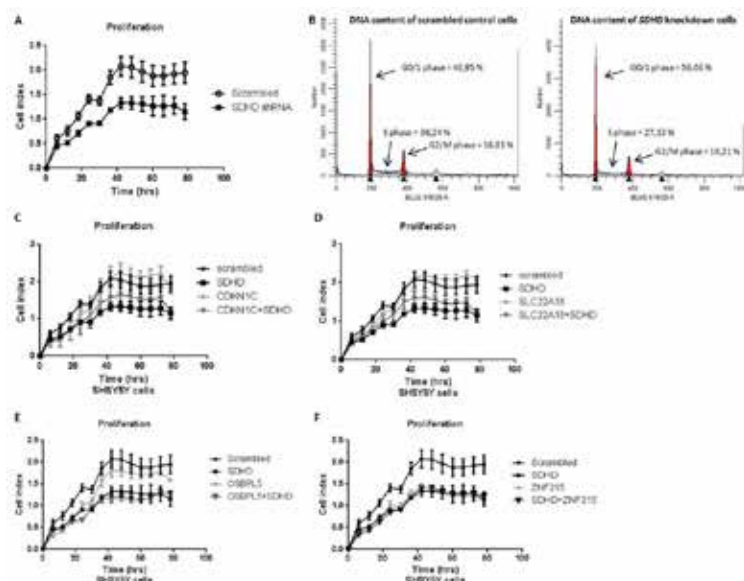


Figure 5. Increased cell proliferation in cells with knockdown of *SDHD* and *CDKN1C* or *SLC22A18*. (A) SHSY5Y cells with stable knockdown of *SDHD* demonstrate a reduced cell proliferation compared to scrambled control cells, measured in real-time using xCelligence. (B) Using propidium iodide and FACS analysis, DNA content histograms showed a decreased S phase fraction and increased G0/1 fraction in *SDHD* knockdown cells compared to scrambled cells. The acquired FACS data were analyzed by ModFit LT software (Verity Software House, Inc.). (C) Using xCelligence, SHSY5Y cells with stable knockdown of *SDHD* and *CDKN1C* or (D) *SLC22A18* show increased proliferation compared to single knockdown of *SDHD*. (E) No differences in cell proliferation were observed when comparing single knockdown of *SDHD* to combined knockdown of *SDHD* and *OSBP15* or (F) *SDHD* and *ZNF215*.

Knockdown of SDHD and SLC22A18 results in apoptosis resistance

No significant apoptotic activity has been detected in HNPGLs, suggesting that apoptotic mechanisms may be impaired or blocked (22). Using *SDHD* knockdown SHSY5Y cells, we induced apoptosis using various concentrations of staurosporine or cisplatin and studied key features of apoptosis such as nuclear fragmentation and activation of caspase 3/7. Staurosporine was significantly less proficient in inducing apoptosis upon *SDHD* knockdown (Figure 6A), and SNB19 cells showed similar results, but with lower overall sensitivity to apoptosis (Fig. 6B). *SDHD* knockdown also resulted in resistance to cisplatin-induced apoptosis, compared to control cells (Fig. 6C). Induction of apoptosis using staurosporine or cisplatin was also accompanied by decreased cell viability (Fig. 6D). Only one candidate gene showed significant differences in apoptosis resistance following double knockdown, *SLC22A18*. In SNB19 cells the combined knockdown of *SDHD* and *SLC22A18* resulted in significant apoptosis resistance compared to single knockdown of *SDHD* (Fig. 6F).

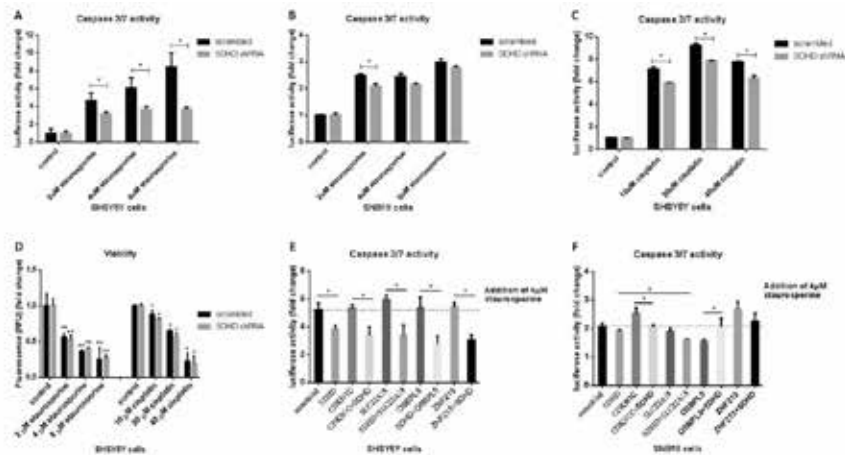


Figure 6. Knockdown of *SDHD* together with *SLC22A18* results in apoptosis resistance. (A) Apoptosis was induced with 2µM, 4µM or 8µM staurosporine for 2 hours in SHSY5Y cells and caspase 3/7 activity was measured using the APOlive-GLO Multiplex Assay (Promega). (B) Apoptosis was induced in SNB19 cells following exposure to 2µM, 4µM or 8µM staurosporine (for 24 hours). SNB19 cells showed lower sensitivity to apoptosis induction than SHSY5Y cells. (C) SHSY5Y cells were exposed to 10µM, 20µM or 40µM cisplatin for 18 hours. (D) Cell viability is decreased by the addition of 2µM, 4µM and 8µM staurosporine or 10µM, 20µM and 40µM cisplatin, measured by APOlive-GLO Multiplex Assay. (E) Using 4µM staurosporine for 2 hours, apoptosis was induced in SHSY5Y cells and double knockdown cells were analyzed. Silencing of *SDHD* together with *CDKN1C*, *SLC22A18*, *OSBP15* or *ZNF215* resulted in small but non-significant decreases in apoptosis compared to *SDHD* knockdown alone. (F) Apoptosis was induced by 4µM staurosporine for 24 hours in SNB19 cells. Double knockdown of *SDHD* and *SLC22A18* led to a small but significant reduction in apoptosis compared to knockdown of *SDHD* alone. Error bars represent standard deviation for duplicate experiments. *p<0.05, **p<0.01.

Gene expression changes characteristic for SDH-related PGL/PCC by the combined loss of *SDHD* and *SLC22A18* or *CDKN1C*

SDHD PGLs display distinctive gene expression patterns compared to paragangliomas and pheochromocytomas linked to other genes. Unsupervised hierarchical cluster analysis of gene expression in SNB19 and SHSY5Y cells showed that while cell type is the primary determinant of clustering (Supplemental Figure 3), a large number of genes are significantly differentially expressed in both SNB19 cells and SHSY5Y cells depending on single *SDHD*, or double knockdown together with *SLC22A18* or *CDKN1C*. Focusing on pathways believed to play a role in PGL/PCC (12;13) and exploiting the pathway database KEGG, we selected functional gene sets for analysis, including oxidative phosphorylation, citrate cycle (TCA cycle), apoptosis, glycolysis, VEGF signaling pathway, pathways in cancer including HIF, glutathione metabolism and beta-alanine metabolism.

Analysis using the global test revealed a synchronized suppression of mitochondrial functions in *SDHD* knockdown SNB19 cells compared to scrambled control cells, characterized by significant differential expression of components of the oxidative response and TCA cycle (Table 2). Interestingly, double knockdown of *SDHD* together with either *CDKN1C* or *SLC22A18* in SNB19 cells led to greater (significant) differential expression of additional PGL/PCC-associated pathways (Table

2). These changes were not observed in SHSY5Y cells using the global test (Supplemental Figure 3). To identify further cellular functions that might be affected by the observed gene expression changes, we performed a series of comparisons using Ingenuity Pathway Analysis (IPA). This analysis revealed that double knockdown of *SDHD* and *SLC22A18* or of *SDHD* and *CDKN1C* strongly decreased apoptosis and cell death-associated gene expression in both SNB19 cells (Fig. 7A) and SHSY5Y cells (Fig. 7B), compared to single *SDHD* knockdown. In addition, both double knockdowns induced gene expression signatures for increased cell proliferation and cell survival compared to single *SDHD* knockdown.

Table 2. Global test of KEGG pathways in three SNB19 cell subgroups

Pathway ID	KEGG pathway name	Number of genes	P-value Control vs SDHD shRNA	P-value Control vs SDHD + CDKN1C shRNA	P-value Control vs SDHD + SLC22A18 shRNA
00190	Oxidative phosphorylation	158	0,002	0,001	0,005
00020	Citrate cycle	50	0,002	0,0005	0,01
00410	beta-Alanine metabolism	34	0,05	0,04	0,01
04210	Apoptosis	151	0,1	0,00002	0,003
00480	Glutathione metabolism	83	0,9	0,1	0,01
00010	Glycolysis	122	0,9	0,5	0,5
05200	Pathways in cancer	601	1	0,008	0,05
04370	VEGF signaling pathway	130	1	0,2	0,1

Number of genes indicates the number of genes involved in the KEGG pathway. P-value is corrected for multiple testing using Benjamini–Hochberg, as described in Material and Methods.

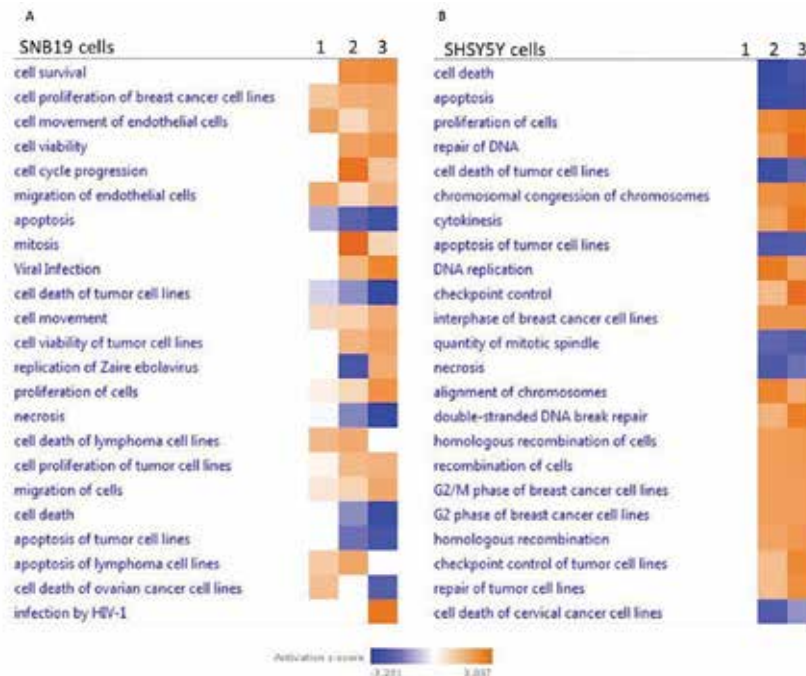


Figure 7. Comparison between the cell subgroups in functional classifications. (A) Heatmap of functional classifications associated with different SNB19 and (B) SHSYSY cell subgroups, selected by IPA. Changes in gene expression of cellular functions for the 3 subgroup comparisons are included in this analysis. 1= scrambled control cells versus knockdown of *SDHD*. 2= scrambled control cells versus knockdown of *SDHD* and *CDKN1C*. 3= scrambled control cells versus knockdown of *SDHD* and *SLC22A18*. Double knockdown of *SDHD* and *SLC22A18* or of *SDHD* and *CDKN1C* strongly decreased apoptosis and cell death-associated gene expression in both SNB19 and SHSYSY cells, and increased cell proliferation and cell survival-related gene expression when compared to single knockdown of *SDHD*. Orange indicates increased and blue indicates decreased Z-scores.

Protein expression of SLC22A18 and CDKN1C and somatic mutation analysis in SDHD mutant tumors without loss of chromosome 11

Most *SDHD*-linked HNPGLs show loss of the entire maternal copy of chromosome 11 (16-18), effectively preventing further genetic or functional analysis of genes and gene products found on the maternal chromosome. However, surveying 60 *SDHD* mutant tumors, we identified four (6.6%) tumors that were heterozygous (no LOH) for microsatellite markers on chromosome 11, indicating retention of chromosome 11 (Fig 8A). Reasoning that retention of maternal chromosome 11 would lead to an alternative pathway of inactivation of a bona fide *SDHD* modifier gene, we analyzed *SLC22A18* and *CDKN1C* protein loss in all 60 tumors by IHC. Interestingly, four tumors with retention of chromosome 11 showed similarly reduced expression levels of *SLC22A18* and *CDKN1C* compared to tumors showing loss of chromosome 11 (Fig 8B-C).

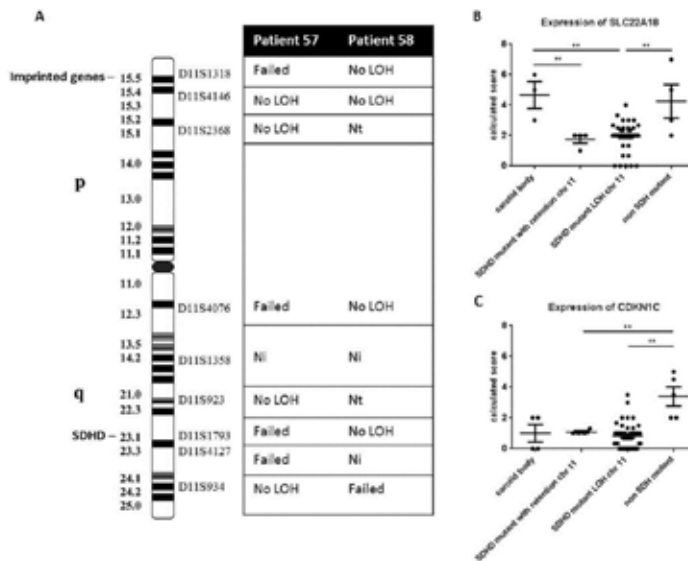


Figure 8. *SDHD* mutant tumors with retention of chromosome 11. (A) Microsatellite markers located on chromosome 11 were used for LOH analyses. Summary of LOH results for two patients, indicating no LOH (e.g. retention) of chromosome 11, which was found in a total of four patients. Nt – not tested. Ni – not informative. (B) Dot plot presenting results of immunohistochemical SLC22A18 expression demonstrating a high expression in normal post-mortem carotid bodies and non-*SDHD* mutant tumors, including *RET*, *NF1* and *MEN1*-linked pheochromocytomas, which is significantly decreased in *SDHD* mutant paragangliomas with retention of chromosome 11 and loss of chromosome 11. (C) Dot plot presenting results of immunohistochemical CDKN1C expression demonstrating comparable expression levels in the 4 *SDHD*-linked tumors showing retention of chromosome 11 to *SDHD* mutant paragangliomas with LOH of chromosome 11 and significantly increased expression levels in non-*SDHD* mutant tumors. Data are represented as calculated mean score \pm standard error of the mean. ** $p < 0.01$.

To investigate whether somatic mutation in *CDKN1C* or *SLC22A18* might underlie protein loss, we analyzed all exons of both genes by Sanger sequencing. While no variants were found in *CDKN1C*, a missense variant was found in the coding region of *SLC22A18*, c.65G>A (p.Arg22Gln) in tumors and in normal matched DNAs in 2 cases. However, as this variant was frequent in a large population database (<http://exac.broadinstitute.org>), this variant is unlikely to explain *CDKN1C* or *SLC22A18* inactivation in this specific group of *SDHD* mutant PGLs/PCCs.

Discussion

Our goal in this study was to identify genes that, upon knockdown together with *SDHD*, would enhance cellular characteristics previously associated with paraganglioma/pheochromocytoma (PGL/PCC). The Hensen model postulates that tumor formation in *SDHD*-linked PGL/PCC occurs upon loss of the *SDHD* wild type gene together with a maternally-expressed tumor modifier gene probably located in the 11p15 region (17). Our evaluation of protein expression in the chief cell component of *SDHD*-mutated tumors showed that *KCNQ1* and *PHLDA2* were expressed and thus excluded as candidates, whereas *CDKN1C*, *SLC22A18* and *ZNF215* all showed loss of protein expression consistent with the Hensen model. The protein expression of the candidate genes *H19* (noncoding RNA) and *KCNQ1DN* (noncoding RNA) could not be explored for obvious reasons, or due to lack of reliable antibodies (*OSBPL5*).

Using two distinct neural-derived cell lines, we then developed stable single and double knockdowns of *SDHD* in combination with the candidate genes *OSBPL5*, *CDKN1C*, *SLC22A18* and *ZNF215*. Consistent with earlier reports (11;23;24), we showed knockdown of *SDHD* results in a disturbed metabolism indicated by changed levels of TCA cycle metabolites and ATP in cells, and by differential gene expression of components of the oxidative response and TCA cycle. We anticipated that *SDHD* gene knockdown together with the knockdown of the relevant 11p15 tumor modifier gene would enhance PGL-related cellular characteristics compared to *SDHD* knockdown alone. Indeed, additional knockdown produced small but significant increases in cell proliferation and apoptosis resistance. Although relatively modest enhancements, similar changes found in benign, slow-growing *SDHD* mutant PGLs are also small. Large changes would in fact be intrinsically suspect. Most importantly, comparative analysis of gene expression confirmed these broader functional differences by showing decreased levels of apoptosis and increased cell proliferation compared to single knockdown.

Results from the cell line-based functional assays were further supported by the finding that *SDHD* mutant tumors with either retention or loss of chromosome 11 showed equally low levels of *SLC22A18* and *CDKN1C* protein expression. *SDHx* mutations are associated with DNA hypermethylation and histone methylation (25), suggesting a possible mechanism underlying the lowered expression of *SLC22A18* and/or *CDKN1C* in *SDHD* mutant tumors with retention of chromosome 11.

A limitation of our *in vitro* work is that all observations were made with tumor cell lines that have already acquired genetic changes that endow them with tumorigenic growth properties. It is therefore remarkable that the knockdown of *SDHD* with or without concomitant knockdown of 11p15 candidate genes was nonetheless capable of causing additional cellular phenotypes resembling those found in primary PGLs (22). While it would have been more appropriate to perform knockdowns in normal carotid body cells, these are currently unavailable as *in vitro* cell lines. Likewise, reintroduction of *SDHD*, *SLC22A18* or *CDKN1C* into a PGL tumor cell line to revert the phenotype wasn't possible for the same reason.

The concept that *SDHD* knockdown (or knockout) alone is insufficient to trigger tumorigenesis in the carotid body is supported by work carried out in genetically engineered mice. No engineered mouse germline knockout of *Sdhb*, *Sdhc*, or *Sdhd* has developed tumors to date (26-28), and conditional tissue-specific homozygous knockout leads only to severe apoptotic loss of neuronal and chromaffin cells and early death of newborn mice (29). Starting from what we understand of *SDHD* PGLs in man

- the almost complete resistance to tumor development of carriers of maternally-inherited, and the loss of entire maternal chromosome 11 – we would argue that the loss of mitochondrial complex II activity in chromaffin cells can only be tolerated on a background of other genetic changes that allows them to overcome cellular lethality. Simultaneous loss of *SDHD* and *SLC22A8* and/or *CDKN1C* may create a favorable genetic landscape via a single genetic event, whole chromosome loss of chromosome 11 (30).

Loss-of-function mutations in *CDKN1C* are associated with Beckwith-Wiedemann syndrome, an overgrowth disorder related to disruption of imprinted expression of 11p15 (31). *CDKN1C*, encoding the cyclin-dependent kinase inhibitor 1C, inhibits cell cycle progression and may therefore lead to increased cell proliferation when lost in *SDHD* mutant PGLs. *SLC22A18* is a member of a family of polyspecific transporters and multidrug resistance genes and has been reported to be a tumor suppressor candidate and a substrate for RING105, a conserved E3 ubiquitin ligase (32). Genetic mutations in *SLC22A18* are rare, with isolated reports of point mutations in a breast cancer cell line (33), a rhabdomyosarcoma cell line (34), and Wilms' tumors and lung tumors (35;36). In glioma cells, *SLC22A18* has a pro-apoptotic function and confers drug resistance (37) and more recently, downregulation of *SLC22A18* in colorectal cancer cell lines has been shown to lead to slower growth by inducing G2/M arrest (38), supporting a role for *SLC22A18* as a tumor suppressor in certain cell types. Our results showed that the combined loss of *SDHD* and *SLC22A18* leads to apoptosis resistance and may, in combination with the increased cell proliferation, result in tumor formation in *SDHD* mutant PGLs. Future studies should address this mechanism, together with the triple knockdown of these genes to assess possible synergistic interactions.

In conclusion, this study has identified two credible candidate 11p15 tumor modifier genes that may be involved in *SDHD*-linked PGL/PCC, and provides further insight into the consequences of *SDHD* knockdown in cells with a neuronal background.

References

- (1) Lenders JW, Eisenhofer G, Mannelli M, Pacak K. Pheochromocytoma. *Lancet* 2005 August 20;366(9486):665-75.
- (2) Jansen JC, van den BR, Kuiper A, Van Der Mey AG, Zwinderman AH, Cornelisse CJ. Estimation of growth rate in patients with head and neck paragangliomas influences the treatment proposal. *Cancer* 2000 June 15;88(12):2811-6.
- (3) Burnichon N, Briere JJ, Libe R, Vescovo L, Riviere J, Tissier F, Jouanno E, Jeunemaitre X, Benit P, Tzagoloff A, Rustin P, Bertherat J, Favier J, Gimenez-Roqueplo AP. SDHA is a tumor suppressor gene causing paraganglioma. *Hum Mol Genet* 2010 August 1;19(15):3011-20.
- (4) Astuti D, Latif F, Dallol A, Dahia PL, Douglas F, George E, Skoldberg F, Husebye ES, Eng C, Maher ER. Gene mutations in the succinate dehydrogenase subunit SDHB cause susceptibility to familial pheochromocytoma and to familial paraganglioma. *Am J Hum Genet* 2001 July;69(1):49-54.
- (5) Niemann S, Muller U. Mutations in SDHC cause autosomal dominant paraganglioma, type 3. *Nat Genet* 2000 November;26(3):268-70.
- (6) Baysal BE, Ferrell RE, Willett-Brozick JE, Lawrence EC, Myssiorek D, Bosch A, van der MA, Taschner PE, Rubinstein WS, Myers EN, Richard CW, III, Cornelisse CJ, Devilee P, Devlin B. Mutations in SDHD, a mitochondrial complex II gene, in hereditary paraganglioma. *Science* 2000 February 4;287(5454):848-51.
- (7) Hao HX, Khalimonchuk O, Schraders M, Dephoure N, Bayley JP, Kunst H, Devilee P, Cremers CW, Schiffman JD, Bentz BG, Gygi SP, Winge DR, Kremer H, Rutter J. SDH5, a gene required for flavination of succinate dehydrogenase, is mutated in paraganglioma. *Science* 2009 August 28;325(5944):1139-42.
- (8) Koivunen P, Hirsila M, Remes AM, Hassinen IE, Kivirikko KI, Myllyharju J. Inhibition of hypoxia-inducible factor (HIF) hydroxylases by citric acid cycle intermediates - Possible links between cell metabolism and stabilization of HIF. *Journal of Biological Chemistry* 2007 February 16;282(7):4524-32.
- (9) Pollard PJ, Briere JJ, Alam NA, Barwell J, Barclay E, Wortham NC, Hunt T, Mitchell M, Olpin S, Moat SJ, Hargreaves IP, Heales SJ, Chung YL, Griffiths JR, Dalglish A, McGrath JA, Gleeson MJ, Hodgson SV, Poulson R, Rustin P, Tomlinson IP. Accumulation of Krebs cycle intermediates and over-expression of HIF1alpha in tumours which result from germline FH and SDH mutations. *Hum Mol Genet* 2005 August 1;14(15):2231-9.
- (10) Selak MA, Armour SM, MacKenzie ED, Boulahbel H, Watson DG, Mansfield KD, Pan Y, Simon MC, Thompson CB, Gottlieb E. Succinate links TCA cycle dysfunction to oncogenesis by inhibiting HIF-alpha prolyl hydroxylase. *Cancer Cell* 2005 January;7(1):77-85.
- (11) Xiao M, Yang H, Xu W, Ma S, Lin H, Zhu H, Liu L, Liu Y, Yang C, Xu Y, Zhao S, Ye D, Xiong Y, Guan KL. Inhibition of alpha-KG-dependent histone and DNA demethylases by fumarate and succinate that are accumulated in mutations of FH and SDH tumor suppressors. *Genes Dev* 2012 June 15;26(12):1326-38.
- (12) Dahia PL, Ross KN, Wright ME, Hayashida CY, Santagata S, Barontini M, Kung AL, Sanso G, Powers JF, Tischler AS, Hodin R, Heitritter S, Moore F, Dluhy R, Sosa JA, Ocal IT, Benn DE, Marsh DJ, Robinson BG, Schneider K, Garber J, Arum SM, Korbonits M, Grossman A, Pigny P et al. A HIF1alpha regulatory loop links hypoxia and mitochondrial signals in pheochromocytomas. *PLoS Genet* 2005 July;1(1):72-80.
- (13) Lopez-Jimenez E, Gomez-Lopez G, Leandro-Garcia LJ, Munoz I, Schiavi F, Montero-Conde C, De Cubas AA, Ramires R, Landa I, Leskela S, Maliszewska A, Inglada-Perez L, de I, V, Rodriguez-Antona C, Leton R, Bernal C, de Campos JM, Diez-Tascon C, Fraga MF, Boullosa C, Pisano DG, Opocher G, Robledo M, Cascon A. Research resource: Transcriptional profiling reveals different pseudohypoxic signatures in SDHB and VHL-related pheochromocytomas. *Mol Endocrinol* 2010 December;24(12):2382-91.
- (14) Kunst HP, Rutten MH, De Monnik JP, Hoefsloot LH, Timmers HJ, Marres HA, Jansen JC, Kremer H, Bayley JP, Cremers CW. SDHAF2 (PGL2-SDH5) and Hereditary Head and Neck Paraganglioma. *Clin Cancer Res* 2011 January 15;17(2):247-54.
- (15) Van Der Mey AG, Maaswinkel-Mooy PD, Cornelisse CJ, Schmidt PH, van de Kamp JJ. Genomic imprinting in hereditary glomus tumours: evidence for new genetic theory. *Lancet* 1989 December 2;2(8675):1291-4.
- (16) Dannenberg H, de Krijger RR, Zhao J, Speel EJ, Saremaslani P, Dinjens WN, Mooi WJ, Roth J, Heitz PU, Komminoth P. Differential loss of chromosome 11q in familial and sporadic parasymphathetic paragangliomas detected by comparative genomic hybridization. *Am J Pathol* 2001 June;158(6):1937-42.

- (17) Hensen EF, Jordanova ES, van Minderhout IJHM, Hogendoorn PCW, Taschner PEM, van der Mey AGL, Devilee P, Cornelisse CJ. Somatic loss of maternal chromosome 11 causes parent-of-origin-dependent inheritance in SDHD-linked paraganglioma and pheochromocytoma families. *Oncogene* 2004 May 20;23(23):4076-83.
- (18) Riemann K, Sotlar K, Kupka S, Braun S, Zenner HP, Preyer S, Pfister M, Pusch CM, Blin N. Chromosome 11 monosomy in conjunction with a mutated SDHD initiation codon in nonfamilial paraganglioma cases. *Cancer Genet Cytogenet* 2004 April 15;150(2):128-35.
- (19) Bayley JP, Oldenburg RA, Nuk J, Hoekstra AS, van der Meer CA, Korpershoek E, McGillivray B, Corssmit EP, Dinjens WN, de Krijger RR, Devilee P, Jansen JC, Hes FJ. Paraganglioma and pheochromocytoma upon maternal transmission of SDHD mutations. *BMC Med Genet* 2014;15:111.
- (20) Yeap PM, Tobias ES, Mavraki E, Fletcher A, Bradshaw N, Freel EM, Cooke A, Murday VA, Davidson HR, Perry CG, Lindsay RS. Molecular Analysis of Pheochromocytoma after Maternal Transmission of SDHD Mutation Elucidates Mechanism of Parent-of-Origin Effect. *J Clin Endocrinol Metab* 2011 September 21.
- (21) van Nederveen FH, Gaal J, Favier J, Korpershoek E, Oldenburg RA, de Bruyn EM, Sleddens HF, Derkx P, Riviere J, Dannenberg H, Petri BJ, Komminoth P, Pacak K, Hop WC, Pollard PJ, Mannelli M, Bayley JP, Perren A, Niemann S, Verhofstad AA, de Bruine AP, Maher ER, Tissier F, Meatchi T, Badoual C et al. An immunohistochemical procedure to detect patients with paraganglioma and pheochromocytoma with germline SDHB, SDHC, or SDHD gene mutations: a retrospective and prospective analysis. *Lancet Oncol* 2009 August;10(8):764-71.
- (22) Dekker PB, Kuipers-Dijkshoorn N, Hogendoorn PC, Van Der Mey AG, Cornelisse CJ. G2M arrest, blocked apoptosis, and low growth fraction may explain indolent behavior of head and neck paragangliomas. *Hum Pathol* 2003 July;34(7):690-8.
- (23) Imperiale A, Moussallieh FM, Sebag F, Brunaud L, Barlier A, Elbayed K, Bachellier P, Goichot B, Pacak K, Namer IJ, Taieb D. A new specific succinate-glutamate metabolomic hallmark in SDHx-related paragangliomas. *PLoS One* 2013;8(11):e80539.
- (24) Rao JU, Engelke UF, Rodenburg RJ, Wevers RA, Pacak K, Eisenhofer G, Qin N, Kusters B, Goudswaard AG, Lenders JW, Hermus AR, Mensenkamp AR, Kunst HP, Sweep FC, Timmers HJ. Genotype-specific abnormalities in mitochondrial function associate with distinct profiles of energy metabolism and catecholamine content in pheochromocytoma and paraganglioma. *Clin Cancer Res* 2013 July 15;19(14):3787-95.
- (25) Hoekstra AS, de Graaff MA, Briaire-de Bruijn IH, Ras C, Seifar RM, van M, I, Cornelisse CJ, Hogendoorn PC, Breuning MH, Suijker J, Korpershoek E, Kunst HP, Frizzell N, Devilee P, Bayley JP, Bovee JV. Inactivation of SDH and FH cause loss of 5hmC and increased H3K9me3 in paraganglioma/pheochromocytoma and smooth muscle tumors. *Oncotarget* 2015 November 17;6(36):38777-88.
- (26) Letouze E, Martinelli C, Lorient C, Burnichon N, Abermil N, Ottolenghi C, Janin M, Menara M, Nguyen AT, Benit P, Buffet A, Marcaillou C, Bertherat J, Amar L, Rustin P, De RA, Gimenez-Roqueplo AP, Favier J. SDH mutations establish a hypermethylator phenotype in paraganglioma. *Cancer Cell* 2013 June 10;23(6):739-52.
- (27) Miyazawa M, Ishii T, Kirinashizawa M, Yasuda K, Hino O, Hartman PS, Ishii N. Cell growth of the mouse SDHC mutant cells was suppressed by apoptosis throughout mitochondrial pathway. *Biosci Trends* 2008 February;2(1):22-30.
- (28) Piruat JJ, Pintado CO, Ortega-Saenz P, Roche M, Lopez-Barneo J. The mitochondrial SDHD gene is required for early embryogenesis, and its partial deficiency results in persistent carotid body glomus cell activation with full responsiveness to hypoxia. *Mol Cell Biol* 2004 December;24(24):10933-40.
- (29) Lepoutre-Lussey C, Thibault C, Buffet A, Morin A, Badoual C, Benit P, Rustin P, Ottolenghi C, Janin M, Castro-Vega LJ, Trapman J, Gimenez-Roqueplo AP, Favier J. From Nf1 to Sdhb knockout: Successes and failures in the quest for animal models of pheochromocytoma. *Mol Cell Endocrinol* 2016 February 5;421:40-8.
- (30) Hoekstra AS, Devilee P, Bayley JP. Models of parent-of-origin tumorigenesis in hereditary paraganglioma. *Semin Cell Dev Biol* 2015 July;43:117-24.
- (31) Brioude F, Netchine I, Praz F, Le JM, Calmel C, Lacombe D, Edery P, Catala M, Odent S, Isidor B, Lyonnet S, Sigaudy S, Leheup B, Audebert-Bellanger S, Burglen L, Giuliano F, Alessandri JL, Cormier-Daire V, Laffargue F, Blesson S, Coupier I, Lespinasse J, Blanchet P, Boute O, Baumann C et al. Mutations of the Imprinted CDKN1C Gene as a Cause of the Overgrowth Beckwith-Wiedemann

- Syndrome: Clinical Spectrum and Functional Characterization. *Hum Mutat* 2015 September;36(9):894-902.
- (32) Yamada HY, Gorbsky GJ. Tumor suppressor candidate TSSC5 is regulated by Ubch6 and a novel ubiquitin ligase RING105. *Oncogene* 2006 March 2;25(9):1330-9.
- (33) Gallagher E, Mc GA, Chung WY, Mc CO, Harrison M, Kerin M, Dervan PA, Mc CA. Gain of imprinting of SLC22A18 sense and antisense transcripts in human breast cancer. *Genomics* 2006 July;88(1):12-7.
- (34) Schwienbacher C, Sabbioni S, Campi M, Veronese A, Bernardi G, Menegatti A, Hatada I, Mukai T, Ohashi H, Barbanti-Brodano G, Croce CM, Negrini M. Transcriptional map of 170-kb region at chromosome 11p15.5: identification and mutational analysis of the BWR1A gene reveals the presence of mutations in tumor samples. *Proc Natl Acad Sci U S A* 1998 March 31;95(7):3873-8.
- (35) Lee MP, Reeves C, Schmitt A, Su K, Connors TD, Hu RJ, Brandenburg S, Lee MJ, Miller G, Feinberg AP. Somatic mutation of TSSC5, a novel imprinted gene from human chromosome 11p15.5. *Cancer Res* 1998 September 15;58(18):4155-9.
- (36) Schwienbacher C, Angioni A, Scelfo R, Veronese A, Calin GA, Massazza G, Hatada I, Barbanti-Brodano G, Negrini M. Abnormal RNA expression of 11p15 imprinted genes and kidney developmental genes in Wilms' tumor. *Cancer Res* 2000 March 15;60(6):1521-5.
- (37) Chu SH, Ma YB, Feng DF, Zhang H, Qiu JH, Zhu ZA. Elevated expression of solute carrier family 22 member 18 increases the sensitivity of U251 glioma cells to BCNU. *Oncol Lett* 2011 November;2(6):1139-42.
- (38) Jung Y, Jun Y, Lee HY, Kim S, Jung Y, Keum J, Lee YS, Cho YB, Lee S, Kim J. Characterization of SLC22A18 as a tumor suppressor and novel biomarker in colorectal cancer. *Oncotarget* 2015 September 22;6(28):25368-80.
- (39) Margetts CDE, Astuti D, Gentle DC, Cooper WN, Cascon A, Catchpoole D, Robledo M, Neumann HPH, Latif F, Maher ER. Epigenetic analysis of HIC1, CASP8, FLIP, TSP1, DCR1, DCR2, DR4, DR5, KvDMR1, H19 and preferential 11p15.5 maternal-allele loss in von Hippel-Lindau and sporadic pheochromocytomas. *Endocrine-Related Cancer* 2005 March;12(1):161-72.
- (40) Li LC, Dahiya R. MethPrimer: designing primers for methylation PCRs. *Bioinformatics* 2002 November;18(11):1427-31.
- (41) Lewin J, Schmitt AO, Adorjan P, Hildmann T, Piepenbrock C. Quantitative DNA methylation analysis based on four-dye trace data from direct sequencing of PCR amplicates. *Bioinformatics* 2004 November 22;20(17):3005-12.
- (42) Carlotti F, Bazuine M, Kekalainen T, Seppen J, Pogoniec P, Maassen JA, Hoeben RC. Lentiviral vectors efficiently transduce quiescent mature 3T3-L1 adipocytes. *Mol Ther* 2004 February;9(2):209-17.
- (43) Livak KJ, Schmittgen TD. Analysis of relative gene expression data using real-time quantitative PCR and the 2⁻(Delta Delta C(T)) Method. *Methods* 2001 December;25(4):402-8.
- (44) Du P, Kibbe WA, Lin SM. lumi: a pipeline for processing Illumina microarray. *Bioinformatics* 2008 July 1;24(13):1547-8.
- (45) Smyth GK, Michaud J, Scott HS. Use of within-array replicate spots for assessing differential expression in microarray experiments. *Bioinformatics* 2005 May 1;21(9):2067-75.
- (46) Goeman JJ, van de Geer SA, de KF, van Houwelingen HC. A global test for groups of genes: testing association with a clinical outcome. *Bioinformatics* 2004 January 1;20(1):93-9.
- (47) Manoli T, Gretz N, Grone HJ, Kenzelmann M, Eils R, Brors B. Group testing for pathway analysis improves comparability of different microarray datasets. *Bioinformatics* 2006 October 15;22(20):2500-6.
- (48) Ogata H, Goto S, Sato K, Fujibuchi W, Bono H, Kanehisa M. KEGG: Kyoto Encyclopedia of Genes and Genomes. *Nucleic Acids Res* 1999 January 1;27(1):29-34.
- (49) Hensen EF, Goeman JJ, Oosting J, Van Der Mey AG, Hogendoorn PC, Cremers CW, Devilee P, Cornelisse CJ. Similar gene expression profiles of sporadic, PGL2-, and SDHD-linked paragangliomas suggest a common pathway to tumorigenesis. *BMC Med Genomics* 2009;2:25.
- (50) Hochberg Y, Benjamini Y. More powerful procedures for multiple significance testing. *Stat Med* 1990 July;9(7):811-8.
- (51) Vindelov LL, Christensen IJ, Nissen NI. A detergent-trypsin method for the preparation of nuclei for flow cytometric DNA analysis. *Cytometry* 1983 March;3(5):323-7.
- (52) Lorenz MA, Burant CF, Kennedy RT. Reducing time and increasing sensitivity in sample preparation for adherent mammalian cell metabolomics. *Anal Chem* 2011 May 1;83(9):3406-14.

- (53) Canelas AB, ten PA, Ras C, Seifar RM, van Dam JC, van Gulik WM, Heijnen JJ. Quantitative evaluation of intracellular metabolite extraction techniques for yeast metabolomics. *Anal Chem* 2009 September 1;81(17):7379-89.
- (54) Seifar RM, Ras C, van Dam JC, van Gulik WM, Heijnen JJ, van Winden WA. Simultaneous quantification of free nucleotides in complex biological samples using ion pair reversed phase liquid chromatography isotope dilution tandem mass spectrometry. *Anal Biochem* 2009 May 15;388(2):213-9.

Supplementary data

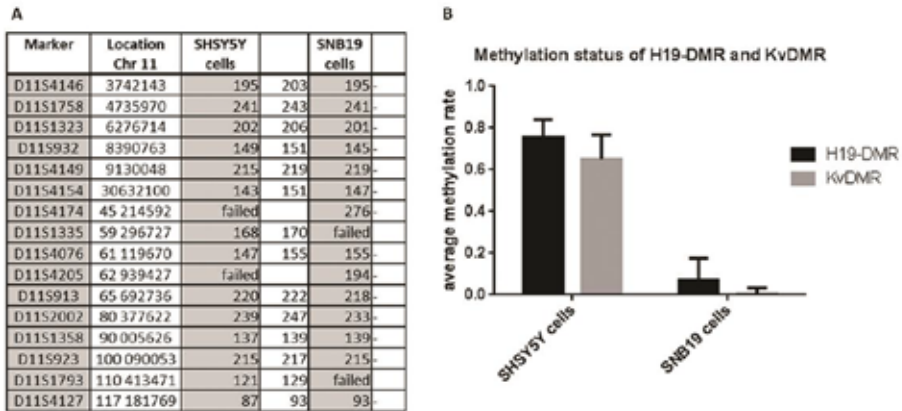


Figure S1. (A) SHSY5Y cells were heterozygous for chromosome 11 as detected by microsatellite markers, while SNB19 cells were homozygous for chromosome 11. (B) SHSY5Y cells showed an average methylation rate of 0.75 ± 0.08 for H19-DMR and 0.65 ± 0.1 for KvDMR, resulting in a ratio of 1.1. The average methylation rate for H19-DMR in SNB19 cells was 0.1 ± 0.1 , while the average methylation rate for KvDMR 0.005 ± 0.03 .

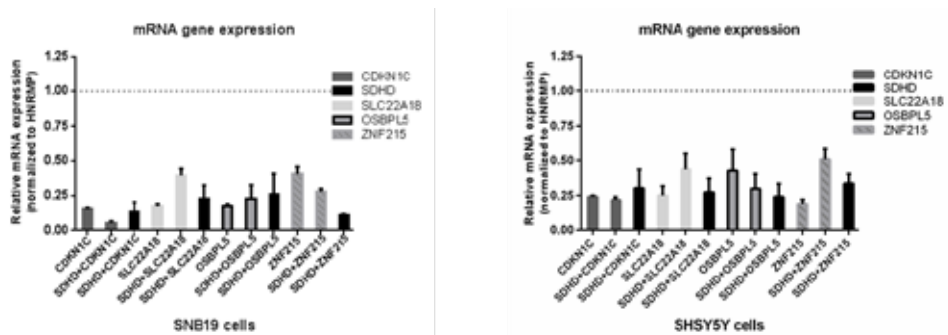
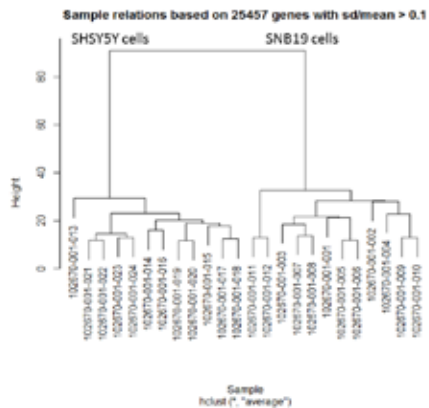


Figure S2. mRNA expression of *CDKN1C*, *SLC22A18*, *OSBP15*, *ZNF215* and *SDHD* in SNB19 and SHSY5Y cells. SNB19 and SHSY5Y cells with stable knockdown of *CDKN1C*, *SLC22A18*, *OSBP15*, or *ZNF215* using lentival shRNA and in combination with knockdown of *SDHD* results in decreased mRNA expression of *CDKN1C*, *SLC22A18*, *OSBP15*, *ZNF215* and *SDHD* compared to scrambled control cells (dashed line).



Pathway ID	KEGG pathway name	Number of genes	P-value Control vs SDHD shRNA	P-value Control vs SDHD + CDKN1C shRNA	P-value Control vs SDHD + SLC22A18 shRNA
00190	Oxidative phosphorylation	158	0,3	0,2	0,1
00020	Citrate cycle	50	0,3	0,03	0,05
00410	beta Alanine metabolism	34	0,6	0,2	0,2
04210	Apoptosis	151	0,6	0,2	0,3
00480	Glutathione metabolism	83	0,6	0,2	0,1
00010	Glycolysis	122	0,6	0,2	0,2
05200	Pathways in cancer	601	0,6	0,2	0,3
04370	VEGF signaling pathway	130	0,6	0,2	0,3

Figure S3. Unsupervised hierarchical cluster analysis of all cells revealed two dominant expression clusters, one including all SHSY5Y samples and the other consisting of all SNB19 samples. Pathway-based analysis using the global test on pathways described in Kyoto Encyclopedia of Genes and Genomes (KEGG) revealed no significant differences between SHSY5Y cells with *SDHD* knockdown versus control cells (scrambled shRNA), whereas *SDHD+CDKN1C* knockdown or *SDHD+SLC22A18* knockdown cells compared to scrambled control cells showed significant differential expression of components of the TCA cycle.

CHAPTER 4

Loss of maternal chromosome 11 is a signature event in SDHAF2, SDHD, and VHL-related paragangliomas, but less significant in SDHB-related paragangliomas

Attje S Hoekstra¹, Erik F Hensen², Ekaterina S Jordanova³, Esther Korpershoek⁴, Anouk NA van der Horst-Schrivers⁵, Eleonora PM Corssmit⁶, Frederik J Hes⁷, Jeroen C Jansen⁸, Henricus PM Kunst⁹, Henri JLM Timmers¹⁰, Adrian Bateman¹¹, Diana Eccles¹², Judith VMG Bovée³, Peter Devilee^{1,3}, Jean-Pierre Bayley¹

¹ Department of Human Genetics, Leiden University Medical Center, Leiden, The Netherlands

² Department of Otolaryngology/ Head and Neck Surgery, VU University Medical Center, Amsterdam, The Netherlands

³ Department of Pathology, Leiden University Medical Center, Leiden, The Netherlands

⁴ Department of Pathology, Josephine Nefkens Institute, Erasmus Medical Center Rotterdam, Rotterdam, The Netherlands

⁵ Department of Endocrinology, University of Groningen, University Medical Center Groningen, Groningen, The Netherlands

⁶ Department of Endocrinology and Metabolic Diseases, Leiden University Medical Center, Leiden, The Netherlands

⁷ Department of Clinical Genetics, Leiden University Medical Center, Leiden, The Netherlands

⁸ Department of Otorhinolaryngology, Leiden University Medical Center, Leiden, The Netherlands

⁹ Department of Otorhinolaryngology, Head and Neck Surgery, Radboud University Nijmegen Medical Centre, Nijmegen, The Netherlands

¹⁰ Department of Medicine, Division of Endocrinology, Radboud University Nijmegen Medical Centre, Nijmegen, The Netherlands

¹¹ Department of Cellular Pathology, University Hospital Southampton, Southampton, UK

¹² University of Southampton School of Medicine, Cancer Sciences Division, Somers Cancer Research Building, Southampton, UK

Submitted

Abstract

Germline mutations in the succinate dehydrogenase (SDHA, SDHB, SDHC, SDHD, SDHAF2) or Von Hippel-Lindau (VHL) genes cause hereditary paraganglioma/pheochromocytoma. While *SDHB* (1p36) and *VHL* (3p25) are associated with autosomal dominant disease, *SDHD* (11q23) and *SDHAF2* (11q13) show a remarkable parent-of-origin effect whereby tumor formation is almost completely dependent on paternal transmission of the mutant allele. Loss of the entire maternal copy of chromosome 11 occurs frequently in *SDHD*-linked tumors, and has been suggested to be the basis for this typical inheritance pattern.

Using fluorescent in situ hybridization, microsatellite marker and SNP array analysis, we demonstrate that loss of the entire copy of chromosome 11 is also frequent in *SDHAF2*-related PGLs, occurring in 89% of tumors. Analysis of two imprinted differentially methylated regions (DMR) in 11p15, H19-DMR and KvDMR, showed that this loss always affected the maternal copy of chromosome 11. Likewise, loss of maternal chromosome 11p15 was demonstrated in 85% of *SDHD* and 75% of *VHL*-related PGLs/PCCs. By contrast, both copies of chromosome 11 were found to be retained in 62% of *SDHB*-mutated PGLs/PCCs, while only 31% showed loss of maternal chromosome 11p15. Genome-wide copy number analysis revealed frequent loss of 1p in *SDHB* mutant tumors and indicated that *SDHB* tumors show greater genomic instability compared to *SDHD* and *SDHAF2*.

These results show that loss of the entire copy of maternal chromosome 11 is a highly specific and statistically significant event in *SDHAF2*, *SDHD* and *VHL*-related PGLs/PCCs, but is less significant in *SDHB*-mutated tumors, suggesting that these tumors have a distinct genetic etiology.

Introduction

Paragangliomas (PGLs) are neuroendocrine tumors derived from cells of the parasympathetic or sympathetic ganglia. Parasympathetic PGLs occur most commonly in the head and neck region (carotid body, glomus jugulare, and glomus tympanicum), are typically benign, and are rarely associated with catecholamine secretion (1;2). PGLs arising from the sympathetic ganglia occur in the abdomen and thorax, often secrete catecholamines, and are associated with a higher risk of malignancy. Pheochromocytomas (PCCs) are generally benign paragangliomas that arise in the chromaffin cells of the adrenal medulla, but are frequently associated with hypertension due to excessive catecholamine secretion (3).

Germline mutations in genes encoding subunits of succinate dehydrogenase (SDH, complex II of the mitochondrial respiratory chain) are the most common genetic cause of PGL/PCC, occurring in up to 25% of all cases (4;5). SDH is a heterotetramer consisting of two catalytic subunits, SDHA and SDHB, and two membrane-spanning subunits, SDHC and SDHD. SDHAF2 encodes an accessory factor required for the flavination of SDHA. SDH is an essential component of the tricarboxylic acid (TCA) cycle and the mitochondrial respiratory chain. A puzzling aspect of *SDHx*-related disease is that despite the close functional relationship of the SDH proteins, mutations lead to marked differences in both tumor location and clinical phenotype.

Another striking difference is that only mutations in *SDHD* and *SDHAF2*, both located on chromosome 11, show a parent-of-origin inheritance effect in which carriers develop tumors almost exclusively following paternal transmission of the mutation (6;7). An important role in causing this inheritance pattern has been ascribed to the loss of the entire *maternal* copy of chromosome 11 in *SDHD*-linked tumors. A cluster of maternally expressed imprinted genes is located on chromosome 11p15, which formed the basis for a hypothesis now known as the 'Hensen model'. The model proposes that maternal chromosomal 11 loss results in the simultaneous deletion of the *SDHD* wild type gene and an as yet unidentified exclusively maternally expressed gene (or genes), resulting in tumor formation (7). This hypothesis predicts that loss of the maternal copy of chromosome 11 might be similarly important for *SDHAF2*-linked tumors, but has yet to be demonstrated.

To further clarify the role of loss of the maternal copy of 11p in relation to loss of the long arm of chromosome 11 in paragangliomas, we used several genetic approaches to determine the allelic status of chromosome 11 in *SDHAF2*, *SDHD*, *SDHB*, and *VHL* mutant PGLs/PCCs. *SDHB* and *VHL*-related tumors were included because these genes map to other chromosomes than 11. The results show that tumorigenesis in *SDHAF2*-related tumors are fully compatible with the Hensen model, and that 11p loss is less important in *SDHB*-related tumors than for the other three tumor subgroups.

Material and methods

Patients and samples

A total of 44 formalin-fixed, paraffin-embedded (FFPE) tissue samples of PGL/PCC from 41 different patients were used for DNA extraction, including 12 *SDHB*, 16 *SDHD*, 9 *SDHAF2* and 8 *VHL*-related tumors. In addition, we included 12 fresh frozen tumor samples for DNA extraction; 11 *SDHD* and 1 *SDHB*-mutated tumors. The histology of all tumors was reviewed (JVMGB, JPB, ASH) and the mutation detection was confirmed by routine *SDHA* and *SDHB* immunohistochemical staining (Supplemental Figure 1), as described previously (8). For 7 *SDHAF2* mutant tumors and 4 *SDHB* mutant tumors, paired blood lymphocyte DNA samples were available. In addition, parental blood lymphocyte DNA was available for 3 *SDHAF2*-linked patients. Following the original identification of the *SDHAF2* mutation, c.232G>A, p.Gly78Arg, all patients were analyzed by sequencing for the presence of the mutation (9). The following primers were used for the amplification of exon 2 of the *SDHAF2* gene: 5'-GTTGACCTTCCCAGGCTC-3' (forward) and 5'-GAGGTTACGCTGCTTTTCTG-3' (reverse). Thirty nanograms of genomic DNA from each patient was amplified, and primer annealing was performed at 58°C. PCR fragments were purified using the Nucleospin gel and PCR clean-up kit (Macherey-Nagel). Sequencing was performed using standard protocols. Sequences were analyzed using the Mutation Surveyor software package (Softgenetics).

The *SDHB*-related samples were obtained from Radboud UMC, Nijmegen, The Netherlands, from UMCG, Groningen, The Netherlands and from University Hospital Southampton, UK. *SDHD*-related samples were obtained from the LUMC, Leiden, The Netherlands. *SDHAF2*-related samples were obtained from Radboud UMC and LUMC. *VHL*-related samples were obtained from the Erasmus MC, Rotterdam, The Netherlands. Written informed consent was obtained for DNA testing, further analyses and publication of all results, according to protocols approved by the Ethics Committees of the Erasmus MC, Radboud UMC, and University Hospital Southampton. Tissues from UMCG were used anonymously in accordance with the code for adequate secondary use of tissue, code of conduct: "Proper Secondary Use of Human Tissue" established by the Dutch Federation of Medical Scientific Societies (<http://www.federa.org>). Oral informed consent was obtained from patients according to protocols approved by the Ethics Committees of the LUMC, Protocol P12.082.

Triple colour interphase FISH on nuclei isolated from paraffin-embedded tissue

The PUC1.77 probe for the centromeric alphoid repeat DNA of chromosomes 1 was kindly provided by Dr J Wiegant (Department of Molecular Cell Biology, LUMC, Leiden, The Netherlands) (10;11). The BAC probes 371C18 (telomere 11p) and 469N6 (telomere 11q) were obtained from the Children's Hospital Oakland Research Institute (Peter de Jong BAC library RP11). All probes were labelled by standard nick translation with biotin-16-aUTP, digoxigenin-11-dUTP or fluorescein-12-dUTP (Roche, Basel, Switzerland).

Isolation of intact nuclei, hybridization and immunodetection were performed as previously described (12), with some modifications. The hybridization mix contained 50% formamide, 3 ng/ μ l of each of the three probes (either PUC1.77, pLC11A and 3F7 or PUC1.77, 371C18 and 469N6) and a 50-fold excess of human Cot-1 DNA (Invitrogen Life tech., Paisley, UK). A volume of 5 μ l of the mix was applied directly onto the slides and covered with an 18x18 mm² coverslip. After a denaturation step of 8 min at 80°C, the slides were incubated overnight at 37°C in a moisture chamber. A total of 200

nuclei were analysed for each sample and probe combination by two independent investigators (EFH and ESJ).

LOH analysis by microsatellite genotyping

Representative tumor areas from FFPE samples were selected to punch 3 cores of 0.6 mm in diameter for DNA isolation. Microdissection was performed on 8 *SDHB*-related tumors, using a total of two 10µm thick sections for each case. A tumor percentage of greater than 80% was achieved for all tumors. FFPE and fresh frozen tumor samples were incubated overnight with proteinase K at 60°C and DNA was isolated using the Qiagen FFPE DNA kit or QIAamp DNA Mini Kit (Qiagen Benelux B.V., Venlo, The Netherlands), respectively, according to the manufacturer's instructions. Tumor and blood samples were genotyped for microsatellite markers located on chromosome 11, as described in the results section. For each marker, 40 ng of DNA was amplified over 40 cycles using FastStar Taq DNA Polymerase (Roche). Forward primers were labeled with 6-FAM, HEX or NED fluorophore (Sigma-Aldrich, St. Louis, MO, USA). Amplicons of microsatellite markers were run on an ABI 3730 genetic analyzer and data were analyzed using Gene Marker software (Soft Genetics, State College, PA 16803, USA), using ABI GeneScan Rox 400 as the internal size standards. LOH was calculated using the allelic imbalance ratio: $AIR = (Tumor1/Tumor2)/(Normal1/Normal2)$. Tumors were regarded as positive for LOH when the mean allele ratio between tumor and blood was <0.7 for all informative markers, as described earlier (13). In cases where no matching blood lymphocyte DNA sample was available, allele peak ratios were compared to DNA samples with the same or very similar allele combinations. Some markers were either not informative in the patient or did not perform well enough on tumor DNA samples to give a reliable result and were therefore excluded.

Methylation analysis of H19-DMR and KvDMR

Bisulfite conversion of 250 ng of tumor DNA was performed with the EZ DNA Methylation Kit (Zymo Research, Irvine, CA, USA) according to the manufacturer's instructions. Bisulfite treated DNA was amplified by PCR with primers specific for modified DNA, designed using Methprimer (14). Primer sequences for the H19-DMR were 5'-GGTTT TAGTGTGAAATTTTTT-3' (forward) and 5'-CCATAAATATCCTATTCCTCCCAATAAC-3' (reverse) and for the KvDMR 5'-TTGAGGAGTTTTTGGAGGTT-3' (forward) and 5'-ACCC AACCAATACCTCATAC-3' (reverse). The PCR program consisted of an initial denaturation step at 94°C for 15 minutes followed by 44 cycles of 20 seconds at 94°C, 30 seconds at 55°C for the KvDMR and 52.5°C for the H19-DMR, followed by 5 minutes at 72°C. PCR fragments were purified using the Nucleospin gel and PCR clean-up kit (Macherey-Nagel, Düren, Germany). Sanger sequencing was performed using standard protocols and methylation rates were evaluated using ESME software (15).

Oncoscan analysis

Twelve *SDHD*, four *SDHAF2*, nine *SDHB*, and three *VHL* mutant tumors (Supplemental Table 1) were further investigated for whole genome copy number by OncoScan analysis (molecular inversion probe technology), as described in (16). This array consists of ~335.000 probes of which the majority (~283.000) are SNP-based. DNA was processed by the Affymetrix Research Services Laboratory (Santa Clara, California, USA) using the OncoScan™ FFPE Assay. The normalized OncoScan data (2Log (test/reference)-ratios and B-allele frequency plots) were analyzed with the Nexus Express software version 3.1 (Biodiscovery, Inc, El Segundo, California, USA) for copy number calling.

Statistical analysis

IBM SPSS Statistics 20.0 for Windows software package (SPSS, Armonk, NY: IBM Corp) was used to analyze the results. Statistical significance between two groups was determined by Mann-Whitney U test. $P < 0.05$ was considered statistically significant.

Results

Loss of heterozygosity in SDHAF2-related PGL

Since *SDHAF2*-related PGLs show a parent-of-origin effect, similar to *SDHD* mutations (7), we hypothesized that their tumorigenesis might also critically depend on loss of the maternal copy of chromosome 11. We first established *SDHAF2* mutation status in germline DNA from 9 patients from *SDHAF2*-related families. All patients showed a missense mutation of *SDHAF2*, c.232G>A (p.Gly78Arg), in a conserved region of the gene (9). We then sequenced DNA isolated from tumors of all nine patients, and compared this to matched DNA from blood samples. This comparison showed that the wild type allele (guanine (G) nucleotide – arrow, Figure 1A) is underrepresented in tumor DNA (Figure 1B), and the mutant allele is (adenine (A) nucleotide) overrepresented, indicating loss of the wild type allele (loss of heterozygosity - LOH) in the tumor. Partial retention of the wild type allele is characteristic of LOH in PGLs, and is due to admixture with normal cells that proliferate together with tumor cells (17).

Loss of chromosome 11 in SDHAF2-related PGL

To investigate whether the entire copy of chromosome 11 is lost in *SDHAF2*-related tumors, we performed fluorescence in situ hybridization (FISH) studies on 6 *SDHAF2*-linked tumors using a probe for the centromere of chromosome 1 as a ploidy reference as described earlier (7), and BAC probes for the subtelomeric regions of 11p and 11q. Simultaneous loss of both probes located on chromosome 11 relative to centromere 1 was found in all *SDHAF2*-related PGLs, in 15-44% of nuclei (Figure 1C, red and orange). Loss of one of the two probes located on chromosome 11 relative to the other was observed in only a very small minority of nuclei (<0.5%), demonstrating that the observed relative loss involves the entire copy of chromosome 11.

Parental origin of chromosomal loss in SDHAF2-related PGL

To further evaluate LOH in all *SDHAF2*-related tumors and study the parental origin of chromosomal loss, tumor DNA was analyzed for LOH using 24 highly polymorphic microsatellite markers selected from a custom microsatellite database. In the 9 *SDHAF2*-related PGLs investigated, 8 (89%) showed chromosome 11-wide LOH, with allelic imbalance ratios of <0.7 or >1.3 (Figure 1D). Parental blood DNA samples were available for 3 *SDHAF2*-related patients. Microsatellite analysis of parental DNA confirmed that the copy of chromosome 11 lost in all 3 *SDHAF2*-mutated tumors was maternal (Figure 1E).

Table 1. Methylation status of 11p15 imprinted regions KvDMR and H19-DMR in *SDHAF2* mutant PGLs with and without chr 11 LOH

Gene mutation and number	11p15 status	11q12 status	Methylation rate of tumor DNA	H19-DMR/KvDMR Methylation rate Ratio of tumor DNA	Methylation rate of matched blood DNA
<i>SDHAF2</i> (1)	LOH	LOH (maternal)	KvDMR: 0,07 H19-DMR: 0,57	8,1	
<i>SDHAF2</i> (2)	LOH	LOH	KvDMR: 0,01 H19-DMR: 0,94	>10	KvDMR: 0,59 H19 DMR: 0,52
<i>SDHAF2</i> (3)	LOH	LOH	KvDMR: 0,001 H19-DMR:0,82	>10	
<i>SDHAF2</i> (4)	LOH	n.i	KvDMR: 0,03 H19-DMR: 0,97	>10	
<i>SDHAF2</i> (5)	LOH	LOH (maternal)	KvDMR: 0,08 H19-DMR: 0,79	9,8	KvDMR: 0,47 H19 DMR: 0,53
<i>SDHAF2</i> (6)	No LOH	No LOH	KvDMR: 0,63 H19-DMR: 0,57	0,9	KvDMR: 0,57 H19 DMR: 0,54
<i>SDHAF2</i> (7)	LOH	LOH (maternal)	KvDMR: 0,22 H19-DMR: 0,81	3,7	KvDMR: 0,37 H19 DMR: 0,47
<i>SDHAF2</i> (8)	LOH	LOH	KvDMR: 0,03 H19-DMR: 0,9	>10	
<i>SDHAF2</i> (9)	LOH	LOH	KvDMR: 0,0001 H19-DMR: failed	-	

LOH: loss of heterozygosity, n.i: not informative

*Frequent loss of maternal chromosome 11 in *SDHD* and *VHL*-related tumors*

To investigate the extent and nature of chromosome 11 loss across the various paraganglioma subgroups, we assembled a panel of 26 *SDHD*, 13 *SDHB*, and 8 *VHL*-related PGLs/PCCs. Of the 26 *SDHD*-related tumors investigated using polymorphic microsatellite marker analysis, LOH at all informative markers of chromosome 11 was observed in 22 (85%) tumors (Table 2). In four *SDHD*-related tumors almost all markers showed allele ratios between 0.8 and 1, indicating retention of heterozygosity. Methylation analysis of H19-DMR and KvDMR demonstrated hypermethylation of H19-DMR and hypomethylation of KvDMR in all *SDHD* mutant PGLs with LOH for chromosome 11, consistent with loss of the maternal allele and significantly different from methylation rates of H19-DMR ($p=0.004$) and KvDMR ($p=0.002$) in blood DNA (Table 2). In the four *SDHD*-related tumors without chromosomal loss, the ratio of H19-DMR to KvDMR was 1, comparable to blood DNA.

All 8 *VHL*-associated PCCs demonstrated loss of chromosome 11 (Table 3), although in 3 tumors, microsatellite markers were uninformative at 11p15 or at 11q23, while other markers on chromosome 11 showed allelic imbalance ratios of <0.7 or >1.3.

Methylation status of H19-DMR and KvDMR revealed loss of the maternal copy of chromosome 11 in 6 of 8 (75%) *VHL*-associated PCCs (Table 3), while the methylation status of the H19-DMR could not be determined in 2 (25%) tumors. However, both these tumors showed hypomethylated KvDMR, suggestive of maternal allele loss.

Table 2. Methylation status of KvDMR and H19-DMR in *SDHD* mutant PGLs with and without chr 11 LOH

Gene mutation and number	11p15 status	11q23 status	KvDMR Methylation rate	H19-DMR Methylation rate	H19-DMR/KvDMR Methylation rate Ratio
<i>SDHD</i> (10)	LOH	LOH	0,01	0,62	>10
<i>SDHD</i> (11)	LOH	LOH	0,0	1,0	>10
<i>SDHD</i> (12)	LOH	LOH	0,01	0,96	>10
<i>SDHD</i> (13)	LOH	LOH	0,10	0,86	8,6
<i>SDHD</i> (14)	LOH	n.i	0,04	0,97	>10
<i>SDHD</i> (15)	LOH	LOH	0,07	1	>10
<i>SDHD</i> (16)	LOH	n.i	0,02	0,75	>10
<i>SDHD</i> (17)	n.i	LOH	0,03	0,45	>10
<i>SDHD</i> (18)	LOH	LOH	0,02	0,96	>10
<i>SDHD</i> (19)	LOH	n.i	0,0	0,91	>10
<i>SDHD</i> (20)	LOH	LOH	0,0	0,87	>10
<i>SDHD</i> (21)	LOH	LOH	0,08	0,76	>10
<i>SDHD</i> (22)	LOH	n.i	0,14	0,90	6,4

SDHD (23)	No LOH	No LOH	0,51	0,56	1
SDHD (24)	LOH	LOH	0,01	0,7	>10
SDHD (25)	LOH	LOH	0,04	0,86	>10
SDHD (26)	No LOH	No LOH	0,57	0,59	1
SDHD (27)	No LOH	No LOH	0,53	0,57	1
SDHD (28)	LOH	LOH	0,17	0,66	3,9
SDHD (29)	LOH	LOH	0,15	0,68	4,4
SDHD (30)	LOH	LOH	0,21	0,70	3,3
SDHD (31)	LOH	LOH	0,16	0,68	4,4
SDHD (32)	LOH	LOH	0,12	0,71	5,9
SDHD (33)	LOH	LOH	0,13	0,65	5,2
SDHD (34)	LOH	LOH	0,11	0,70	6,4
SDHD (35)	LOH	LOH	0,13	0,69	5,4
SDHD (36)	No LOH	No LOH	0,48	0,61	1,2

LOH: loss of heterozygosity, n.i: not informative

Table 3. Methylation status of KvDMR and H19-DMR in VHL mutant PCCs with and without chr 11 LOH

Gene mutation and number	11p15 status	11q23 status	KvDMR Methylation rate	H19-DMR Methylation rate	H19-DMR/KvDMR Methylation rate Ratio
VHL (37)	LOH	n.i	0	0,65	>10
VHL (38)	LOH	LOH	0,01	0,89	>10
VHL (39)	LOH	LOH	0,03	0,75	>10
VHL (40)	LOH	LOH	0,01	1	>10
VHL (41)	LOH	LOH	0,01	1	>10
VHL (42)	LOH	LOH	0,01	0,83	>10
VHL (43)	n.i	LOH	0,01	failed	-
VHL (44)	n.i	LOH	0	failed	-

LOH: loss of heterozygosity, n.i: not informative

Low frequency maternal chromosome 11 loss in SDHB-related tumors

Almost all (92%) *SDHB*-mutated tumors retained heterozygosity in the 11q region, while 4 (31%) tumors showed LOH exclusively in the 11p15 region, in 1 tumor microsatellite markers were uninformative at 11p15 (Table 4). Moreover, in all cases with LOH, this LOH affected multiple small regions of chromosome 11 alternated with regions of retention of heterozygosity. Methylation analysis of H19-DMR and KvDMR in 8 (62%) *SDHB* mutant tumors showed the ratio of H19-DMR to KvDMR was ~1, comparable to blood DNA. Of the 4 tumors with indications for LOH of 11p15, 1 (tumor 51) showed hypermethylation of H19-DMR and hypomethylation of KvDMR. Tumors 48 and 50 showed hypermethylation of H19-DMR but normal methylation of KvDMR, resulting in a ratio of H19-DMR/KvDMR <3 (Table 4). In the remaining *SDHB* mutant tumor (tumor 49), no methylation was detected at KvDMR, whereas the methylation rate of H19-DMR was normal. These results are in stark contrast to the unequivocal findings in *SDHAF2*, *SDHD* and *VHL*-related PGLs/PCCs. To investigate whether *SDHB*-mutated tumors show a scattered pattern of LOH on other chromosomes, we used microsatellite markers from chromosomes known to be affected in PGL/PCC (19), including chromosomes 1, 3, 5, 14 and 17. All *SDHB* mutant tumors showed LOH for chromosome 1p, presumably affecting the *SDHB* wild type allele (Figure 2). In addition, LOH of other chromosomes, defined as allelic imbalance ratios of <0.7 or >1.3, was observed in most *SDHB*-related tumors, in contrast to *SDHD* mutant tumors (Figure 2).

Table 4. Methylation status of KvDMR and H19-DMR in *SDHB* mutant tumors with and without chr 11 LOH

Gene mutation and number	11p15 status	11q23 status	KvDMR Methylation rate	H19-DMR Methylation rate	H19-DMR/KvDMR Methylation rate Ratio	Methylation rate of matched blood DNA
<i>SDHB</i> (45)	No LOH	No LOH	0,39	0,45	1,1	KvDMR: 0,39 H19: 0,44
<i>SDHB</i> (46)	No LOH	No LOH	0,68	0,60	0,9	
<i>SDHB</i> (47)	No LOH	No LOH	0,48	0,31	0,6	
<i>SDHB</i> (48)	LOH	No LOH	0,57	0,81	1,4	KvDMR: 0,30 H19: 0,51
<i>SDHB</i> (49)	LOH	No LOH	0,09	0,43	4,8	KvDMR: 0,37 H19: 0,51
<i>SDHB</i> (50)	LOH	No LOH	0,33	0,91	2,8	
<i>SDHB</i> (51)	LOH	LOH	0,04	0,86	>10	
<i>SDHB</i> (52)	n.i	No LOH	0,004	0,47	>10	
<i>SDHB</i> (53)	No LOH	No LOH	0,41	0,69	1,7	
<i>SDHB</i> (54)	No LOH	No LOH	0,89	0,97	1,1	KvDMR: 0,50 H19: 0,54
<i>SDHB</i> (55)	No LOH	No LOH	0,91	0,92	1,0	
<i>SDHB</i> (56)	No LOH	No LOH	0,46	0,52	1,1	
<i>SDHB</i> (57)	No LOH	No LOH	0,23	0,33	1,4	

LOH: loss of heterozygosity, n.i: not informative

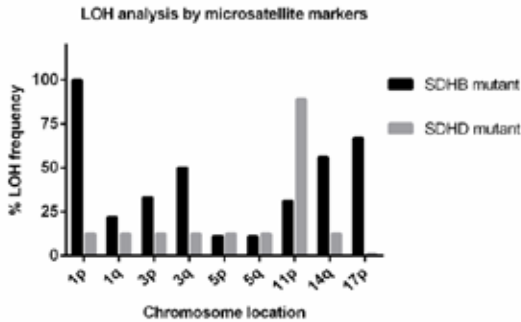


Figure 2. Frequency (%) plot of loss of heterozygosity (LOH) of different chromosomes in *SDHB* (black bars) and *SDHD* (grey bars) mutant tumors, determined by microsatellite marker analysis. A higher frequency of LOH of chromosomes 1, 3, 14, and 17 is observed in *SDHB*-related tumors compared to *SDHD*-related tumors. LOH of chromosome 11p is the most frequent event in *SDHD* mutant tumors.

Greater genomic instability in SDHB tumors compared to SDHD and SDHAF2-related tumors

To further explore genomic instability in these tumors, we analyzed genome-wide copy number changes and LOH in a total of 28 tumors (12 *SDHD*, 4 *SDHAF2*, 9 *SDHB* and 3 *VHL*-related PGLs/PCCs) using SNP array analysis. In agreement with our microsatellite marker results and with other studies (19-23), the most frequent copy number alterations in these tumors were deletions of 1p (48%), 3p/q (28%/32%), and 11p/q (88%/68%) (Figure 3). Although the *SDHB*, *VHL*, *SDHD*, and *SDHAF2* genes are located in these chromosomal regions, losses occurred independently of the presence of germline mutations in these genes (Supplemental Figure 2). SNP array analysis revealed patterns of chromosomal gains and losses that were more heterogeneous in *SDHB* mutant tumors compared to *SDHD* and *SDHAF2*-mutated tumors. We evaluated the level of chromosomal instability in each tumor by calculating the 'Fraction of Aberrant Arms' (i.e. the proportion of chromosome arms altered over more than 40% of their length (24)). This analysis confirmed the greater degree of genome instability in *SDHB* mutant tumors (mean 12%) compared to *SDHD* mutant tumors (mean 4%) or to *SDHAF2* mutant tumors (mean 4,5%). One *SDHD* and two *SDHB*-linked tumors appeared to be tetraploid as determined by the 2Log (test/reference) ratios (Supplemental Figure 3). The most commonly affected chromosomal regions in *SDHB*-related tumors were gain of 1q (57%), chromosome 7 (28%) and 17q (28%), and loss of 1p (100%) (*SDHB* locus) and 17p (57%). These regions have also been shown to be affected in *RET*, *NF1* and sporadic paragangliomas/pheochromocytomas (19), indicating the potential presence of driver genes on these autosomes.

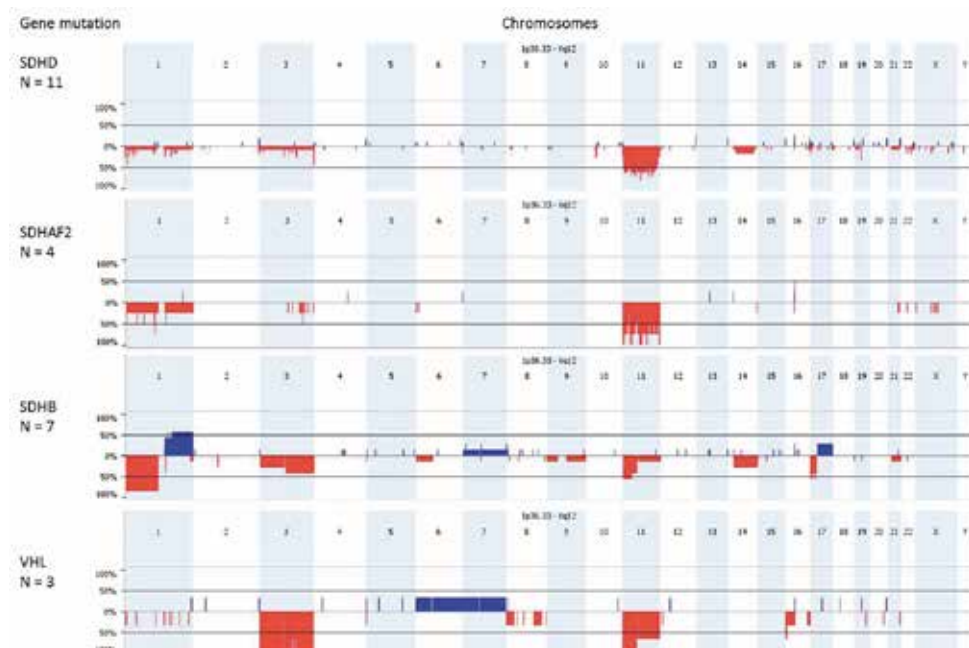


Figure 3. SNP array results of *SDHx* and *VHL*-mutated paragangliomas/pheochromocytomas. Genomic frequency plots of gains (in blue) and deletions (in red) among 11 *SDHD*, 4 *SDHAF2*, 7 *SDHB* and 3 *VHL*-mutated tumors, obtained with Nexus Express. *SDHD*, *SDHAF2* and *VHL* mutant paragangliomas/pheochromocytomas have the highest frequency of 11p loss, while the loss of 1p is a frequent event in *SDHB* mutant tumors. The X-axis shows the genomic position along the chromosomes and the Y-axis shows the frequency (%) of copy number gains and losses.

Discussion

In this study we showed that loss of maternal chromosome 11 is also a cardinal feature of *SDHAF2*-linked paragangliomas. The selective loss of maternal chromosome 11 conforms to the Hensen model and explains why *SDHAF2*-linked tumors arise in principal upon paternal transmission of the mutation, comparable to most *SDHD*-linked tumors (7;20;25). The presence of a paternal parent-of-origin effect in both *SDHAF2* and *SDHD*-related PGLs, a phenomenon absent in other *SDH*-related PGLs, argues that their location on chromosome 11 reveals the fundamental role of another chromosome 11 gene in tumorigenesis.

The specific loss of maternal chromosome 11 in *VHL*-related PCCs suggests that a maternally-expressed gene on chromosome 11 also plays a crucial role in these tumors. In this case no parent-of-origin effect for the *VHL* mutation is predicted because loss of the wild type *VHL* allele on chromosome 3 can occur independently of maternal chromosome 11 loss. These findings agree with earlier reports (18;19;22;26) showing a high frequency of chromosome 11p loss in *VHL* mutant tumors. It is likely that loss of chromosome 11p confers further growth advantage to the tumors besides the inactivation of the *VHL* gene.

The 11p15 region contains several imprinted genes that are exclusively maternally expressed and paternally silenced. LOH of maternal chromosome 11 will result in complete loss of expression of these genes. Our results lend further support to the notion that loss of an as yet unidentified locus (or loci) in 11p15 could contribute to tumor formation in *SDHD*, *SDHAF2* and *VHL*-related PGLs/PCCs.

Of the potential candidate genes, the paternally expressed growth promoter insulin like growth factor 2 (IGF2) and the maternally expressed candidate tumor suppressor genes *CDKN1C* and *H19*, have been most consistently implicated in imprinting disorders, such as Beckwith-Wiedemann Syndrome and Silver-Russell Syndrome (27). Interestingly, we recently found loss of *CDKN1C* and *SLC22A18* expression in *SDHD*-related PGLs compared with normal carotid body tissue and established that knockdown of *SDHD* together with *SLC22A18* or with *CDKN1C* led to small increases in cell proliferation and resistance to apoptosis in neuronal cells (28). Further studies are needed to clarify the role of imprinted genes located on 11p15 in tumor development of *SDHx* and *VHL* mutant PGL/PCC.

While partial or entire loss of chromosome 11 is a signature event in a proportion of *SDHB*-related tumors, many *SDHB* tumors exhibit gains and losses confined to other chromosomes. Compared to *SDHD* and *SDHAF2*, *SDHB* tumors show a more complex pattern of chromosome 11 loss and characteristic changes affecting other chromosomes. Closer analysis to the allele ratios of various microsatellite markers in all tumors revealed a scattered segmental LOH pattern (Supplemental Table 5). While loss might be partly masked by tumor heterogeneity and copy neutral LOH, either of which could impair the detection of genomic alterations (29), the complex pattern of chromosome 11 loss we observed was specific to *SDHB* tumors. Nevertheless, 4 (31%) *SDHB*-related tumors showed loss of maternal chromosome 11p, perhaps signifying a role for the same modifier genes that play such a prominent role in *SDHD* and *SDHAF2* tumors. A low frequency of chromosome 11 loss in *SDHB*-related tumors is in agreement with previous reports (19;23). While a proportion of the greater heterogeneity of chromosomal gains and losses we observed in *SDHB* mutant tumors might simply be a byproduct of genomic instability, many changes are recurrent and thus apparently under the influence of selection, especially losses on chromosomes 1p, 3q, 11p, and 17p and somatic gain of chromosome 1q. One or more modifier genes on these autosomes may work in specific synergistic combinations to initiate or promote tumor growth. These recurring and often non-overlapping chromosomal changes also point to a potential redundancy in modifiers, and as such, altered expression of different groups of modifier genes might be involved in *SDHB* tumorigenesis. Analysis of a much larger number of *SDHB* tumors will be required to resolve this question.

Interestingly, recent work (30;31) showed that engineering *in vitro* the loss of chromosome 8p in cells alters fatty acid and ceramide metabolism. The shift in lipid metabolism triggered tumorigenic potential under stress conditions. Such a complex metabolic shift is difficult to ascribe to a dosage effect of a single gene, and is more likely the result of multiple genes on 8p coordinately undergoing a dosage change. This mechanism might also be at work in *SDHx*-related tumors, with chromosome 11p loss necessary and sufficient to trigger *SDHD* and *SDHAF2* tumorigenesis, whereas *SDHB* tumors require amplification or deletion of multiple driver genes located on different chromosomes.

This speculation is supported by the striking difference in penetrance. A characteristic feature of *SDHD* and *SDHAF2*-related mutations is very high penetrance (90-100%) (9;34), in contrast to *SDHB*-related PGLs/PCCs that have an estimated penetrance of only 20-30% (35-37). This striking

difference cannot be readily explained by functional differences between the respective proteins and therefore suggests a role for genetic effects, such as chromosomal location. In this scenario, tumorigenesis in *SDHD* and *SDHAF2* mutation carriers requires only a single somatic genetic event (chromosome 11 loss), as opposed to the two or more independent somatic events required in *SDHB* mutation carriers (loss of the respective wild type allele, together with loss or gain of other chromosomal regions). In conclusion, our results clearly show that *SDHB* tumors follow a more complex and possibly different path to tumorigenesis compared to *SDHD* and *SDHAF2*-related PGLs, involving loss or gain of a greater proportion of the genome.

Despite the apparently integrated function of the SDH subunits, mutations in individual subunit genes result in a number of striking genetic, phenotypic and clinical differences. Our data now highlight further differences between *SDHB*-related PGL/PCC compared to *SDHD*, *SDHAF2* or *VHL* mutant PGL/PCC in terms of maternal chromosome 11 loss and additional genomic instability. Loss of maternal chromosome 11 is a highly specific and statistically significant event in the latter tumors, suggesting an important role for a still unidentified chromosome 11 factor in the genesis of paraganglioma.

References

- (1) Jansen JC, van den BR, Kuiper A, Van Der Mey AG, Zwinderman AH, Cornelisse CJ. Estimation of growth rate in patients with head and neck paragangliomas influences the treatment proposal. *Cancer* 2000 June 15;88(12):2811-6.
- (2) Lack EE, Cubilla AL, Woodruff JM. Paragangliomas of the head and neck region. A pathologic study of tumors from 71 patients. *Hum Pathol* 1979 March;10(2):191-218.
- (3) Galan SR, Kann PH. Genetics and molecular pathogenesis of pheochromocytoma and paraganglioma. *Clin Endocrinol (Oxf)* 2013 February;78(2):165-75.
- (4) Baysal BE, Willett-Brozick JE, Lawrence EC, Drovdic CM, Savul SA, McLeod DR, Yee HA, Brackmann DE, Slattery WH, III, Myers EN, Ferrell RE, Rubinstein WS. Prevalence of SDHB, SDHC, and SDHD germline mutations in clinic patients with head and neck paragangliomas. *J Med Genet* 2002 March;39(3):178-83.
- (5) Neumann HP, Bausch B, McWhinney SR, Bender BU, Gimm O, Franke G, Schipper J, Klisch J, Althoefer C, Zerres K, Januszewicz A, Eng C, Smith WM, Munk R, Manz T, Glaesker S, Apel TW, Treier M, Reineke M, Walz MK, Hoang-Vu C, Brauckhoff M, Klein-Franke A, Klose P, Schmidt H et al. Germline mutations in nonsyndromic pheochromocytoma. *N Engl J Med* 2002 May 9;346(19):1459-66.
- (6) Hao HX, Khalimonchuk O, Schraders M, Dephoure N, Bayley JP, Kunst H, Devilee P, Cremers CW, Schiffman JD, Bentz BG, Gygi SP, Winge DR, Kremer H, Rutter J. SDH5, a gene required for flavination of succinate dehydrogenase, is mutated in paraganglioma. *Science* 2009 August 28;325(5944):1139-42.
- (7) Hensen EF, Jordanova ES, van Minderhout IJHM, Hogendoorn PCW, Taschner PEM, van der Mey AGL, Devilee P, Cornelisse CJ. Somatic loss of maternal chromosome 11 causes parent-of-origin-dependent inheritance in SDHD-linked paraganglioma and pheochromocytoma families. *Oncogene* 2004 May 20;23(23):4076-83.
- (8) Kunst HP, Rutten MH, De Monnik JP, Hoefsloot LH, Timmers HJ, Marres HA, Jansen JC, Kremer H, Bayley JP, Cremers CW. SDHAF2 (PGL2-SDH5) and Hereditary Head and Neck Paraganglioma. *Clin Cancer Res* 2011 January 15;17(2):247-54.
- (9) Douwes Dekker PB, Corver WE, Hogendoorn PC, Van Der Mey AG, Cornelisse CJ. Multiparameter DNA flow-sorting demonstrates diploidy and SDHD wild-type gene retention in the sustentacular cell compartment of head and neck paragangliomas: chief cells are the only neoplastic component. *J Pathol* 2004 April;202(4):456-62.
- (10) Margetts CDE, Astuti D, Gentle DC, Cooper WN, Cascon A, Catchpoole D, Robledo M, Neumann HPH, Latif F, Maher ER. Epigenetic analysis of HIC1, CASP8, FLIP, TSP1, DCR1, DCR2, DR4, DR5, KvDMR1, H19 and preferential 11p15.5 maternal-allele loss in von Hippel-Lindau and sporadic pheochromocytomas. *Endocrine-Related Cancer* 2005 March;12(1):161-72.
- (11) Castro-Vega LJ, Letouze E, Burnichon N, Buffet A, Disderot PH, Khalifa E, Loriot C, Elarouci N, Morin A, Menara M, Lepoutre-Lussey C, Badoual C, Sibony M, Dousset B, Libe R, Zinzindohoue F, Plouin PF, Bertherat J, Amar L, De RA, Favier J, Gimenez-Roqueplo AP. Multi-omics analysis defines core genomic alterations in pheochromocytomas and paragangliomas. *Nat Commun* 2015;6:6044.
- (12) Dannenberg H, de Krijger RR, Zhao J, Speel EJ, Saremaslani P, Dinjens WN, Mooi WJ, Roth J, Heitz PU, Komminoth P. Differential loss of chromosome 11q in familial and sporadic parasympathetic paragangliomas detected by comparative genomic hybridization. *Am J Pathol* 2001 June;158(6):1937-42.
- (13) Edstrom E, Mahlamaki E, Nord B, Kjellman M, Karhu R, Hoog A, Goncharov N, Teh BT, Backdahl M, Larsson C. Comparative genomic hybridization reveals frequent losses of chromosomes 1p and 3q in pheochromocytomas and abdominal paragangliomas, suggesting a common genetic etiology. *Am J Pathol* 2000 February;156(2):651-9.
- (14) Lui WO, Chen J, Glasker S, Bender BU, Madura C, Khoo SK, Kort E, Larsson C, Neumann HP, Teh BT. Selective loss of chromosome 11 in pheochromocytomas associated with the VHL syndrome. *Oncogene* 2002 February 7;21(7):1117-22.
- (15) Sandgren J, Diaz de ST, Andersson R, Menzel U, Piotrowski A, Nord H, Backdahl M, Kiss NB, Brauckhoff M, Komorowski J, Dralle H, Hessman O, Larsson C, Akerstrom G, Bruder C, Dumanski JP, Westin G. Recurrent genomic alterations in benign and malignant pheochromocytomas and paragangliomas revealed by whole-genome array comparative genomic hybridization analysis. *Endocr Relat Cancer* 2010 September;17(3):561-79.

- (16) Guichard C, Amaddeo G, Imbeaud S, Ladeiro Y, Pelletier L, Maad IB, Calderaro J, Bioulac-Sage P, Letexier M, Degos F, Clement B, Balabaud C, Chevet E, Laurent A, Couchy G, Letouze E, Calvo F, Zucman-Rossi J. Integrated analysis of somatic mutations and focal copy-number changes identifies key genes and pathways in hepatocellular carcinoma. *Nat Genet* 2012 June;44(6):694-8.
- (17) Riemann K, Sotlar K, Kupka S, Braun S, Zenner HP, Preyer S, Pfister M, Pusch CM, Blin N. Chromosome 11 monosomy in conjunction with a mutated SDHD initiation codon in nonfamilial paraganglioma cases. *Cancer Genet Cytogenet* 2004 April 15;150(2):128-35.
- (18) Flynn A, Benn D, Clifton-Bligh R, Robinson B, Trainer AH, James P, Hogg A, Waldeck K, George J, Li J, Fox SB, Gill AJ, McArthur G, Hicks RJ, Tothill RW. The genomic landscape of pheochromocytoma. *J Pathol* 2015 May;236(1):78-89.
- (19) Azzi S, Abi HW, Netchine I. Beckwith-Wiedemann and Russell-Silver Syndromes: from new molecular insights to the comprehension of imprinting regulation. *Curr Opin Endocrinol Diabetes Obes* 2014 February;21(1):30-8.
- (20) Hoekstra AS, Addie RD, Ras C, Seifar RM, Ruivenkamp CA, Briaire-de Bruijn IH, Hes FJ, Jansen JC, Corssmit EP, Corver WE, Morreau H, Bovee JV, Bayley JP, Devilee P. Parent-of-origin tumorigenesis is mediated by an essential imprinted modifier in SDHD-linked paragangliomas: SLC22A18 and CDKN1C are candidate tumor modifiers. *Hum Mol Genet* 2016 July 8.
- (21) Corver WE, Middeldorp A, ter Haar NT, Jordanova ES, van PM, van ER, Cornelisse CJ, Fleuren GJ, Morreau H, Oosting J, van WT. Genome-wide allelic state analysis on flow-sorted tumor fractions provides an accurate measure of chromosomal aberrations. *Cancer Res* 2008 December 15;68(24):10333-40.
- (22) Cai Y, Crowther J, Pastor T, Abbasi AL, Baietti MF, De TM, Vazquez I, Talebi A, Renzi F, Dehairs J, Swinnen JV, Sablina AA. Loss of Chromosome 8p Governs Tumor Progression and Drug Response by Altering Lipid Metabolism. *Cancer Cell* 2016 May 9;29(5):751-66.
- (23) Tschaharganeh DF, Bosbach B, Lowe SW. Coordinated Tumor Suppression by Chromosome 8p. *Cancer Cell* 2016 May 9;29(5):617-9.
- (24) Hensen EF, Jansen JC, Siemers MD, Oosterwijk JC, Vriends AH, Corssmit EP, Bayley JP, Van Der Mey AG, Cornelisse CJ, Devilee P. The Dutch founder mutation SDHD.D92Y shows a reduced penetrance for the development of paragangliomas in a large multigenerational family. *Eur J Hum Genet* 2010 January;18(1):62-6.
- (25) Hes FJ, Weiss MM, Woortman SA, de Miranda NF, van Bunderen PA, Bonsing BA, Stokkel MP, Morreau H, Romijn JA, Jansen JC, Vriends AH, Bayley JP, Corssmit EP. Low penetrance of a SDHB mutation in a large Dutch paraganglioma family. *BMC Med Genet* 2010;11:92.
- (26) Schiavi F, Milne RL, Anda E, Blay P, Castellano M, Opocher G, Robledo M, Cascon A. Are we overestimating the penetrance of mutations in SDHB? *Hum Mutat* 2010 June;31(6):761-2.
- (27) Solis DC, Burnichon N, Timmers HJ, Raygada MJ, Kozupa A, Merino MJ, Makey D, Adams KT, Venisse A, Gimenez-Roqueplo AP, Pacak K. Penetrance and clinical consequences of a gross SDHB deletion in a large family. *Clin Genet* 2009 April;75(4):354-63.
- (28) Hoekstra AS, de Graaff MA, Briaire-de Bruijn IH, Ras C, Seifar RM, van M, I, Cornelisse CJ, Hogendoorn PC, Breuning MH, Suijker J, Korpershoek E, Kunst HP, Frizzell N, Devilee P, Bayley JP, Bovee JV. Inactivation of SDH and FH cause loss of 5hmC and increased H3K9me3 in paraganglioma/pheochromocytoma and smooth muscle tumors. *Oncotarget* 2015 November 17;6(36):38777-88.
- (29) Cooke HJ, Hindley J. Cloning of human satellite III DNA: different components are on different chromosomes. *Nucleic Acids Res* 1979 July 25;6(10):3177-97.
- (30) Wayne JS, Creeper LA, Willard HF. Organization and evolution of alpha satellite DNA from human chromosome 11. *Chromosoma* 1987;95(3):182-8.
- (31) Jordanova ES, Riemersma SA, Philippo K, Giphart-Gassler M, Schuurin E, Kluin PM. Hemizygous deletions in the HLA region account for loss of heterozygosity in the majority of diffuse large B-cell lymphomas of the testis and the central nervous system. *Genes Chromosomes Cancer* 2002 September;35(1):38-48.
- (32) Bayley JP, Oldenburg RA, Nuk J, Hoekstra AS, van der Meer CA, Korpershoek E, McGillivray B, Corssmit EP, Dinjens WN, de Krijger RR, Devilee P, Jansen JC, Hes FJ. Paraganglioma and pheochromocytoma upon maternal transmission of SDHD mutations. *BMC Med Genet* 2014;15:111.
- (33) Li LC, Dahiya R. MethPrimer: designing primers for methylation PCRs. *Bioinformatics* 2002 November;18(11):1427-31.

- (34) Lewin J, Schmitt AO, Adorjan P, Hildmann T, Piepenbrock C. Quantitative DNA methylation analysis based on four-dye trace data from direct sequencing of PCR amplicates. *Bioinformatics* 2004 November 22;20(17):3005-12.
- (35) Wang Y, Carlton VE, Karlin-Neumann G, Sapolsky R, Zhang L, Moorhead M, Wang ZC, Richardson AL, Warren R, Walther A, Bondy M, Sahin A, Krahe R, Tuna M, Thompson PA, Spellman PT, Gray JW, Mills GB, Faham M. High quality copy number and genotype data from FFPE samples using Molecular Inversion Probe (MIP) microarrays. *BMC Med Genomics* 2009;2:8.

Supplementary data

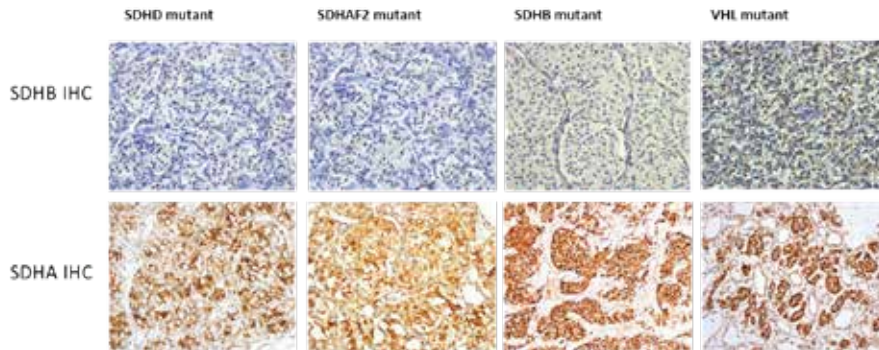
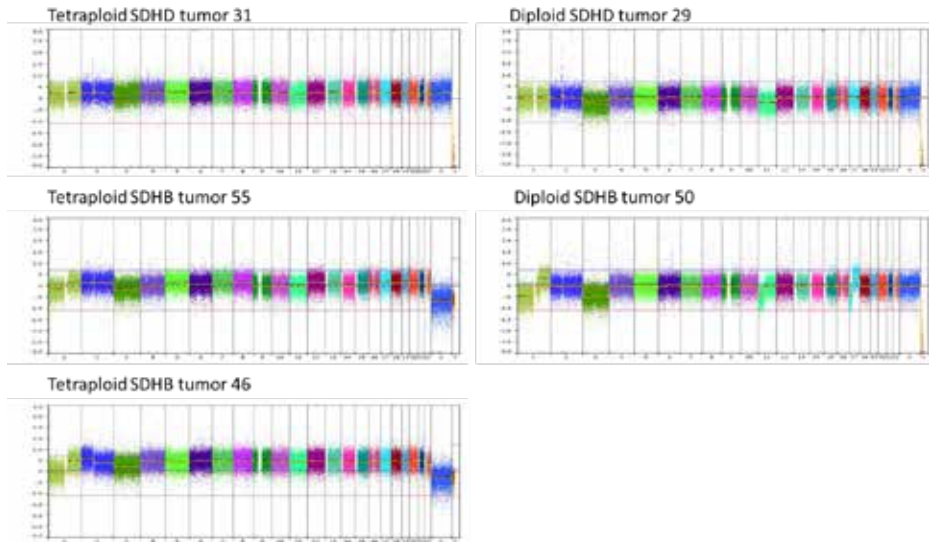


Figure S1. Immunohistochemical staining of *SDHx* and *VHL*-mutated paragangliomas/pheochromocytomas. *SDHB* protein expression is negative in *SDHx*-related tumors and positive in *VHL* mutant tumors. *SDHA* protein expression is positive in *SDHD*, *SDHAF2*, *SDHB* and *VHL*-mutated tumors.



Supplemental figure 2. Overview of the copy-number profiles exported from Nexus Express. Each line represents the profile of a tumor, with gains in blue and deletions in red. Samples are ordered according to the gene mutation, as indicated on the left.



Supplemental figure 3. Log Ratio profiles of five different tumors. The left panel represents three different tetraploid tumors from 1 SDHD and 2 SDHB mutation carriers. The right panel represents two diploid tumors from 1 SDHD and 1 SDHB mutation carriers.

CHAPTER 5

Simple and rapid characterization of novel large germline deletions in SDHB, SDHC and SDHD-related paraganglioma

Attje S Hoekstra¹, Bas van den Ende¹, Xavier Prado Julià¹, Lars van Breemen¹, Kimberly Scheurwater¹, Carli M Tops⁴, Angelica Malinoc³, Peter Devilee^{1,2}, Hartmut PH Neumann³, Jean-Pierre Bayley¹

¹ Department of Human Genetics, Leiden University Medical Center, Leiden, The Netherlands

² Department of Pathology, Leiden University Medical Center, Leiden, The Netherlands

³ Department of Nephrology, University Medical Center Freiburg, Freiburg, Germany

⁴ Department of Clinical Genetics, Leiden University Medical Center, Leiden, The Netherlands

Accepted in Clinical Genetics

Abstract

Germline mutations in genes encoding subunits of succinate dehydrogenase (SDH) are associated with hereditary paraganglioma and pheochromocytoma. Although most mutations in *SDHB*, *SDHC* and *SDHD* are intraexonic variants, large germline deletions may represent up to 10% of all variants but are rarely characterized at the DNA sequence level. Additional phenotypic effects resulting from deletions that affect neighbouring genes are also not understood.

We performed multiplex ligation-dependent probe amplification, followed by a simple long-range PCR 'chromosome walking' protocol to characterize breakpoints in twenty *SDHx*-linked paraganglioma-pheochromocytoma patients. Breakpoints were confirmed by conventional PCR and Sanger sequencing.

Heterozygous germline deletions of up to 104 kb in size were identified in *SDHB*, *SDHC*, *SDHD* and flanking genes in twenty paraganglioma-pheochromocytoma patients. The exact breakpoint could be determined in sixteen paraganglioma-pheochromocytoma patients of which 15 were novel deletions. In six patients proximal genes were also deleted, including *PADI2*, *MFAP2*, *ATP13A2* (*PARK9*), *CFAP126*, *TIMM8B* and *C11orf57*. These genes were either partially or completely deleted, but did not modify the phenotype.

This study increases the number of known *SDHx* deletions by over 50% and demonstrates that a significant proportion of large gene deletions can be resolved at the nucleotide level using a simple and rapid method.

Introduction

Head and neck paragangliomas (HN-PGLs) are generally benign, highly vascularized neuroendocrine tumours that are associated with the parasympathetic nervous system. HN-PGLs most frequently arise in the head and neck region as carotid body tumours at the carotid bifurcation. Extra-adrenal PGLs and pheochromocytomas (PCCs) are associated with the sympathetic nervous system, with extra-adrenal PGLs occurring in the sympathetic paraganglia anywhere from the neck to the pelvic floor, while PCCs originate in the chromaffin cells of the adrenal medulla (1). Extra-adrenal sympathetic PGLs may show an aggressive and metastatic growth pattern (2).

Germline mutations in the genes that encode succinate dehydrogenase (SDH), including *SDHA* (3), *SDHB* (4), *SDHC* (5), *SDHD* (6), and *SDHAF2* (7), are associated with the development of familial PGL/PCC. SDH plays a central role in the tricarboxylic acid cycle, converting succinate to fumarate, while providing electrons for oxidative phosphorylation via the inner mitochondrial membrane. Despite the close functional relationship of the SDH proteins, mutations of subunit genes lead to clear differences in clinical phenotype. While *SDHD* and *SDHAF2* mutations predominantly result in head and neck PGLs, *SDHB* mutations are more closely associated with extra-adrenal PGL and metastatic disease (8;9). *SDHA* and *SDHC* mutations are very rare and are currently associated with both PGL and PCC (10;11).

A wide variety of *SDH* gene mutations have been described and listed in the SDH mutation database at <http://chromium.liacs.nl/LOVD2/SDH/home.php> (12), and over 400 variants are now included. The majority of mutations in the *SDH* genes are point mutations and small deletions, which are easily detected by direct sequencing. Large deletions are rarely detectable using this method, but the widespread adoption of multiplex ligation-dependent probe amplification (MLPA), and other methods has led to the identification of many large deletions (13-16). The SDH mutation database currently contains 31 large deletions, including some relatively common variants such as the *SDHB* Dutch founder deletion in exon 3 (17;18). However, few deletions have been fully characterized and it is not known whether partial or complete deletion of additional genes has any phenotypic effect. In addition, mechanisms underlying deletion such as *Alu* repeat-mediated recombination, which is known to play a major role in germline deletions affecting *VHL* (19), have not yet been extensively explored in the *SDH* genes.

We collected samples from PGL/PCC patients who tested negative for point mutations by Sanger sequencing of the *SDH* genes. MLPA gene deletion analyses of *SDHB*, *SDHC* and *SDHD* in these patients led to the identification of 20 *SDH*-related gene deletions. The exact breakpoint could be determined in 16 PGL/PCC patients and the majority of these deletions were rapidly identified using a simple 'chromosome walking' long-range PCR method. Of the 15 novel deletions identified, 6 also affected neighbouring genes. This study illustrates the ease-of-use of this long-range PCR method and suggests that it may be the most rapid and practical approach for further characterization of single or a small number of deletions. However, this study also illustrates the drawbacks of this method in the analysis of complex or very large deletions (>100 kb).

Material and methods

Patients

DNA samples from 20 index paraganglioma/pheochromocytoma patients were obtained from the Albert-Ludwigs-University, Freiburg. Genomic DNA was extracted using standard methods from EDTA-anticoagulated blood samples. Following initial Sanger sequencing and MLPA analysis at Albert-Ludwigs-University, the samples were further analyzed at the Department of Human Genetics, Leiden University Medical Center. Informed consent was obtained for DNA testing according to protocols approved by ethics committee of the Albert-Ludwigs-University, Freiburg. All included patients were found to be negative for pathogenic mutations by sequencing.

MLPA

Screening for large deletions was carried out using the P226-B1 MLPA kit, following the manufacturer's protocol (MRC-Holland, Amsterdam, The Netherlands). This P226-B1 probemix contains probes for all exons of the *SDHB*, *SDHC* and *SDHD* genes. In addition, 10 reference probes are included in this probemix, detecting 10 different autosomal chromosomal locations.

Long-range PCR

Long-range PCR was carried out using the Takara LA Taq kit (Takara Bio Inc., Lucron Bioproducts, B.V., Gennep, The Netherlands) according to manufacturer's recommendations, except that the final volume was reduced to 20 μ l. Approximately 30 ng of genomic DNA isolated from whole blood was used per reaction. The long range-PCR protocol was as follows: first an initial melting phase at 95°C for 3 minutes, followed by 35 cycles of 30 seconds at 95°C, 15 minutes at 68°C (20 minutes for fragments over 10 kb), and finally an extension phase for 10 minutes at 72°C. Primers were designed using the Primer3 program (<http://frodo.wi.mit.edu/>), with a left or right primer specified and subsequent primers selected using standard parameters (loosened when no primer was found). DNA sequences were downloaded from the UCSC genome browser using the pages *gene sorter*, *genomic sequence*, and *get genomic sequence near gene*, with the extent of appropriate upstream or downstream sequences specified, together with repeat masking. Primer3 allows the analysis of up to 200 kb of genomic sequence, so all primers required for a particular deletion analysis strategy were designed together. *Alu* sequences were analyzed using Repbase (Jurka 2000) (<http://www.girinst.org/repbase/index.html>). PCR fragments spanning a deletion were characterized in detail by Sanger sequencing. Results from the sequenced PCR products were analyzed using either the Multalin program (<http://multalin.toulouse.inra.fr/multalin/multalin.html>) or the Blat program <https://genome.ucsc.edu/cgi-bin/hgBlat>. Deletion nomenclature follows HGVS guidelines.

Quantitative PCR

Broad mapping of selected deletions was carried out by quantitative PCR of DNA using the iQ SYBR Green Supermix (Biorad, California, USA) on a CFX96 Real-Time System (Bio-Rad, USA). BioRad CFX Manager 3.0 software was used to analyze the data. Primers were designed using Primer3 software on repeat masked sequences (primer sequences available upon request). PCR reactions and quantification of PCR products were performed as previously described (20;21). All measurements were carried out in triplicate. Ratios of 0.85-1.25 were accepted as diploid, while values of 0.35-0.70 were considered to be haploid, as described previously (19).

Results

MLPA analysis

MLPA analysis, which is based on the quantification of multiplexed amplified DNA fragments, allows the identification of large deletions. MLPA screening identified ten cases with partial or complete germline deletions of *SDHB*, four cases with deletions of *SDHC* and six cases with deletions of *SDHD* (Table 1). Patients with *SDHB* deletions showed a variety of deletions in the proximal part of the gene including the *SDHB* promoter, exons 1 and 2 (patients 1, 2, 3 and 6), complete gene deletions (patients 4 and 5), and deletions affecting distal exons (patients 8, 9 and 10). A previously described Dutch founder deletion affecting exon 3 of the *SDHB* gene was identified in one patient (patient 7) (17).

Of the four patients with *SDHC*-related deletions, three had deletions that extended beyond the boundaries of the gene, including two patients with deletions in exons 4, 5 and 6 (patients 11 and 12), and patient 14 with a deletion of exons 5 and 6 (Table 1). Only patient 13 showed a deletion confined to the internal exons 3 and 4.

Of the six patients with deletions in *SDHD*, five had deletions that affected extragenic regions, including distal deletions affecting exons 3 and 4 (patient 15 and 20), deletions of the *SDHD* promoter and proximal exons (patients 16 and 17) and a complete gene deletion (patient 18). One patient appeared to have an internal deletion confined to exon 3 of *SDHD* (patient 19).

Table 1. MLPA results of 20 SDH-related patients

Patient number	Gene mutation	Description MLPA
1	<i>SDHB</i>	Del Promoter + exon 1
2	<i>SDHB</i>	Del Promoter + exon 1
3	<i>SDHB</i>	Del Promoter + exon 1+2
4	<i>SDHB</i>	Del Promoter + exon 1-8
5	<i>SDHB</i>	Del Promoter + exon 1-8
6	<i>SDHB</i>	Del exon 1
7	<i>SDHB</i>	Del exon 3
8	<i>SDHB</i>	Del exon 6+7
9	<i>SDHB</i>	Del exon 6-8
10	<i>SDHB</i>	Del exon 2-8
11	<i>SDHC</i>	Del exon 4-6
12	<i>SDHC</i>	Del exon 4-6
13	<i>SDHC</i>	Del exon 3+4
14	<i>SDHC</i>	Del exon 5+6
15	<i>SDHD</i>	Del exon 4
16	<i>SDHD</i>	Del Promoter + exon 1
17	<i>SDHD</i>	Del Promoter + exon 1-3
18	<i>SDHD</i>	Del Promoter + exon 1-4
19	<i>SDHD</i>	Del exon 3
20	<i>SDHD</i>	Del exon 3+4

Long-range 'chromosome walking' PCR

We used long-range PCR to refine deleted regions and, in some cases, to immediately identify exact breakpoints. Long-range PCR is conventionally used as a secondary method to narrow regions around deletions that have been located approximately by other methods such as qPCR or microsatellite mapping. In a previous publication we briefly described exclusive use of long-range PCR in the rapid mapping of the breakpoints of four *SDH* gene deletions (13). Here we wished to further explore the practicality of using this approach as a primary method of breakpoint identification. Forward or reverse primers were designed in undeleted regions of the *SDH* genes when known, with strategies for individual deletions developed based on the known location of deleted and retained regions as defined by MLPA. For example, in the case of a proximal deletion extending for an unknown distance upstream of a gene, several reverse primers are designed in a retained exon and into the possibly retained proximal intron region (Figure 1A). Forward primers are concurrently designed at increasing distances beyond the region known to be deleted, with steps of around 5 kb, depending on the location of masked repeat regions in the gene sequence. Following long-range PCR, amplified products are analyzed by gel electrophoresis and compared to theoretical products from the wild type allele and possible deletion alleles. The staggered design of primers pairs (R1+F1, R1+F2, R1+F3, etc.) will in some cases produce a ladder effect on an agarose gel that immediately suggests the presence of a deletion. In other cases a single dominant product of the correct size will suggest a specific PCR product. Suspected positive PCR products must be confirmed by Sanger sequencing (Figure 1B). The breakpoint can then be directly sequenced from such deletion junction-containing fragments or further refined by conventional PCR and sequencing.

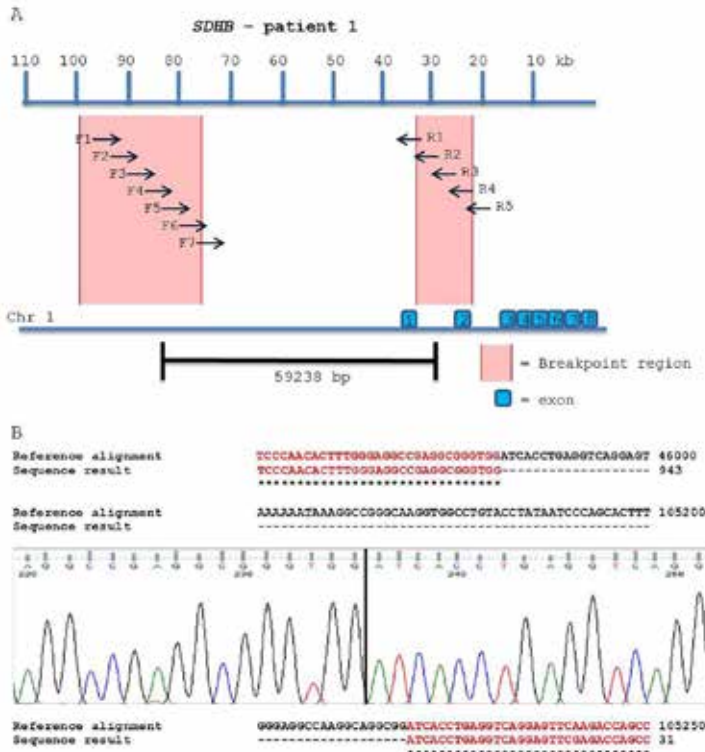


Figure 1. Long-range PCR mapping strategy to identify the breakpoints of the deletion. (A) Patient 1. F and R indicate approximate positions of the forward and reverse primers used for *SDHB*. Genomic DNA is represented by horizontal lines with exons as blue boxes. The size of the deletion was 59238 bp. (B) The breakpoint is identified by sequencing with the black line indicating the breakpoint. Alignment of the *SDHB* gene (red) shows the continuous region of mismatch and the breakpoints (black).

Thirteen of 20 deletions were rapidly identified using this ‘chromosome walking’ long-range PCR approach. Ranging from 2.5 kb up to 44 kb, 10 deletions included extragenic regions. A total of 288 PCR reactions were required to identify the breakpoints of 13 deletions, representing an average of 22 PCR reactions per deletion. Even using the relatively basic and low-throughput approach of 96-well PCR followed by gel electrophoresis, little more than 3 PCR plates were required to identify these deletion breakpoints. In some cases where products were too large for convenient sequencing across a breakpoint or mononucleotide repeats hindered sequencing, additional primers were designed to simplify Sanger sequencing.

By contrast, an additional 629 PCR reactions failed to identify the 7 unresolved deletion breakpoints (approx. 90 per deletion). Deletions encompassing an entire gene were particularly problematic, because in the absence of an anchoring gene sequence the number of forward and reverse primer combinations expands rapidly and results in significant numbers of false positive PCR products that have to be further analyzed. Extended analysis can also lead to the depletion of DNA samples that are only available in limited quantities.

Mapping of deletions by qPCR

The 7 deletions (patients 1, 4, 5, 13, 14, 15, 18) that could not be resolved by long-range PCR analyses were subjected to broad mapping by SYBR Green qPCR (20). Primers were designed to amplify 100-300 bp DNA fragments of the genomic sequence of the *SDHB*, *SDHC* and *SDHD* genes, using steps of around 8 kb between primer sets and including 100 kb upstream and 100 kb downstream of the coding regions where appropriate. Amplicons of patient DNA with an unresolved deletion were compared to amplicons derived from DNA lacking an *SDH* gene deletion. Relative ratios of 0.85-1.25 were considered to be diploid, while values of 0.35-0.70 were taken as indicators of a haploid genome region.

The deletion breakpoint for patient 1 (deletion of *SDHB* promoter and exon 1) was narrowed by qPCR analysis to a region 44 kb upstream of *SDHB* (Figure 2A). The breakpoints for patient 4 were mapped to regions 21 kb upstream and 95 kb downstream of *SDHB*. However, downstream qPCR results were variable, with ratios of 0.70-0.90 in the region 96 kb to 165 kb of *SDHB*. Breakpoints for patient 5 were mapped to areas 76 kb upstream and 28 kb downstream of *SDHB* (Figure 2A). A deletion in *SDHC* exons 3 and 4 (patient 13) determined by MLPA analysis gave inconclusive qPCR results in this region with ratios of 0.75-0.85 (Figure 2B). The deletion breakpoint for patient 14 (deletion of *SDHC* exons 5 and 6) was narrowed to a 56 kb region downstream of *SDHC* (Figure 2B).

Patient 15 carried a deletion of exon 4 of the *SDHD* gene that extended only slightly beyond the end of gene (Figure 2C). The breakpoints of patient 18, with a complete *SDHD* gene deletion, were narrowed by qPCR mapping to regions 2 kb upstream and 38 kb downstream of *SDHD* (Figure 2C). However, the downstream region was uncertain, due to borderline ratios of 0.75-0.85.

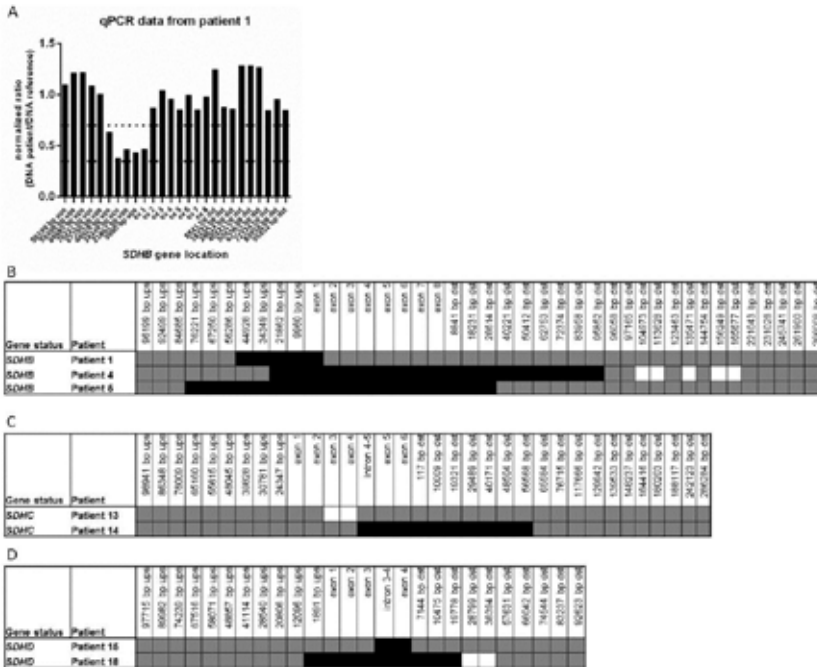


Figure 2. Result of fine mapping of deletions by qPCR. Primers were designed to amplify 100-300 bp DNA fragments of the genomic sequence of the *SDH* gene, using steps of around 10 kb between primer sets and including 100 kb upstream and 100 kb downstream of the coding regions. (A) Normalized qPCR result of patient 1, with the dashed line indicating the deleted region based on ratio values of 0.35-0.70. (B) Primers 96 kb upstream and 266 kb downstream of *SDHB* are used for qPCR. (C) Primers 98 kb upstream and 286 kb downstream of *SDHC* are used for qPCR. (D) Primers 97 kb upstream and 92 kb downstream of *SDHD* are used for qPCR. Black blocks represents the deleted region based on ratio values of 0.35-0.70. Grey blocks represents the retained region based on ratio values of 0.85-1.25. Inconclusive results are indicated by white blocks based on ratio values of 0.75-0.85.

Breakpoint characterization

Following the further refinement of deleted regions by qPCR, we again applied the long-range PCR approach described above to identify exact breakpoints. Exact positions of the breakpoints could be determined in a further three patients (patients 1, 5, 15). Of the four unresolved patients, three showed poor results suggesting low-quality DNA (patients 4, 13 and 14), and one could not be resolved due to exhaustion of available DNA (patient 18). All results are listed in Table 2, which also provides information on neighbouring genes affected by deletions. We have included schematic figures of all deletions and the location of the breakpoints identified in *SDHB* (Figure S1), *SDHC* (Figure S2), and *SDHD* carriers (Figure S3). Of the 16 deletions, 13 were simple deletions and 3 were deletions-insertions, including a 17 bp insertion (patient 8), a 6 bp insertion (patient 9), and an insertion of 133 bp in patient 20 that was identified as an *AluS* repeat.

We also analyzed the breakpoint regions using Repbase (22) to determine whether *Alu-Alu* recombination is an underlying mechanism driving deletion in the *SDH* genes. Single deletion breakpoints were located in *Alu* repeats (patients 5, 7, 15) or in a mammalian long terminal repeat



(LTR)-transposon 1 (MLT1) element (patients 11, 12) in the *SDHD* and *SDHC* genes providing no evidence for an influence of repeat sequences. Evidence for *Alu-Alu* recombination-mediated deletion was found for 4 *SDHB* gene deletions (patients 1, 3, 6, 7).

Proximal genes

Several of the identified *SDH* gene deletions also affected neighbouring genes. Patient 1 showed a deletion in the *SDHB* promoter together with exon 1 that also extended to include exons 2-16 of *PADI2* (Peptidyl Arginine Deiminase 2) upstream of *SDHB*. In addition to complete gene deletion of *SDHB* in patient 5, upstream of *SDHB* exons 11-16 of *PADI2* were lost and downstream the *MFAP2* (Microfibrillar-Associated Protein 2) and *ATP13A2* (*PARK9*) genes were entirely deleted. Mutations in *ATP13A2/PARK9* have been linked to genetic forms of early onset Parkinsonism (23). Patients 11 and 12 showed, in addition to deletion of *SDHC* exons 4-6, complete deletion of *CFAP126* (Cilia And Flagella Associated Protein 126) (Table 2). Complete gene deletion of *TIMM8B* (Mitochondrial import inner membrane translocase subunit Tim8 B) upstream of *SDHD* was found in patient 16. Patient 17 also showed deletion of the entire *TIMM8B* gene, in addition to partial deletion of *C11orf57*, upstream of *SDHD*.

Table 2. Exactly defined breakpoints and deletion sizes in 16 *SDH*-linked patients

Patient number	Description MLPA information	Size deletion (bp)	HGVS description	Associated repeats/other features	Other affected genes
1	<i>SDHB</i> del promoter + exon 1	59238	NG_012340.1 (NM_003000.2): c.1-54121_73-4014del	5' <i>AluSq</i> 3' <i>AluSq</i>	<i>PADI2</i> all but 1 st exon deleted
2	<i>SDHB</i> del promoter + exon 1	3019	NG_012340.1 (NM_003000.2): c.1-516_72+333del	None	None
3	<i>SDHB</i> del promoter + exon 1+2	28199	NG_012340.1 (NM_003000.2): c.1-8570_201-1396del	5' <i>AluSz</i> 3' <i>AluSz</i>	None
4	<i>SDHB</i> del promoter + exon 1-8	?	NG_012340.1 (NM_003000.2): c.1+1_*1_?del		
5	<i>SDHB</i> del promoter + exon 1-8	103903	NG_012340.1 (NM_003000.2): c.1-24771_*1+43992del	5' <i>AluJb</i>	<i>MFAP2</i> complete deletion, <i>ATP13A2</i> complete deletion, <i>PADI2</i> last 5 exons deleted
6	<i>SDHB</i> del exon 1	2530	NG_012340.1 (NM_003000.2): c.1-584_72+1872del	5' <i>AluSq</i> 3' <i>AluSq</i>	None

7	<i>SDHB</i> del exon 3	7905	NG_012340.1 (NM_003000.2): c.201-4429_287-933del	5' <i>AluS</i>	None
8	<i>SDHB</i> del exon 6+7	8240	NG_012340.1 (NM_003000.2): c.540+266_766-341del.ins17	17 bp insertion	None
9	<i>SDHB</i> del exon 6-8	8182	NG_012340.1 (NM_003000.2): c.541-1549_*1+1692del.ins6	6 bp insertion	None
10	<i>SDHB</i> del exon 2-8	33973	NG_012340.1 (NM_003000.2):c.72+2025_*1 +931del	5' <i>AluSx1</i> 3' <i>AluSx1</i>	None
11	<i>SDHC</i> del exon 4-6	44028	NG_012767.1 (NM_001278172.1): c.179+1931_*1+12026del	5' <i>MLT1-int</i>	<i>CFAP126</i> complete deletion
12	<i>SDHC</i> del exon 4-6	44028	NG_012767.1 (NM_001278172.1): c.179+1931_*1+12026del	5' <i>MLT1-int</i>	<i>CFAP126</i> complete deletion
13	<i>SDHC</i> del exon 3+4	?	NG_012767.1 (NM_001278172.1): c.77-?_c.179+?del		
14	<i>SDHC</i> del exon 5+6	?	NG_012767.1 (NM_001278172.1): c.241+*1_?del		
15	<i>SDHD</i> del exon 4	4944	NG_012337.3 (NM_001276506.1): c.315-726_*1+4052del	5' <i>AluSq</i>	None
16	<i>SDHD</i> del promoter + exon 1	2409	NG_012337.3 (NM_001276506.1): c.1-1949_52+408del	None	<i>TIMM8B (DDP2)</i> complete deletion
17	<i>SDHD</i> del promoter + exon 1-3	10636	NG_012337.3 (NM_001276506.1): c.1-2651_315del	None	<i>TIMM8B (DDP2)</i> complete deletion, <i>C11orf57</i> 3'UTR partially deleted
18	<i>SDHD</i> del promoter + exon 1-4	?	NG_012337.3 (NM_001276506.1): c.1+*1_?del		
19	<i>SDHD</i> del exon 3	2640	NG_012337.3 (NM_001276506.1): c.169+168_314+177del	None	None
20	<i>SDHD</i> del exon 3+4	6571	NG_012337.3 (NM_001276506.1): c.170- 80_*1+895del.ins133	133bp insertion	None

SDH: succinate dehydrogenase, PADI2: peptidyl arginine deiminase 2, MFAP2: microfibrillar-associated protein 2, CFAP126: cilia and flagella associated protein 126, TIMM8B (DDP2): mitochondrial import inner membrane translocase subunit tim8 B, MLT1: mammalian long terminal repeat (LTR)-transposon 1.

Discussion

In this study we characterized germline deletions of the *SDH* genes and flanking genes, identifying precise deletion breakpoints in sixteen patients and deletions of up to 104 kb in size. The average size of a deletion was 23 kb. This study underlines the fact that clinically relevant deletions may encompass neighbouring genes, with the potential to modify phenotype. Six of the deletions affected genes proximal to *SDH*. Deletions affecting neighbouring genes may influence phenotypes, as apparent in the case of the *VHL* gene in which deletion of the actin regulator gene *BRK1* together with the *VHL* gene reduces risk for renal cell carcinoma, kidney cysts and retinal angiomas (19;24;25). Patient 1, with a deletion of the *SDHB* gene promoter and exon 1, also showed a deletion of exons 2 to 16 of *PADI2*. PAD enzymes convert protein arginine to citrulline, and citrullination has been associated with autoimmune responses such as those seen in rheumatoid arthritis (RA) (26). Certain polymorphisms of the *PADI2* gene are also associated with RA (27). No additional phenotype is currently recognized in patient 1. In addition to complete gene deletion of *SDHB*, patient 5 was also affected by deletion of exons 11-16 of *PADI2* and complete deletion of the genes *MFAP2* and *ATP13A2* (PARK9). *MFAP2* is an antigen of elastin-associated microfibrils and may affect hematopoiesis (28). *Mfap2*^{-/-} mice show bone abnormalities, hematopoietic changes, increased fat deposition, diabetes, compromised wound repair, and bleeding diathesis (29). However, no human mutations in *MFAP2* are currently known and heterozygous deletion of *MFAP2* in this patient did not lead to an additional phenotype. *ATP13A2* (PARK9) is involved in the pathogenesis of movement disorders and a heterozygous *ATP13A2* gene frameshift mutation has been reported to cause juvenile Parkinsonism, a disease with an onset under 21 years of age (23). Patient 5 had complete loss of one *ATP13A2* allele, but no additional clinical features associated with Parkinsonism. A large *ATP13A2* deletion has never been reported before in the literature. This deletion may not result in a phenotype because it currently appears that mutations with a relatively mild structural effect result in misfolded proteins that are the actual cause of symptoms, probably acting as dominant negative proteins (30). If this patient had a Parkinson-like phenotype it would be the very first report of such a pathogenic mutation in this disease, and would require a re-think of pathogenic mechanisms.

Two patients with a deletion in exons 4-6 of *SDHC* (patient 11 and 12) also showed complete deletion of the *CFAP126* gene. This gene might play a role in Charcot-Marie-Tooth disease, however no mutations in *CFAP126* have been reported to date. In two other patients, genes proximal to *SDHD* were also affected by the deletion of *TIMM8B* (patients 16 and 17) and *C11orf57* (patient 17). Little is known about the function of these genes but heterozygous deletions are not known to result in an additional phenotype (13). Although we did not observe any clinical repercussions that can be attributed to deletions in these neighbouring genes, some patients may be too young for a full phenotype to be manifested.

Of the 32 sequenced breakpoints, 13 (40%) were located in repeats, of which 11 (34% of total) were *Alu* elements. Most breakpoints located in *Alu* elements were identified in *SDHB*-related cases (10/18, 55%). In four *SDHB*-related cases there was evidence for *Alu*-*Alu* recombination-mediated deletion and analysis of the genomic structure of the *SDHB* gene revealed a high density of *Alu* repeats (44 elements that represent 31% of the sequence). A high density of *Alu* elements is likely to contribute to homologous *Alu*-mediated recombination, as shown for *VHL* mutant PCCs where most large *VHL* gene deletions are caused by recombination events driven by *Alu* repeat sequences (19). The *VHL* locus sequence shows a very high *Alu* density of 49%, this may predispose the *VHL* gene to a

high frequency of *Alu*-mediated deletions, in contrast to the *SDH* genes (mean *Alu* density of 29%). Our results suggest that *Alu*-mediated recombination does not play a major role in the deletion of *SDH* genes, since only 34% of all *SDH* deletions were located in *Alu* elements compared to 90% of *VHL* deletions (19).

This study also illustrates the practicality of a long-range 'chromosome walking' PCR strategy in the rapid and efficient mapping of deletion breakpoints. Although large deletions may represent up to 10% of all *SDHx* mutations, on a per center basis they are relatively rare and most centers will find few large deletions. At this point further mapping becomes problematic in terms of return on time invested. On the one hand, benefits of precise breakpoint mapping include exact identification of a variant, which facilitates family studies and the identification of founder mutations. The sequence-related mechanisms underlying large deletions can only be elucidated by breakpoint mapping. Furthermore, as so few deletions have been mapped in detail, we currently know little about possible additional phenotypes or phenotypic modification. On the other hand, drawbacks include the time required to map breakpoints, the expense and relative technical complexity of typical first-line methods such as qPCR, and the uncertainty surrounding the relevance and meaning of results. Our experience in this study suggests that any lab with a basic competence in molecular biology could rapidly map the majority of gene deletion breakpoints using standard equipment, and with personnel with limited experience. We suggest that while all deletions could be considered targets for long-range 'chromosome walking' PCR, this technique is at its most efficient when used to tackle deletions that show retention of some part of a gene. In practical terms, using this technique to analyze more than 100 kb flanking either side of a gene yields diminishing returns and other approaches such as qPCR or microsatellite mapping should perhaps be considered. Limitations of the chromosome walking approach include the lack of a positive control in PCR reactions, the possibility of false negative findings due to primers that produce PCR deletion products too large for efficient amplification (>10-12kb) and the numerous off-target PCR products produced when primers are not consumed in the amplification of bona fide products.

In several cases, we used qPCR for further mapping of large deletions in the *SDH* genes. When successful, upstream or downstream gene regions can be very rapidly narrowed. However, this approach is relatively costly, time-consuming, difficult to interpret, and requires close supervision of inexperienced personnel. Our results were not always conclusive, possibly due to the variable quality of certain DNA samples, the inexperience of staff and to the intrinsically wider variability of this quantitative technique. As newer technologies, such as digital PCR, targeted arrays, targeted panel sequencing, and next-generation sequencing, are increasingly being used for routine clinical screening, and the costs for genome sequencing decreases, these techniques could be used in the future to detect copy-number changes (31).

In conclusion, we identified 15 novel deletions, increasing the number of reported *SDHx* deletions to 46. The majority of deletions found in this study fell within the reach of our 'chromosome walking' approach. In several cases the initial characterization and confirmation of a deletion could be completed in a single long-range PCR experiment, followed directly by Sanger sequencing using the same primers. We hope that this method will provide a low threshold approach for labs facing the dilemma of whether to invest time and resources in the full characterization of deletions. Only by fully characterizing deletions and monitoring patients for possible additional phenotypes can we determine whether specific *SDHx* deletions and/or loss of neighbouring genes have phenotypic

consequences. Improved understanding of the function of deleted neighbouring genes may allow new insights into subtle clinical effects.

References

- (1) Petri BJ, van Eijk CH, de Herder WW, Wagner A, de Krijger RR. Pheochromocytomas and sympathetic paragangliomas. *Br J Surg* 2009 December;96(12):1381-92.
- (2) Benn DE, Gimenez-Roqueplo AP, Reilly JR, Bertherat J, Burgess J, Byth K, Croxson M, Dahia PL, Elston M, Gimm O, Henley D, Herman P, Murday V, Niccoli-Sire P, Pasiaka JL, Rohmer V, Tucker K, Jeunemaitre X, Marsh DJ, Plouin PF, Robinson BG. Clinical presentation and penetrance of pheochromocytoma/paraganglioma syndromes. *J Clin Endocrinol Metab* 2006 March;91(3):827-36.
- (3) Burnichon N, Briere JJ, Libe R, Vescovo L, Riviere J, Tissier F, Jouanno E, Jeunemaitre X, Benit P, Tzagoloff A, Rustin P, Bertherat J, Favier J, Gimenez-Roqueplo AP. SDHA is a tumor suppressor gene causing paraganglioma. *Hum Mol Genet* 2010 August 1;19(15):3011-20.
- (4) Astuti D, Latif F, Dallol A, Dahia PL, Douglas F, George E, Skoldberg F, Husebye ES, Eng C, Maher ER. Gene mutations in the succinate dehydrogenase subunit SDHB cause susceptibility to familial pheochromocytoma and to familial paraganglioma. *Am J Hum Genet* 2001 July;69(1):49-54.
- (5) Niemann S, Muller U. Mutations in SDHC cause autosomal dominant paraganglioma, type 3. *Nat Genet* 2000 November;26(3):268-70.
- (6) Baysal BE, Ferrell RE, Willett-Brozick JE, Lawrence EC, Myssiorek D, Bosch A, van der MA, Taschner PE, Rubinstein WS, Myers EN, Richard CW, III, Cornelisse CJ, Devilee P, Devlin B. Mutations in SDHD, a mitochondrial complex II gene, in hereditary paraganglioma. *Science* 2000 February 4;287(5454):848-51.
- (7) Hao HX, Khalimonchuk O, Schraders M, Dephoure N, Bayley JP, Kunst H, Devilee P, Cremers CW, Schiffman JD, Bentz BG, Gygi SP, Winge DR, Kremer H, Rutter J. SDH5, a gene required for flavination of succinate dehydrogenase, is mutated in paraganglioma. *Science* 2009 August 28;325(5944):1139-42.
- (8) Neumann HP, Pawlu C, Peczkowska M, Bausch B, McWhinney SR, Muresan M, Buchta M, Franke G, Klisch J, Bley TA, Hoegerle S, Boedeker CC, Opocher G, Schipper J, Januszewicz A, Eng C. Distinct clinical features of paraganglioma syndromes associated with SDHB and SDHD gene mutations. *JAMA* 2004 August 25;292(8):943-51.
- (9) Ricketts CJ, Forman JR, Rattenberry E, Bradshaw N, Laloo F, Izatt L, Cole TR, Armstrong R, Kumar VK, Morrison PJ, Atkinson AB, Douglas F, Ball SG, Cook J, Srirangalingam U, Killick P, Kirby G, Aylwin S, Woodward ER, Evans DG, Hodgson SV, Murday V, Chew SL, Connell JM, Blundell TL et al. Tumor risks and genotype-phenotype-proteotype analysis in 358 patients with germline mutations in SDHB and SDHD. *Hum Mutat* 2010 January;31(1):41-51.
- (10) Benn DE, Robinson BG, Clifton-Bligh RJ. 15 YEARS OF PARAGANGLIOMA: Clinical manifestations of paraganglioma syndromes types 1-5. *Endocr Relat Cancer* 2015 August;22(4):T91-103.
- (11) Peczkowska M, Cascon A, Prejbisz A, Kubaszek A, Cwikla BJ, Furmanek M, Eric Z, Eng C, Januszewicz A, Neumann HP. Extra-adrenal and adrenal pheochromocytomas associated with a germline SDHC mutation. *Nat Clin Pract Endocrinol Metab* 2008 February;4(2):111-5.
- (12) Bayley JP, Devilee P, Taschner PE. The SDH mutation database: an online resource for succinate dehydrogenase sequence variants involved in pheochromocytoma, paraganglioma and mitochondrial complex II deficiency. *BMC Med Genet* 2005;6:39.
- (13) Bayley JP, Weiss MM, Grimbergen A, van Brussel BT, Hes FJ, Jansen JC, Verhoef S, Devilee P, Corssmit EP, Vriends AH. Molecular characterization of novel germline deletions affecting SDHD and SDHC in pheochromocytoma and paraganglioma patients. *Endocr Relat Cancer* 2009 September;16(3):929-37.
- (14) Burnichon N, Rohmer V, Amar L, Herman P, Lebouleux S, Darrouzet V, Niccoli P, Gaillard D, Chabrier G, Chabolle F, Coupier I, Thieblot P, Lecomte P, Bertherat J, Wion-Barbot N, Murat A, Venisse A, Plouin PF, Jeunemaitre X, Gimenez-Roqueplo AP. The succinate dehydrogenase genetic testing in a large prospective series of patients with paragangliomas. *J Clin Endocrinol Metab* 2009 August;94(8):2817-27.
- (15) Cascon A, Montero-Conde C, Ruiz-Llorente S, Mercadillo F, Leton R, Rodriguez-Antona C, Martinez-Delgado B, Delgado M, Diez A, Rovira A, Diaz JA, Robledo M. Gross SDHB deletions in patients with paraganglioma detected by multiplex PCR: a possible hot spot? *Genes Chromosomes Cancer* 2006 March;45(3):213-9.
- (16) McWhinney SR, Pilarski RT, Forrester SR, Schneider MC, Sarquis MM, Dias EP, Eng C. Large germline deletions of mitochondrial complex II subunits SDHB and SDHD in hereditary paraganglioma. *J Clin Endocrinol Metab* 2004 November;89(11):5694-9.

- (17) Bayley JP, Grimbergen AE, van Bunderen PA, van der WM, Kunst HP, Lenders JW, Jansen JC, Dullaart RP, Devilee P, Corssmit EP, Vriends AH, Losekoot M, Weiss MM. The first Dutch SDHB founder deletion in paraganglioma-pheochromocytoma patients. *BMC Med Genet* 2009;10:34.
- (18) Hensen EF, van DN, Jansen JC, Corssmit EP, Tops CM, Romijn JA, Vriends AH, Van Der Mey AG, Cornelisse CJ, Devilee P, Bayley JP. High prevalence of founder mutations of the succinate dehydrogenase genes in the Netherlands. *Clin Genet* 2012 March;81(3):284-8.
- (19) Franke G, Bausch B, Hoffmann MM, Cybulla M, Wilhelm C, Kohlhase J, Scherer G, Neumann HP. Alu-Alu recombination underlies the vast majority of large VHL germline deletions: Molecular characterization and genotype-phenotype correlations in VHL patients. *Hum Mutat* 2009 May;30(5):776-86.
- (20) Boehm D, Herold S, Kuechler A, Liehr T, Laccone F. Rapid detection of subtelomeric deletion/duplication by novel real-time quantitative PCR using SYBR-green dye. *Hum Mutat* 2004 April;23(4):368-78.
- (21) Borozdin W, Boehm D, Leipoldt M, Wilhelm C, Reardon W, Clayton-Smith J, Becker K, Muhlendyck H, Winter R, Giray O, Silan F, Kohlhase J. SALL4 deletions are a common cause of Okihiro and acro-renal-ocular syndromes and confirm haploinsufficiency as the pathogenic mechanism. *J Med Genet* 2004 September;41(9):e113.
- (22) Jurka J. Repbase update: a database and an electronic journal of repetitive elements. *Trends Genet* 2000 September;16(9):418-20.
- (23) Fong CY, Rolfs A, Schwarzbraun T, Klein C, O'Callaghan FJ. Juvenile parkinsonism associated with heterozygous frameshift ATP13A2 gene mutation. *Eur J Paediatr Neurol* 2011 May;15(3):271-5.
- (24) Cascon A, Escobar B, Montero-Conde C, Rodriguez-Antona C, Ruiz-Llorente S, Osorio A, Mercadillo F, Leton R, Campos JM, Garcia-Sagredo JM, Benitez J, Malumbres M, Robledo M. Loss of the actin regulator HSPC300 results in clear cell renal cell carcinoma protection in Von Hippel-Lindau patients. *Hum Mutat* 2007 June;28(6):613-21.
- (25) Maranchie JK, Afonso A, Albert PS, Kalyandrug S, Phillips JL, Zhou S, Peterson J, Ghadimi BM, Hurley K, Riss J, Vasselli JR, Ried T, Zbar B, Choyke P, Walthers MM, Klausner RD, Linehan WM. Solid renal tumor severity in von Hippel Lindau disease is related to germline deletion length and location. *Hum Mutat* 2004 January;23(1):40-6.
- (26) Foulquier C, Sebbag M, Clavel C, Chapuy-Regaud S, Al BR, Mechin MC, Vincent C, Nachat R, Yamada M, Takahara H, Simon M, Guerrin M, Serre G. Peptidyl arginine deiminase type 2 (PAD-2) and PAD-4 but not PAD-1, PAD-3, and PAD-6 are expressed in rheumatoid arthritis synovium in close association with tissue inflammation. *Arthritis Rheum* 2007 November;56(11):3541-53.
- (27) Chang X, Xia Y, Pan J, Meng Q, Zhao Y, Yan X. PADI2 is significantly associated with rheumatoid arthritis. *PLoS One* 2013;8(12):e81259.
- (28) Combs MD, Knutsen RH, Broekelmann TJ, Toennies HM, Brett TJ, Miller CA, Kober DL, Craft CS, Atkinson JJ, Shipley JM, Trask BC, Mecham RP. Microfibril-associated glycoprotein 2 (MAGP2) loss of function has pleiotropic effects in vivo. *J Biol Chem* 2013 October 4;288(40):28869-80.
- (29) Weinbaum JS, Broekelmann TJ, Pierce RA, Werneck CC, Segade F, Craft CS, Knutsen RH, Mecham RP. Deficiency in microfibril-associated glycoprotein-1 leads to complex phenotypes in multiple organ systems. *J Biol Chem* 2008 September 12;283(37):25533-43.
- (30) Park JS, Blair NF, Sue CM. The role of ATP13A2 in Parkinson's disease: Clinical phenotypes and molecular mechanisms. *Mov Disord* 2015 May;30(6):770-9.
- (31) Smith MJ, Urquhart JE, Harkness EF, Miles EK, Bowers NL, Byers HJ, Bulman M, Gokhale C, Wallace AJ, Newman WG, Evans DG. The Contribution of Whole Gene Deletions and Large Rearrangements to the Mutation Spectrum in Inherited Tumor Predisposing Syndromes. *Hum Mutat* 2016 March;37(3):250-6.

Supplementary data

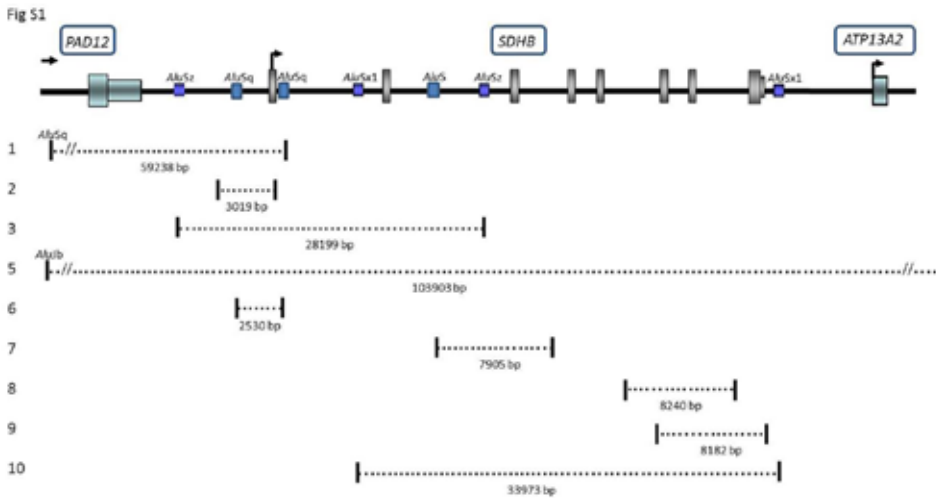


Figure S1. Schematic figure of the deletions in the *SDHB* gene. In total, 9 large deletions were identified and the size of the deletions is provided, varying from 2530 bp to 103903 bp. Patient numbers are indicated on the left as defined in Table 2. In two patients proximal genes were also deleted, including *PADI2* (patient 1), *MFAP2* and *ATP13A2* (*PARK9*) (patient 5). Involvement of *Alu* repeats in deletions are found in 6 *SDHB* carriers (patient 1, 3, 5, 6, 7, 10). Broken lines indicate deletions with breakpoints located beyond the limits chosen for this figure.

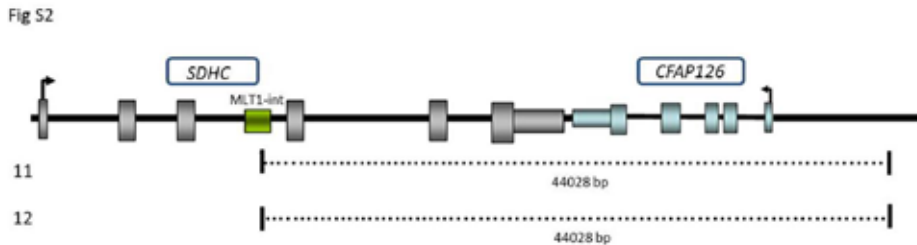


Figure S2. Schematic figure of the deletions in the *SDHC* gene. In total, 2 large deletions were identified and the size of the deletions is 44028 bp. Patient numbers are indicated on the left as defined in Table 2. Both patients also showed complete deletion of the *CFAP126* gene. Single deletion breakpoints were located in *MLT1-int* repeat in both *SDHC* carriers.

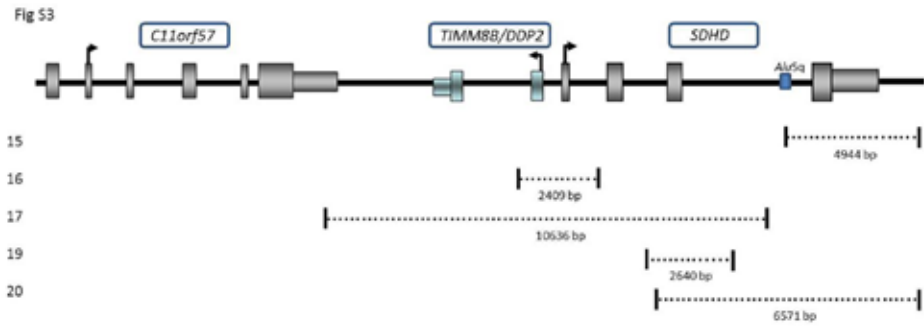



Figure S3. Schematic figure of the deletions in the *SDHD* gene. In total, 5 large deletions were identified and the size of the deletions is provided, varying from 2409 bp to 10636 bp. Patient numbers are indicated on the left as defined in Table 2. In two patients proximal genes were also deleted, including *TIMM8B* (*DDP2*) (patient 16) and *C11orf5* (patient 17). A single deletion breakpoint was located in an *Alu* repeat in 1 *SDHD* carrier (patient 15).

The background features a complex arrangement of overlapping, semi-transparent spheres and thin white lines. The spheres vary in size and color, including shades of light blue, pink, and white. Some spheres are partially obscured by others, creating a sense of depth. The overall aesthetic is clean and modern, typical of a technical or scientific document cover.

CHAPTER 6
Summary and Discussion

TCA cycle defects

Paranglioma and pheochromocytoma are associated with more than 20 genes to date, in which germline and/or somatic mutations have been identified. A subgroup of these genes is associated with hereditary paraganglioma–pheochromocytoma, and encode the subunits forming complex II embedded in the mitochondrial inner membrane. Complex II, also termed succinate dehydrogenase (SDH) consists of *SDHA*, *SDHB*, *SDHC*, *SDHD* and the SDH-assembly factor *SDHAF2*. Tumors caused by mutations in these genes can be grouped together in a cluster (cluster 1) on the basis of their transcriptional profile, enriched for genes that are associated with angiogenesis and the hypoxic response (1). The SDH complex resides in the inner mitochondrial membrane and serves as a core component of both the tricarboxylic acid (TCA) cycle and the electron transport chain coupling the conversion of succinate to fumarate with the reduction of ubiquinone. Another component of the TCA cycle is fumarate hydratase (FH), responsible for the hydroxylation of fumarate to L-malate. *FH*-deficient tumors show gene expression profiles that are very similar of *SDH* mutant tumors, suggesting similarities in the mechanism of tumorigenesis (2). The link between *SDH* and *FH* inactivation was further strengthened by the identification of *FH* gene mutations in PCCs that displayed similar transcriptional and methylation profiles to those of *SDH* mutant tumors (3). Inactivation of either *SDH* or *FH* leads to accumulation of the respective substrates, succinate and fumarate, which act as oncometabolites. ‘Oncometabolite’ is a term coined to describe existing or de novo compounds that accumulate due to the action of a cancer-associated protein and which influence important cellular processes. In the case of succinate and fumarate this involves inhibition of α -ketoglutarate dependent hydroxylases, including prolyl hydroxylases (PHD), histone demethylases and the TET (ten-eleven translocation) family of DNA hydroxylases (Figure 1). TET is responsible for the oxidation of 5-methylcytosine to 5-hydroxymethylcytosine (5hmC).

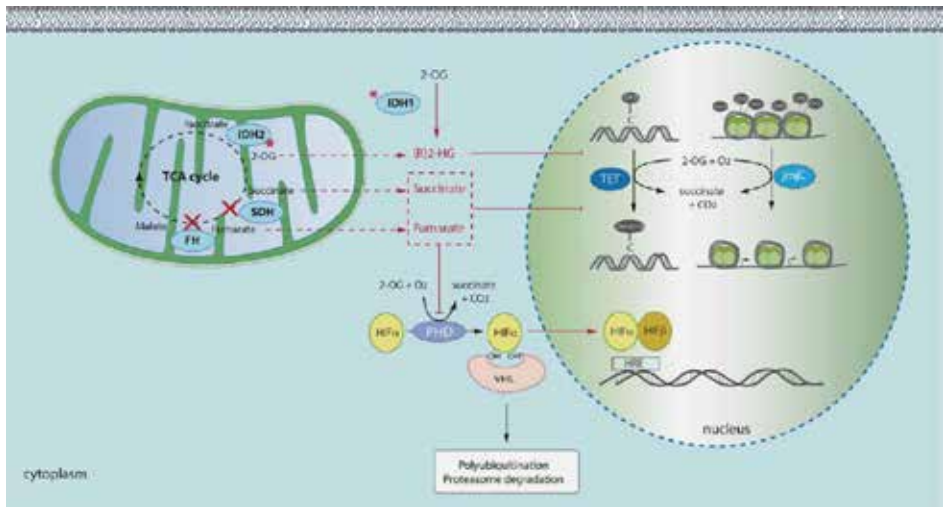


Figure 1. Inactivating mutations (red crosses) in genes encoding succinate dehydrogenase (SDH), fumarate hydratase (FH), and oncogenic mutations (red star) in isocitrate dehydrogenase (IDH1 and IDH2) lead to the accumulation of succinate, fumarate and (R)-2 hydroxyglutarate ((R)-2-HG), respectively. These oncometabolites inhibit α -ketoglutarate (2-OG) dependent hydroxylases, including prolyl hydroxylases (PHD), jumonji C-domain-containing (JmJc) histone demethylases and the TET (ten-eleven translocation) family of DNA hydroxylases, respectively leading to pseudohypoxia, histone and DNA methylation. (Adapted from (4)).

In **chapter two**, we demonstrated that *SDH* and *FH* mutations are associated with inhibition of DNA and histone demethylases, leading to loss of 5hmC and increased H3K9me3 levels in the tumor cells of *SDH*-deficient paragangliomas and *FH*-deficient smooth muscle tumors. Both DNA methylation and H3K9me3 are often associated with regulatory elements of transcriptionally repressed genes and constitutive heterochromatic regions of the genome, resulting in an altered transcriptome. The relationship between methylation and expression changes in *SDHx* and *FH*-related paragangliomas has been examined by Letouzé *et al.* (2), who revealed 191 genes showing both significant CpG island hypermethylation and significant downregulation in these tumors (2). Gene ontology analysis of this set of genes showed a significant enrichment in terms associated with neuroendocrine differentiation, indicating that methylome remodeling results in transcriptional abnormalities in *SDHx* and *FH*-related paragangliomas, directly associated with their phenotypic characteristics. *VHL*, *NF1*, and *RET*-mutated paragangliomas/pheochromocytomas did not display a hypermethylator phenotype (2), while those caused by defects in other genes of the TCA cycle, such as isocitrate dehydrogenase and malate dehydrogenase, did (5;6). These findings suggest clinical opportunities for epigenetic targeting in tumors caused by TCA cycle defects. The DNA methyltransferase inhibitors 5-azacytidine and decitabine are of interest, as 5-azacytidine has been shown to reduce the proliferative index in an *in vivo* IDH1 glioma model (7) and decitabine repressed the migration capacities of *Sdhb*^{-/-} cells (2). Moreover, temozolomide, an alkylating agent, has been shown to be effective in the treatment for glioblastoma and neuroendocrine tumors (8;9). The cytotoxic effect of temozolomide has been attributed to its ability to induce DNA methylation at the O⁶ position of guanine. Methylation of guanine results in DNA mismatch, ultimately resulting in apoptosis and tumor cell death. Efficacy of temozolomide was correlated with loss of the expression of the DNA repair enzyme O(6)-methylguanine-DNA methyltransferase (MGMT) and/or MGMT promoter methylation in glioblastoma and neuroendocrine tumors (8;9). In a limited cohort, temozolomide appeared to be more effective in patients with *SDHB* malignant paragangliomas/pheochromocytomas compared to non-*SDHB* mutant tumors. This increased response is probably explained by the loss of MGMT as its promoter was highly methylated in this subgroup of tumors (10).

The Hensen model

Mutations in *SDHD* or *SDHAF2*, unlike mutations of the other *SDH* subunit genes, show a remarkable parent-of-origin effect in which carriers develop tumors only when the mutation is inherited from the father. *SDHD* and *SDHAF2* share the same location, chromosome 11, in contrast to the *SDHA*, *SDHB* and *SDHC* genes, which are located on chromosome 5 (*SDHA*) and chromosome 1 (*SDHB* and *SDHC*), and in which germline mutations do not give rise to this parent-of-origin effect. Chromosome 11 harbors the main concentration of imprinted genes in the human genome in the 11p15 region, with 8 genes expressed exclusively from the maternal allele while the opposite allele is silenced by epigenetic mechanisms. Loss of the entire maternal copy of chromosome 11 is a frequent event in *SDHD*-linked paragangliomas (11). Hensen and colleagues (11) have proposed that the selective loss of the maternal copy of chromosome 11 results in the simultaneous deletion of the wild type copy of the *SDHD* gene and an exclusively maternally expressed gene, producing a parent-of-origin inheritance pattern (Figure 2). This second locus has remained elusive to date. In **chapter three** we present experiments to identify this second locus/loci. We hypothesized that in a human neuronal

cell line with two parental copies of chromosome 11 in which *SDHD* had been inactivated, the knockdown of candidate genes from the imprinted gene cluster on 11p15 might lead to a cellular phenotype resembling that of primary paragangliomas if the correct combination of genes were targeted. We studied cell proliferation, apoptosis, gene expression profiles and TCA cycle metabolites in these cells and identified two potential tumor modifier genes, *SLC22A18* and *CDKN1C*.

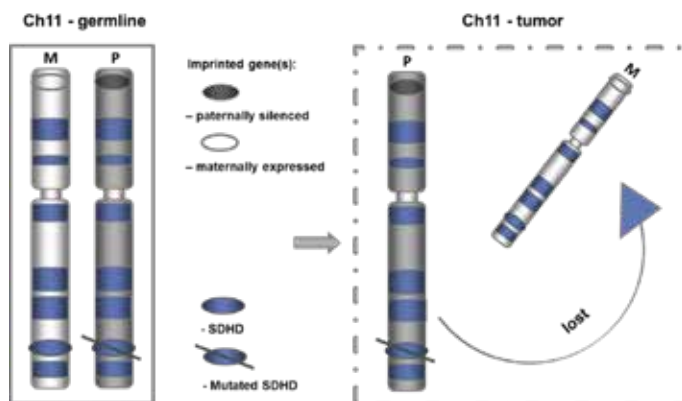


Figure 2. The 'Hensen' hypothesis in outline. Loss of a maternally expressed tumor suppressor gene(s) in the tumor, together with the normal gene copy of *SDHD*, leads to tumor formation. (m – maternal, p – paternal)

Compared to single knockdown of *SDHD*, knockdown of *SDHD* together with *SLC22A18* or with *CDKN1C* led to small but significant increases in cell proliferation and resistance to apoptosis and resulted in a gene expression profile closely related to the known transcriptional profile of *SDH*-deficient tumors. While the results of our cell line-based functional assays supported a role of *SLC22A18* and/or *CDKN1C* in tumor formation, further genetic and protein analyses of *SLC22A18* and *CDKN1C* was performed in 60 *SDHD*-mutated tumors. Of the 60 *SDHD* mutant tumors investigated, 4 tumors showed retention of chromosome 11, suggesting that *SLC22A18* and/or *CDKN1C* might be functionally deleted in these tumors. Indeed, we observed that *SLC22A18* and *CDKN1C* protein expression levels in *SDHD* mutant tumors with retention of chromosome 11 were comparable to levels in tumors showing loss of chromosome 11 by immunohistochemistry and were significantly decreased compared to controls and/or non-*SDH* mutant tumors. In chapter two, we have observed the association of *SDHD*-related tumors with DNA hypermethylation and histone methylation; it is possible that this leads to repressed transcription of *SLC22A18* and *CDKN1C* and might explain the lowered expression of these genes in *SDHD* mutant tumors with retention of chromosome 11. Histone modifications leading to repression of *CDKN1C* transcription has been shown to contribute to breast cancer (12), rhabdoid tumors (13), and gastric cancer (14). Moreover, *SLC22A18* promoter methylation and downregulation is associated with the development and progression of glioma (15;16). Future studies should address whether *SLC22A18* and *CDKN1C* are methylated in this subgroup of *SDHD*-related tumors with retention of chromosome 11. Overall, our data strongly suggest that *SLC22A18* and *CDKN1C* are genes involved in the tumorigenesis of *SDHD*-linked paragangliomas.

CDKN1C, encoding the cyclin-dependent kinase inhibitor 1C, negatively regulates cell proliferation by inhibiting cyclin/Cdk complexes during the G1 phase of the cell cycle and blocks cancer cell growth (17). It is likely that loss of CDKN1C expression in *SDHD* mutant paragangliomas confers further growth advantage to the tumors besides the inactivation of the *SDHD* gene. In agreement with this, our data showed that the double knockdown of *SDHD* and *CDKN1C* increased cell proliferation of neuronal cells and cell proliferation-related gene expression compared to single knockdown of *SDHD*.

SLC22A18 is a member of a family of polyspecific transporters and multidrug resistance genes, but the identity of its physiological substrates is presently unknown. As such, there is no information on molecular pathways that could explain a tumor suppressive function of this transporter. It has been shown that *SLC22A18* has a pro-apoptotic function in glioma cells and confers drug resistance, since the elevated expression of *SLC22A18* increased the expression of caspase-3 and the sensitivity of glioma cells to the anticancer drug BCNU (18). In agreement with this, our findings showed downregulation of apoptosis and cell death-related gene expression in neuronal cells by the knockdown of *SLC22A18*. No significant apoptotic activity has been detected in head and neck paragangliomas (19), and our results showed that by combined knockdown of *SLC22A18* and *SDHD*, cells became more resistant to apoptosis. This suggests that the joint loss of *SLC22A18* and *SDHD* might create a cellular condition that is favourable for tumor progression, i.e., a combination of metabolic and epigenetic changes induced by succinate accumulation, and increased resistance to apoptotic mechanisms. Via which mechanism *SDHD* and *SLC22A18* regulate apoptosis is still unknown. A possible explanation could be through the activation of hypoxia inducible factor 1 (HIF-1). *SDHD* mutations leads to a cellular pseudohypoxic state through the stabilization of HIF-1 caused by the accumulation of succinate (Figure 1). Activated HIF-1 can act as a transcription factor in the nucleus and activates the transcription of a large number of genes, resulting in increased cellular proliferation and reduced apoptosis (1).

Somatic genetic changes

If the loss of chromosome 11 is important for the development of all *SDH*-related tumors, one prediction of the Hensen model is that mutations in *SDHD* and *SDHAF2* will display higher penetrance than mutations in *SDHA*, *SDHB*, or *SDHC*. Tumorigenesis in *SDHD* and *SDHAF2* mutation carriers requires only a single somatic genetic event (chromosome 11 loss), as opposed to the two events required in *SDHA*, *SDHB*, and *SDHC* mutation carriers (loss of the respective wild type allele, together with independent loss of chromosome 11). This prediction appears to be borne out by the wide difference in lifetime penetrance between mutations in *SDHD* (~90%) (20) and *SDHAF2* (>95%) (21), compared to *SDHB* (~30%) (22-24) and *SDHA* and *SDHC* (both with unknown, but probably very low, penetrance). In **chapter four** we studied whether loss of the maternal copy of chromosome 11p is an important feature for the development of *SDHAF2*, *SDHD*, *SDHB*, and *VHL*-linked tumors. We demonstrated in 89% of *SDHAF2*, 85% of *SDHD*, and 75% of *VHL*-related tumors loss of maternal chromosome 11p, using highly polymorphic microsatellite markers. No paternal chromosome 11 loss was found in these tumors. By contrast, both copies of chromosome 11 were found to be retained in 62% of *SDHB*-mutated PGLs/PCCs, while only 31% showed loss maternal chromosome 11p15,

suggesting a different genetic mechanism for tumor development in a substantial group of *SDHB*-related tumors.

SNP array analysis revealed a strikingly simple pattern of chromosome involvement in *SDHAF2* and *SDHD*-related tumors, in which copy number loss/LOH primarily affects chromosome 11 and not much else. *VHL* and *SDHB*-related tumors show a much more complex pattern, involving several other chromosomes beyond those containing *VHL* and *SDHB* (chromosome 3 and 1, respectively). Moreover, *SDHB* mutant tumors have a greater degree of genome instability (mean 12%) compared to *SDHD* (mean 4%) and *SDHAF2* (mean 4,5%) mutant tumors. The most commonly affected chromosomal regions in *SDHB*-related tumors were gain of 1q (57%), chromosome 7 (28%) and 17q (28%), and loss of 1p (100%) and 17p (57%). These regions have also been shown to be similarly affected in *RET*, *NF1* and sporadic paragangliomas/pheochromocytomas (25), indicating the potential presence of modifier genes on these autosomes. Many chromosomal changes are recurrent and often non-overlapping, suggesting a potential redundancy in modifiers. As such, altered expression of different groups of modifier genes might be involved in *SDHB* tumorigenesis. Analysis of a much larger number of *SDHB* tumors will be required to resolve this question.

Interestingly, recent work showed that somatic copy number alterations impact cancer by the concomitant loss of multiple genes, leading to an altered metabolism (26;27). This mechanism might also be at work in *SDHx*-related tumors, with chromosome 11p loss necessary and sufficient to trigger *SDHD* and *SDHAF2* tumorigenesis, while *SDHB* tumors can develop upon amplification or deletion of multiple modifier genes located on different chromosomes. As shown in chapter three, *SLC22A18* and *CDKN1C* could be the genes involved in the tumorigenesis of *SDHD*-linked paragangliomas and might also be involved in *SDHAF2* and *VHL*-related tumors, but this has yet to be determined. In conclusion, our results clearly show that loss of maternal chromosome 11 is a signature event in *SDHAF2*, *SDHD*, and *VHL*-related paragangliomas, while *SDHB* tumors follow a more complex and possibly different path to tumorigenesis, involving loss or gain of a greater proportion of the genome.

Clinical presentation

Despite the fact that the SDH proteins are all associated with the same protein complex, mutations in individual subunit genes lead to clear differences in clinical phenotype (Table 1). The molecular basis for this clinical divergence is as yet unknown. *SDHD* mutations are generally associated with a higher risk of head and neck paragangliomas. For *SDHB* mutations, extra-adrenal and adrenal is more often the presenting feature, and *SDHB* mutation carriers have a higher risk of metastasis (31;32). Metastasis is thought to occur through epithelial–mesenchymal transition (EMT), while gene expression analysis of *SDHB*-related metastatic paragangliomas showed the activation of the EMT programme (26;33). This might confer cancer cells with stem cell-like properties including the ability to migrate to and invade distant anatomic sites.

Table 1. Clinical presentation of *SDH*-related paragangliomas/pheochromocytomas

Gene	Gene locus	Protein function of SDH complex	Inheritance	Penetrance	Malignancy rate	PGL predilection site
<i>SDHA</i>	5p15	Flavoprotein, catalytic subunit	AD	low	-	Extra-adrenal
<i>SDHB</i>	1p36	Iron-sulphur catalytic subunit	AD	20-30%	+++	Extra-adrenal, adrenal
<i>SDHC</i>	1q21	Anchoring subunit	AD	low	+	Head and neck
<i>SDHD</i>	11q23	Anchoring subunit	ADPI	88-100%	+	Head and neck
<i>SDHAF2</i>	11q13	Assembly factor	ADPI	87-100%	-	Head and neck

PGL: paraganglioma, AD: autosomal dominant, ADPI: autosomal dominant paternal imprinting.

It was recently proposed that a quantitative epigenetic switch, more pronounced in *SDHB* mutants than in other *SDHx*-related tumors, explains the increased malignancy risk conferred by *SDHB* mutations (2). Certain methylated genes have been linked to neuroendocrine differentiation (*PNMT*, *NPY* and *SLC6A2*) and EMT differentiation (*KRT19*). And as explained above, epigenetic targeting by the DNA methyltransferase inhibitor decitabine repressed the migration capacities of *SDHB*-deficient cells (2). Whether suppression of certain genes by CpG island or histone methylation provides an advantage in *SDHB*-mutated tumor progression, however, remains to be directly demonstrated.

Genetic heterogeneity of paragangliomas is further highlighted by the identification of the variety of *SDH* germline mutations, with the majority of mutations being point mutations and small deletions (30). In **chapter five**, we have molecularly characterized 16 germline deletions in *SDHB*, *SDHC*, *SDHD* and flanking genes of up to 104 kb in size using a simple and rapid long-range PCR method. This study increases the number of known *SDH* germline deletions by over 50%. It further underlines the fact that clinically relevant deletions may encompass neighboring genes, with the potential to modify phenotype. In 6 patients, we found a deletion affecting genes proximal to *SDHB*, *SDHC*, or *SDHD*, including *PADI2*, *MFAP2*, *ATP13A2* (*PARK9*), *CFAP126*, *TIMM8B* and *C11orf57*. These genes were either partially or completely deleted, but did not influence the phenotype of the patients. In addition, our results suggest that mechanisms underlying deletion such as *Alu* repeat-mediated recombination, which is known to play a major role in the germline deletion of *VHL* (31), does not play a significant role in the deletion of *SDH* genes. Since the *VHL* locus sequence shows a very high *Alu* density of 49%, this may predispose the *VHL* gene to a high frequency of *Alu*-mediated deletions, in contrast to the *SDH* genes, which show a lower *Alu* density (mean of 29%). Benefits of precise breakpoint mapping include exact identification of a variant, which facilitates family studies and the identification of founder mutations. Improved understanding of the function of deleted neighboring genes will bring new insights into subtle clinical effects.

Overall, we and others (25) identified recurrent copy number alterations as well as gene expression and methylation patterns in *SDH*-deficient tumors. However, the particular mechanisms in which these events are involved in paraganglioma tumorigenesis remain to be clarified. We still do not know if the primary link between loss of *SDH* and tumorigenesis is due to the activation of HIF-1 through the accumulation of succinate or due to inhibition of DNA and histone demethylases (Figure

1), leading in both cases to an altered transcriptome. Recently, a causal link between hypoxia and DNA hypermethylation has been identified, leading to altered gene expression (32). Since paragangliomas are hypoxic tumors and show a hypermethylator phenotype, this might suggest these mechanisms are related and both important for tumorigenesis. Whether changes in gene expression are a cause or a consequence of tumor formation needs to be addressed in the future. Progress will require the development of relevant animal and cell culture models that link SDH dysfunction to tumor formation.

References

- (1) Dahia PL. Pheochromocytoma and paraganglioma pathogenesis: learning from genetic heterogeneity. *Nat Rev Cancer* 2014 February;14(2):108-19.
- (2) Letouze E, Martinelli C, Lorient C, Burnichon N, Abermil N, Ottolenghi C, Janin M, Menara M, Nguyen AT, Benit P, Buffet A, Marcaillou C, Bertherat J, Amar L, Rustin P, De RA, Gimenez-Roqueplo AP, Favier J. SDH mutations establish a hypermethylator phenotype in paraganglioma. *Cancer Cell* 2013 June 10;23(6):739-52.
- (3) Castro-Vega LJ, Buffet A, De Cubas AA, Cascon A, Menara M, Khalifa E, Amar L, Azriel S, Bourdeau I, Chabre O, Curras-Freixes M, Franco-Vidal V, Guillaud-Bataille M, Simian C, Morin A, Leton R, Gomez-Grana A, Pollard PJ, Rustin P, Robledo M, Favier J, Gimenez-Roqueplo AP. Germline mutations in FH confer predisposition to malignant pheochromocytomas and paragangliomas. *Hum Mol Genet* 2014 May 1;23(9):2440-6.
- (4) Morin A, Letouze E, Gimenez-Roqueplo AP, Favier J. Oncometabolites-driven tumorigenesis: From genetics to targeted therapy. *Int J Cancer* 2014 November 15;135(10):2237-48.
- (5) Cascon A, Comino-Mendez I, Curras-Freixes M, De Cubas AA, Contreras L, Richter S, Peitzsch M, Mancikova V, Inglada-Perez L, Perez-Barrios A, Calatayud M, Azriel S, Villar-Vicente R, Aller J, Setien F, Moran S, Garcia JF, Rio-Machin A, Leton R, Gomez-Grana A, Apellaniz-Ruiz M, Roncador G, Esteller M, Rodriguez-Antona C, Satrustegui J et al. Whole-exome sequencing identifies MDH2 as a new familial paraganglioma gene. *J Natl Cancer Inst* 2015 May;107(5).
- (6) Xu W, Yang H, Liu Y, Yang Y, Wang P, Kim SH, Ito S, Yang C, Wang P, Xiao MT, Liu LX, Jiang WQ, Liu J, Zhang JY, Wang B, Frye S, Zhang Y, Xu YH, Lei QY, Guan KL, Zhao SM, Xiong Y. Oncometabolite 2-hydroxyglutarate is a competitive inhibitor of alpha-ketoglutarate-dependent dioxygenases. *Cancer Cell* 2011 January 18;19(1):17-30.
- (7) Borodovsky A, Salmasi V, Turcan S, Fabius AW, Baia GS, Eberhart CG, Weingart JD, Gallia GL, Baylin SB, Chan TA, Riggins GJ. 5-azacytidine reduces methylation, promotes differentiation and induces tumor regression in a patient-derived IDH1 mutant glioma xenograft. *Oncotarget* 2013 October;4(10):1737-47.
- (8) Hegi ME, Diserens AC, Gorlia T, Hamou MF, de TN, Weller M, Kros JM, Hainfellner JA, Mason W, Mariani L, Bromberg JE, Hau P, Mirimanoff RO, Cairncross JG, Janzer RC, Stupp R. MGMT gene silencing and benefit from temozolomide in glioblastoma. *N Engl J Med* 2005 March 10;352(10):997-1003.
- (9) Kulke MH, Hornick JL, Frauenhoffer C, Hooshmand S, Ryan DP, Enzinger PC, Meyerhardt JA, Clark JW, Stuart K, Fuchs CS, Redston MS. O6-methylguanine DNA methyltransferase deficiency and response to temozolomide-based therapy in patients with neuroendocrine tumors. *Clin Cancer Res* 2009 January 1;15(1):338-45.
- (10) Hadoux J, Favier J, Scoazec JY, Leboulleux S, Al GA, Caramella C, Deandrei D, Borget I, Lorient C, Chougnat C, Letouze E, Young J, Amar L, Bertherat J, Libe R, Dumont F, Deschamps F, Schlumberger M, Gimenez-Roqueplo AP, Baudin E. SDHB mutations are associated with response to temozolomide in patients with metastatic pheochromocytoma or paraganglioma. *Int J Cancer* 2014 December 1;135(11):2711-20.
- (11) Hensen EF, Jordanova ES, van Minderhout IJHM, Hogendoorn PCW, Taschner PEM, van der Mey AGL, Devilee P, Cornelisse CJ. Somatic loss of maternal chromosome 11 causes parent-of-origin-dependent inheritance in SDHD-linked paraganglioma and pheochromocytoma families. *Oncogene* 2004 May 20;23(23):4076-83.
- (12) Yang X, Karuturi RK, Sun F, Aau M, Yu K, Shao R, Miller LD, Tan PB, Yu Q. CDKN1C (p57) is a direct target of EZH2 and suppressed by multiple epigenetic mechanisms in breast cancer cells. *PLoS One* 2009;4(4):e5011.
- (13) Algar EM, Muscat A, Dagar V, Rickert C, Chow CW, Biegel JA, Ekert PG, Saffery R, Craig J, Johnstone RW, Ashley DM. Imprinted CDKN1C is a tumor suppressor in rhabdoid tumor and activated by restoration of SMARCB1 and histone deacetylase inhibitors. *PLoS One* 2009;4(2):e4482.
- (14) Shin JY, Kim HS, Lee KS, Kim J, Park JB, Won MH, Chae SW, Choi YH, Choi KC, Park YE, Lee JY. Mutation and expression of the p27KIP1 and p57KIP2 genes in human gastric cancer. *Exp Mol Med* 2000 June 30;32(2):79-83.
- (15) Chu SH, Feng DF, Ma YB, Zhang H, Zhu ZA, Li ZQ, Jiang PC. Promoter methylation and downregulation of SLC22A18 are associated with the development and progression of human glioma. *J Transl Med* 2011;9:156.

- (16) Chu SH, Ma YB, Feng DF, Zhang H, Zhu ZA, Li ZQ, Jiang PC. Correlation of low SLC22A18 expression with poor prognosis in patients with glioma. *J Clin Neurosci* 2012 January;19(1):95-8.
- (17) Kavanagh E, Joseph B. The hallmarks of CDKN1C (p57, KIP2) in cancer. *Biochim Biophys Acta* 2011 August;1816(1):50-6.
- (18) Chu SH, Ma YB, Feng DF, Zhang H, Qiu JH, Zhu ZA. Elevated expression of solute carrier family 22 member 18 increases the sensitivity of U251 glioma cells to BCNU. *Oncol Lett* 2011 November;2(6):1139-42.
- (19) Dekker PB, Kuipers-Dijkshoorn N, Hogendoorn PC, Van Der Mey AG, Cornelisse CJ. G2M arrest, blocked apoptosis, and low growth fraction may explain indolent behavior of head and neck paragangliomas. *Hum Pathol* 2003 July;34(7):690-8.
- (20) Hensen EF, Jansen JC, Siemers MD, Oosterwijk JC, Vriends AH, Corssmit EP, Bayley JP, Van Der Mey AG, Cornelisse CJ, Devilee P. The Dutch founder mutation SDHD.D92Y shows a reduced penetrance for the development of paragangliomas in a large multigenerational family. *Eur J Hum Genet* 2010 January;18(1):62-6.
- (21) Kunst HP, Rutten MH, De Monnik JP, Hoefsloot LH, Timmers HJ, Marres HA, Jansen JC, Kremer H, Bayley JP, Cremers CW. SDHAF2 (PGL2-SDH5) and Hereditary Head and Neck Paraganglioma. *Clin Cancer Res* 2011 January 15;17(2):247-54.
- (22) Hes FJ, Weiss MM, Woortman SA, de Miranda NF, van Bunderen PA, Bonsing BA, Stokkel MP, Morreau H, Romijn JA, Jansen JC, Vriends AH, Bayley JP, Corssmit EP. Low penetrance of a SDHB mutation in a large Dutch paraganglioma family. *BMC Med Genet* 2010;11:92.
- (23) Schiavi F, Milne RL, Anda E, Blay P, Castellano M, Opocher G, Robledo M, Cascon A. Are we overestimating the penetrance of mutations in SDHB? *Hum Mutat* 2010 June;31(6):761-2.
- (24) Solis DC, Burnichon N, Timmers HJ, Raygada MJ, Kozupa A, Merino MJ, Makey D, Adams KT, Venisse A, Gimenez-Roqueplo AP, Pacak K. Penetrance and clinical consequences of a gross SDHB deletion in a large family. *Clin Genet* 2009 April;75(4):354-63.
- (25) Castro-Vega LJ, Letouze E, Burnichon N, Buffet A, Disderot PH, Khalifa E, Lorient C, Elarouci N, Morin A, Menara M, Lepoutre-Lussey C, Badoual C, Sibony M, Dousset B, Libe R, Zinzindohoue F, Plouin PF, Bertherat J, Amar L, De RA, Favier J, Gimenez-Roqueplo AP. Multi-omics analysis defines core genomic alterations in pheochromocytomas and paragangliomas. *Nat Commun* 2015;6:6044.
- (26) Cai Y, Crowther J, Pastor T, Abbasi AL, Baietti MF, De TM, Vazquez I, Talebi A, Renzi F, Dehairs J, Swinnen JV, Sablina AA. Loss of Chromosome 8p Governs Tumor Progression and Drug Response by Altering Lipid Metabolism. *Cancer Cell* 2016 May 9;29(5):751-66.
- (27) Tschaharganeh DF, Bosbach B, Lowe SW. Coordinated Tumor Suppression by Chromosome 8p. *Cancer Cell* 2016 May 9;29(5):617-9.
- (28) Bayley JP, Devilee P, Taschner PE. The SDH mutation database: an online resource for succinate dehydrogenase sequence variants involved in pheochromocytoma, paraganglioma and mitochondrial complex II deficiency. *BMC Med Genet* 2005;6:39.
- (29) Franke G, Bausch B, Hoffmann MM, Cybulla M, Wilhelm C, Kohlhasse J, Scherer G, Neumann HP. Alu-Alu recombination underlies the vast majority of large VHL germline deletions: Molecular characterization and genotype-phenotype correlations in VHL patients. *Hum Mutat* 2009 May;30(5):776-86.
- (30) Ye D, Xiong Y. Cancer: Suffocation of gene expression. *Nature* 2016 August 17.



CHAPTER 7
Nederlandse samenvatting

Introductie

Paragangliomen zijn vaatrijke neuro-endocriene tumoren van het autonome zenuwstelsel en zijn afkomstig van paraganglia, die ontstaan uit de embryonale neurale lijst. Paragangliomen kunnen van hoofd-halsgebied tot bekken ontstaan ter plaatse van parasympathische ganglia en de sympathische grensstreng (1). Parasympathische paragangliomen zijn vaak gelegen in het hoofd-halsgebied. De meest voorkomende hoofd-hals paraganglioom, glomus caroticum, ontstaat in de splitsing van de halsslagader en meet de zuurstofspanning in het bloed. Een glomus-caroticum-tumor is een goedaardige tumor en groeit langzaam (2). Sympathische paragangliomen zijn voornamelijk gelokaliseerd in thorax, abdomen of pelvis en hebben een groter risico op maligniteit. Als het paraganglioom uitgaat van het bijniermerg, spreekt men van een feochromocytoom (3).

Paraganglioma kan sporadisch ontstaan of in het kader van familiale syndromen. In dit proefschrift worden klinische kenmerken, de genetica en de tumor biologie van paragangliomen geëvalueerd, waarbij gefocust wordt op *SDH* mutatie dragers.

Hoofdstuk 1

In hoofdstuk 1 wordt een overzicht gegeven van de genen die een rol spelen bij de tumorvorming van paraganglioma. Meer dan de helft van de paragangliomen is erfelijk en kan onder andere veroorzaakt worden door een kiembaanmutatie in *SDH*-gerelateerde genen. SDH, ook mitochondriaal complex II genoemd, is een enzym complex dat zich bevindt in het binnenste membraan van het mitochondriën en maakt onderdeel uit van zowel de citroenzuurcyclus als de elektron-transportketen. Hoewel kiembaanmutaties in de meeste *SDH*-gerelateerde genen tot een autosomaal dominant overervingspatroon van de ziekte in families leidt, zijn er 2 uitzonderingen: *SDHD* en *SDHAF2*. Mutaties in het *SDHD* of *SDHAF2* gen, beide gelegen op chromosoom 11, vertonen een bijzondere overervingspatroon. Paragangliomen ontstaan vrijwel nooit indien de verantwoordelijke mutatie in het *SDHD* of *SDHAF2* gen wordt geërfd via de moeder, terwijl er wel een grote kans is op het ontstaan van paragangliomen als dezelfde mutatie wordt doorgegeven via de vader (4;5). Meerdere modellen om dit overervingspatroon te verklaren worden besproken in dit hoofdstuk.

Hoofdstuk 2

In dit hoofdstuk worden de epigenetische consequenties van mutaties in *SDH*-gerelateerde paragangliomen en *FH*-gerelateerde leiomyosarcomen besproken. De enzymen SDH en FH spelen een rol in de citroenzuurcyclus, waar SDH de oxidatie van succinaat naar fumarate uitvoert en FH fumarate naar malaat omzet. Een mutatie in het *SDH* of *FH* gen leidt respectievelijk tot een ophoping van succinaat of fumarate in het cytoplasma, waardoor α -ketoglutarate afhankelijke dioxygenases, zoals histon demethylases en de TET familie van DNA hydroxylases, geremd worden. Hierdoor wordt histon en DNA methylatie gestimuleerd. Met behulp van immunohistochemie laten we in dit hoofdstuk zien dat histonen van tumorcellen in *SDH*-gerelateerde paragangliomen en *FH*-gerelateerde leiomyosarcomen meer H3K9me3 modificatie bevatten, en het DNA een verlies van 5hmC vertoont ten opzichte van normaal weefsel. Verlies van 5hmC was gecorreleerd aan de

nucleaire exclusie van TET1 eiwit in de tumorcellen van *SDH*-gerelateerde paragangliomen. Onze studie toont aan dat een defect in twee genen van de citroenzuurcyclus vergelijkbare epigenetische consequenties kan hebben en resulteert in histon en DNA methylering. Histon en DNA methylering kan leiden tot het moduleren van genexpressie, waardoor het transcriptoom verandert. Eerder onderzoek heeft aangetoond dat *FH*-gerelateerde tumoren dezelfde genexpressie patronen vertonen als *SDH*-gerelateerde tumoren (6), en dat *FH* mutaties paragangliomen kunnen veroorzaken (7). Deze data suggereert dat *SDH* en *FH* mutaties een vergelijkbaar mechanisme tot tumorvorming kunnen hebben en door metabolische veranderingen het epigenoom wordt gemodificeerd. Daarnaast is ook aangetoond dat een defect in andere genen van de citroenzuurcyclus zoals isocitraat dehydrogenase en malaat dehydrogenase kan leiden tot DNA methylering. Deze bevindingen geven aanleiding tot klinische mogelijkheden voor epigenetische therapie voor tumoren veroorzaakt door een mutatie in een gen onderdeel van de citroenzuurcyclus.

Hoofdstuk 3

In hoofdstuk 3 wordt een model uitgewerkt dat het bijzondere overervingspatroon van *SDHD*-geassocieerde paragangliomen verklaart. Eerder onderzoek heeft aangetoond dat in *SDHD*-geassocieerde paragangliomen niet alleen het wild type *SDHD* allel verloren gaat, maar dat er sprake is van selectief verlies van de gehele maternale kopie van chromosoom 11 (4). Dit somatische verlies van het gehele chromosoom suggereert dat een ander gen, gelegen elders op chromosoom 11, een essentiële rol speelt bij de tumorvorming. Volgens dit zogenaamde “Hensen” model is het aannemelijk dat naast het wild type *SDHD* allel, ook een actief matернаal tumor suppressor gen verloren moet gaan, welke onderhevig is aan paternale imprinting (4). Imprinting is een epigenetisch fenomeen waarbij een gen, afhankelijk van de ouder die het doorgeeft, wel of niet tot expressie komt. Aangezien de maternale kopie selectief verloren gaat in *SDHD*-geassocieerde paragangliomen, zal het tweede gen alleen actief zijn op het maternale allel. Wij hebben aangenomen dat dit gen zou gelokaliseerd moeten worden in de 11p15 regio, omdat dit een gebied is dat bekend staat vanwege het uitgebreide cluster van geïmprinte genen dat er gelegen is.

In dit hoofdstuk hebben we uitgezocht welk gen in de 11p15 regio betrokken zou kunnen zijn bij de tumorvorming van *SDHD*-geassocieerde paragangliomen. Dit is gedaan met behulp van een *in vitro* model van neuronale oorsprong, waarin *SDHD* is uitgeschakeld. Vervolgens zijn verschillende 11p15 genen uitgeschakeld en is uitgezocht welke combinatie resulteerde in een cellulair fenotype vergelijkbaar aan primaire tumoren. Onze resultaten laten zien dat het uitschakelen van *SDHD* en *CDKN1C* of van *SDHD* en *SLC22A18* beide leiden tot een verhoging in celproliferatie en resistentie tegen apoptose (celdood) ten opzichte van *SDHD* uitschakeling alleen. Verder hebben we een verlaging van de eiwit expressie van *CDKN1C* en *SLC22A18* in 60 *SDHD*-geassocieerde tumoren aangetoond en deze tumoren onderzocht op chromosoom 11 verlies. Van de 60 *SDHD*-geassocieerde tumoren vertoonden 4 tumoren geen chromosoom 11 verlies. In deze 4 tumoren zouden de geïmprinte genen functioneel uitgeschakeld kunnen zijn. DNA sequentie analyse liet zien dat deze tumoren geen somatische mutaties in *CDKN1C* of *SLC22A18* hebben. Het zou kunnen dat *CDKN1C* en *SLC22A18* gemethyleerd zijn in deze tumoren en op die manier niet tot expressie komen, maar nader onderzoek zal dit moeten uitwijzen.

In dit hoofdstuk tonen wij aan dat *CDKN1C* en/of *SLC22A18* goede kandidaat genen zijn welke betrokken kunnen zijn bij de tumorvorming van *SDHD* mutatie dragers. *CDKN1C* is een remmer van cycline-afhankelijke kinases die de transitie van de G1-fase naar de S-fase van de celcyclus, en dus celdeling, mediëren (8). Verlies van *CDKN1C* zal een stijging in celdeling veroorzaken en kan op deze wijze een rol spelen bij de tumorvorming van *SDHD* mutatie dragers.

SLC22A18 behoort tot de familie van de organische cation transporters, maar het is nog onbekend via welk mechanisme *SLC22A18* zijn tumor suppressor functie uitoefent. Recent onderzoek heeft aangetoond dat overexpressie van *SLC22A18* een pro-apoptotische functie heeft in glioma cellen en dat deze cellen resistent zijn tegen chemotherapie (BCNU) (9). Dit komt overeen met onze resultaten waarin wij aantonen dat onderdrukking van *SLC22A18* in neuronale cellen apoptose resistentie veroorzaakt. In hoofd-hals paragangliomen is ook geen apoptose gemeten (10), wat suggereert dat apoptose wordt geblokkeerd tijdens tumorvorming. Onze resultaten tonen aan dat uitschakeling van *SDHD* en *SLC22A18* in neuronale cellen een blokkering van apoptose veroorzaakt, dit zou een mogelijke verklaring kunnen zijn van de tumorgenese in *SDHD*-geassocieerde paragangliomen. Via welk mechanisme dit optreedt is nog niet bekend. Echter, een mogelijk mechanisme zou kunnen zijn via de activatie van hypoxia-inducerende factor 1 (HIF1). De ophoping van succinaat in *SDHD*-geassocieerde paragangliomen kan proxyl hydroxylase remmen, waardoor HIF1 wordt gestabiliseerd (11). Vervolgens kan HIF1 in de kern van de cel reageren als een transcriptiefactor en de transcriptie van verschillende genen activeren die betrokken zijn bij onder andere glucose metabolisme, angiogenese, celdeling en apoptose. Meer onderzoek is nodig om de onderliggende mechanismen in het ontstaan van paragangliomen te begrijpen en de rol van *CDKN1C* en *SLC22A18* bij tumorvorming uit te zoeken.

Hoofdstuk 4

In hoofdstuk 4 hebben we een groot cohort van paragangliomen en feochromocytomen met *SDHAF2*, *SDHD*, *SDHB* en *VHL* mutaties geanalyseerd op het verlies van de maternale kopie van chromosoom 11. Uit onze resultaten blijkt dat in 89% van *SDHAF2*, 85% van *SDHD* en 75% van *VHL*-geassocieerde tumoren de maternale 11p regio verloren is gegaan. In tegenstelling tot *SDHB*-gerelateerde tumoren, waar in 62% van de tumoren beide kopieën van chromosoom 11 aanwezig is en maar 31% verlies toont van de maternale 11p regio. Onze resultaten suggereren dat een subgroep van *SDHB*-gerelateerde tumoren een ander genetisch mechanisme tot tumorvorming heeft ten opzichte van *SDHAF2*, *SDHD* en *VHL*-geassocieerde tumoren.

SNP array analyse toont aan dat er naast het verlies van chromosoom 11 in *SDHAF2* en *SDHD*-gerelateerde tumoren niet veel andere chromosomale veranderingen plaatsvinden. *VHL* en *SDHB*-gemuteerde tumoren laten een veel complexer patroon zien, waar naast het verlies van het wild type allel ook andere chromosomale veranderingen plaatsvinden. Voorts vertonen *SDHB*-gerelateerde tumoren meer heterogene patronen van amplificaties en deleties van chromosomen en is de genomische instabiliteit hoger in vergelijking met *SDHAF2* en *SDHD*-geassocieerde paragangliomen. Uit onze studie blijkt dat *SDHB*-gerelateerde tumoren voornamelijk een verlies van chromosoom 1p (100%) en 17p (57%) vertonen, maar ook amplificatie van chromosoom 1q (57%), chromosoom 7 (28%) en 17q (28%). Deze chromosomale regio's zijn ook aangedaan in *RET*, *NF1* en sporadische paragangliomen en feochromocytomen (12), wat suggereert dat er potentiële driver

genen in deze chromosomale regio's kunnen liggen. Eén of meerdere genen gelegen op deze chromosomen zouden in synergie kunnen werken om zo tumorgroei te initiëren. Analyse van een groter cohort *SDHB* tumoren is nodig om deze vraag te kunnen beantwoorden.

Recent onderzoek heeft aangetoond dat somatische kopie-aantal veranderingen het metabolisme van een cel kan veranderen door het gelijktijdig verlies van meerdere driver genen gelokaliseerd in een enkele chromosoom regio (13;14). Dit mechanisme zou ook van toepassing kunnen zijn voor *SDHx* of *VHL*-geassocieerde tumoren, waar chromosoom 11p verlies belangrijk is voor *SDHAF2*, *SDHD* en *VHL*-gemuteerde tumoren. Voor *SDHB*-gerelateerde paragangliomen is dat minder eenduidig en lijken ze te kunnen ontstaan door amplificatie of deletie van verschillende driver genen gelokaliseerd op verschillende chromosomen.

Deze speculatie wordt ondersteund door de opvallende verschillen in penetrantie van *SDHx* mutaties. *SDHD* en *SDHAF2* mutaties hebben een zeer hoge penetrantie (90-100%), terwijl *SDHB* mutaties een lage penetrantie hebben (20-30%) (5;17-19). Het verschil in penetrantie kan niet verklaard worden door functionele verschillen tussen de respectieve eiwitten en suggereert een rol voor genetische effecten, zoals chromosoom locatie. In het geval van paternaal overerfde *SDHD* en *SDHAF2* mutaties is slechts één gebeurtenis voldoende voor de initiatie van tumorgroei, namelijk het wegvallen van het maternale chromosoom 11. In het geval van *SDHB* mutaties zijn twee onafhankelijke stappen nodig voor de initiatie van tumorgroei, namelijk het verlies van het wild type allel (chromosoom 1p) en een tweede die een ander chromosoom regio treft. Aangezien dit soort genetische gebeurtenissen met een bepaalde waarschijnlijkheid optreden tijdens de celdeling, is het zeer aannemelijk dat dit laatste scenario veel minder frequent voorkomt.

Hoofdstuk 5

Hoofdstuk 5 betreft een studie waarin 16 deleties in *SDHB*, *SDHC*, *SDHD* en aangrenzende genen zijn gekarakteriseerd en de exacte breukpunten van de deleties beschreven worden. Van de 16 beschreven deleties zijn 15 *SDH* deleties nieuw, wat resulteert in een stijging van meer dan 50% van het aantal bekende *SDH* deleties. In de studie is gebruik gemaakt van MLPA om *SDH* deleties te identificeren, gevolgd door een simpele en snelle techniek genaamd 'long-range PCR' om de breukpunten van de deleties te karakteriseren. De breukpunten zijn bevestigd met behulp van Sanger sequencing. Onze resultaten laten zien dat de deleties kunnen variëren in grootte van 2,5 kb tot 104 kb. Voorts wordt aangetoond dat 6 patiënten een heterozygote deletie hebben in *SDHB*, *SDHC* of *SDHD* en ook in aangrenzende genen, zoals *PADI2*, *MFAP2*, *ATP13A2* (*PARK9*), *CFAP126*, *TIMM8B* en *C11orf57*. Deze genen zijn voor een deel of volledig gedeleteerd, maar hebben geen invloed op de fenotype van de patiënten. Daarnaast laat onze studie zien dat *Alu-Alu* recombinatie geen prominente mechanisme voor *SDH* deleties is. Eerder onderzoek heeft aangetoond dat *Alu-Alu* recombinatie een grote rol speelt bij kiembaan deleties in het *VHL* gen (20), dit kan verklaard worden door een hoog aantal kopieën van *Alu* sequenties in *VHL* (49%) ten opzichte van *SDH* genen (gemiddelde van 29%). Alleen door het volledig karakteriseren van deleties en het monitoren van patiënten op additionele fenotypes zullen we kunnen bepalen of een specifieke *SDH* deletie en verlies van aangrenzende genen een verandering in fenotype kan veroorzaken. Op deze manier kunnen we beter de functie van het verloren gen begrijpen wat kan leiden tot nieuwe inzichten in subtiele klinische effecten.

Conclusies

In dit proefschrift wordt een aantal nieuwe bevindingen gepresenteerd die de tumorontwikkeling volgens het Hensen model in *SDHD* en *SDHAF2*-geassocieerde paragangliomen bevestigen en verder invulling geven. Er zijn twee tumor suppressor genen geïdentificeerd die mogelijk een rol spelen in de initiatie van tumorgroei in *SDHD* (en *SDHAF2*)-geassocieerde paragangliomen: *CDKN1C* en *SLC22A18*. Nader onderzoek zal dit moeten bevestigen.

Er is voortgang geboekt in het begrip van de moleculair biologische mechanismen die tumorgroei als gevolg van *SDH* mutaties kunnen verklaren. Succinaat ophoping als gevolg van een *SDH* mutatie kan α -ketoglutaraat afhankelijke dioxygenases remmen. Hierdoor ontstaat er HIF1 stabilisatie en DNA hypermethylatie, wat resulteert in (epi)genetische veranderingen. De precieze link tussen deze veranderingen en tumorontwikkeling is nog onbekend. Dat mutaties in andere genen van de citroenzuurcyclus vergelijkbare epigenetische veranderingen veroorzaakt, kan inzicht geven in de moleculaire wegen die metabolische veranderingen verbinden met tumorgroei.

Het paragangliomen onderzoek heeft het inzicht doen toenemen in de verschillen in genomische instabiliteit tussen *SDHAF2*, *SDHD*, *VHL* en *SDHB*-gerelateerde tumoren, waar het verlies van chromosoom 11p een duidelijke rol speelt in *SDHAF2*, *SDHD* en *VHL*-geassocieerde paragangliomen/feochromocytomen, maar niet zozeer in *SDHB*-gerelateerde tumoren. Een belangrijke vraag welke onbeantwoord blijft is waarom mutaties in genen die allen onderdelen van hetzelfde SDH complex coderen, en allen leiden tot een verstoorde functie van dit enzym, toch tot duidelijke verschillen in klinische presentatie kunnen leiden (Tabel 1).

Toekomstig onderzoek zal moeten uitwijzen wat de onderliggende mechanismes zijn die verantwoordelijk zijn voor de tumorontwikkeling en het gedrag van paragangliomen als gevolg van mutaties in het SDH complex. Progressie zou gemaakt kunnen worden door de ontwikkeling van relevante diermodellen en cellijnen.

Tabel 1. Klinische presentatie van *SDH*-gerelateerde paragangliomen/feochromocytomen

Gen	Genlocus	Eiwit functie van SDH complex	Overerving	Penetrantie	Maligniteit	Typische tumor lokalisatie
<i>SDHA</i>	5p15	Flavoproteïne, katalytisch subeenheid	AD	Laag	-	Extra-adrenaal
<i>SDHB</i>	1p36	IJzer-zwavelproteïne, katalytisch subeenheid	AD	20-30%	+++	Extra-adrenaal, adrenaal
<i>SDHC</i>	1q21	Cytochroom b subeenheid, ankereiwit	AD	Laag	+	Hoofd-halsgebied
<i>SDHD</i>	11q23	Cytochroom b subeenheid, ankereiwit	ADPI	88-100%	+	Hoofd-halsgebied
<i>SDHAF2</i>	11q13	Cofactor	ADPI	87-100%	-	Hoofd-halsgebied

SDH: succinaat dehydrogenase, AD: autosomaal dominant, ADPI: autosomaal dominant paternale imprinting.

References

- (1) Wasserman PG, Savargaonkar P. Paragangliomas: classification, pathology, and differential diagnosis. *Otolaryngol Clin North Am* 2001 October;34(5):845-vi.
- (2) Jansen JC, van den BR, Kuiper A, Van Der Mey AG, Zwinderman AH, Cornelisse CJ. Estimation of growth rate in patients with head and neck paragangliomas influences the treatment proposal. *Cancer* 2000 June 15;88(12):2811-6.
- (3) Petri BJ, van Eijck CH, de Herder WW, Wagner A, de Krijger RR. Pheochromocytomas and sympathetic paragangliomas. *Br J Surg* 2009 December;96(12):1381-92.
- (4) Hensen EF, Jordanova ES, van Minderhout IJHM, Hogendoorn PCW, Taschner PEM, van der Mey AGL, Devilee P, Cornelisse CJ. Somatic loss of maternal chromosome 11 causes parent-of-origin-dependent inheritance in SDHD-linked paraganglioma and pheochromocytoma families. *Oncogene* 2004 May 20;23(23):4076-83.
- (5) Kunst HP, Rutten MH, De Monnik JP, Hoefsloot LH, Timmers HJ, Marres HA, Jansen JC, Kremer H, Bayley JP, Cremers CW. SDHAF2 (PGL2-SDH5) and Hereditary Head and Neck Paraganglioma. *Clin Cancer Res* 2011 January 15;17(2):247-54.
- (6) Letouze E, Martinelli C, Lorient C, Burnichon N, Abermil N, Ottolenghi C, Janin M, Menara M, Nguyen AT, Benit P, Buffet A, Marcaillou C, Bertherat J, Amar L, Rustin P, De RA, Gimenez-Roqueplo AP, Favier J. SDH mutations establish a hypermethylator phenotype in paraganglioma. *Cancer Cell* 2013 June 10;23(6):739-52.
- (7) Castro-Vega LJ, Buffet A, De Cubas AA, Cascon A, Menara M, Khalifa E, Amar L, Azriel S, Bourdeau I, Chabre O, Curras-Freixes M, Franco-Vidal V, Guillaud-Bataille M, Simian C, Morin A, Leton R, Gomez-Grana A, Pollard PJ, Rustin P, Robledo M, Favier J, Gimenez-Roqueplo AP. Germline mutations in FH confer predisposition to malignant pheochromocytomas and paragangliomas. *Hum Mol Genet* 2014 May 1;23(9):2440-6.
- (8) Kavanagh E, Joseph B. The hallmarks of CDKN1C (p57, KIP2) in cancer. *Biochim Biophys Acta* 2011 August;1816(1):50-6.
- (9) Chu SH, Ma YB, Feng DF, Zhang H, Qiu JH, Zhu ZA. Elevated expression of solute carrier family 22 member 18 increases the sensitivity of U251 glioma cells to BCNU. *Oncol Lett* 2011 November;2(6):1139-42.
- (10) Dekker PB, Kuipers-Dijkshoorn N, Hogendoorn PC, Van Der Mey AG, Cornelisse CJ. G2M arrest, blocked apoptosis, and low growth fraction may explain indolent behavior of head and neck paragangliomas. *Hum Pathol* 2003 July;34(7):690-8.
- (11) Selak MA, Armour SM, MacKenzie ED, Boulahbel H, Watson DG, Mansfield KD, Pan Y, Simon MC, Thompson CB, Gottlieb E. Succinate links TCA cycle dysfunction to oncogenesis by inhibiting HIF- α prolyl hydroxylase. *Cancer Cell* 2005 January;7(1):77-85.
- (12) Castro-Vega LJ, Letouze E, Burnichon N, Buffet A, Disderot PH, Khalifa E, Lorient C, Elarouci N, Morin A, Menara M, Lepoutre-Lussey C, Badoual C, Sibony M, Dousset B, Libe R, Zinzindohoue F, Plouin PF, Bertherat J, Amar L, De RA, Favier J, Gimenez-Roqueplo AP. Multi-omics analysis defines core genomic alterations in pheochromocytomas and paragangliomas. *Nat Commun* 2015;6:6044.
- (13) Cai Y, Crowther J, Pastor T, Abbasi AL, Baietti MF, De TM, Vazquez I, Talebi A, Renzi F, Dehairs J, Swinnen JV, Sablina AA. Loss of Chromosome 8p Governs Tumor Progression and Drug Response by Altering Lipid Metabolism. *Cancer Cell* 2016 May 9;29(5):751-66.
- (14) Tschaharganeh DF, Bosbach B, Lowe SW. Coordinated Tumor Suppression by Chromosome 8p. *Cancer Cell* 2016 May 9;29(5):617-9.
- (15) Hensen EF, Jansen JC, Siemers MD, Oosterwijk JC, Vriends AH, Corssmit EP, Bayley JP, Van Der Mey AG, Cornelisse CJ, Devilee P. The Dutch founder mutation SDHD.D92Y shows a reduced penetrance for the development of paragangliomas in a large multigenerational family. *Eur J Hum Genet* 2010 January;18(1):62-6.
- (16) Hes FJ, Weiss MM, Woortman SA, de Miranda NF, van Bunderen PA, Bonsing BA, Stokkel MP, Morreau H, Romijn JA, Jansen JC, Vriends AH, Bayley JP, Corssmit EP. Low penetrance of a SDHB mutation in a large Dutch paraganglioma family. *BMC Med Genet* 2010;11:92.
- (17) Schiavi F, Milne RL, Anda E, Blay P, Castellano M, Opocher G, Robledo M, Cascon A. Are we overestimating the penetrance of mutations in SDHB? *Hum Mutat* 2010 June;31(6):761-2.
- (18) Franke G, Bausch B, Hoffmann MM, Cybulla M, Wilhelm C, Kohlhase J, Scherer G, Neumann HP. Alu-Alu recombination underlies the vast majority of large VHL germline deletions: Molecular

characterization and genotype-phenotype correlations in VHL patients. Hum Mutat 2009
May;30(5):776-86.

DANKWOORD

Promoveren is samenwerken. Ik heb dit enerverende traject tot een succesvol einde kunnen brengen dankzij het vertrouwen van mijn promotor en co-promotor. Graag wil ik een woord van dank richten aan allen met wie ik de afgelopen jaren heb mogen samenwerken, met daarbij een paar mensen in het bijzonder.

Peter Devilee, dank voor de kans die je me hebt geboden in het onderzoek en voor de coördinatie van het promotietraject. De altijd open deur maakt dat het erg prettig was om zomaar binnen te lopen.

Jean-Pierre Bayley, ik ben erg dankbaar dat ik de afgelopen jaren met jou heb mogen samenwerken. Je kritische blik op mijn werk heeft me scherp gehouden en ik heb dan ook veel van je geleerd.

Inge Briaire-de Bruijn, bedankt voor je altijd enthousiaste en welwillende houding. Ik vond het zeer prettig om met jou te mogen samenwerken tijdens mijn promotietraject.

TumGen groep, Heggert Rebel, Juan Zhang, Ellen Thomassen, Nandi Celosse, Inge Lakeman, Els Robanus, Maaïke Vreeswijk, Heleen van der Klift, Caro Meijers, Florentine Hilbers, Celia Dingemans-van der Spek, Shanti Jagmohan, Marije Geilenkirchen, Juul Wijnen, Anne Jansen, bedankt voor de gezellige tijd die ik heb mogen beleven met jullie de afgelopen jaren en voor alle leuke thee/koffie/lunch gesprekken.

Paraganglioma Groep Leiden, Noortje van der Kleij-Corssmit, Frederik Hes, Jeroen Jansen en alle betrokken chirurgen, ik wil jullie allen zeer bedanken voor jullie enorme betrokkenheid en jullie enthousiasme voor het onderzoek.

Alle co-auteurs en de vele anderen die een essentiële bijdrage hebben geleverd aan dit proefschrift wil ik bedanken. Judith Boveé, Esther Korpershoek, Marieke de Graaff, Cor Ras, Reza Seifar, Ivonne van Minderhout, Pancras Hogendoorn, Martijn Breuning, Johnny Suijker, Dirk Kunst, Henri Timmers, Norma Frizzell, Ruben Addie, Claudia Ruivenkamp, Wim Corver, Hans Morreau, Bas van den Ende, Xavi Julià, Lars van Breemen, Kimberly Scheurwater, Carli Tops, Angelica Malinoc, Hartmut Neumann, Adrian Bateman, Diana Eccles, Judit Balog, Yvonne Fillie-Grijpma, Anouk van der Horst-Schrijvers, Katja Jordanova, Cees Cornelisse en Erik Hensen, zonder jullie inzet hadden deze studies niet tot stand kunnen komen.

Manon, Olivia, Berber, Agmar, Elisa, Jessica, Marijn, Lianne, Mariëlle en Maaïke; onze vriendschap is heel bijzonder en ik geniet enorm van onze weekendjes in de Achterhoek en de goede gesprekken die we voeren, maar ook zeker van alle goede grappen die gemaakt worden.

Paranimfen Baukje en Nynke, super bedankt voor jullie vertrouwen in mij. Ik vind het erg fijn dat jullie vandaag naast me zitten.

De solide basis en steun van mijn familie, schoonfamilie en alle vrienden heeft me altijd positief gehouden, daar ben ik jullie enorm dankbaar voor!

Lieve heit en mem, ik wil jullie speciaal bedanken voor alle kansen die jullie mij bieden en voor het feit dat jullie altijd voor me klaar staan.

Lieve Marcus, vanaf het begin van mijn onderzoek ben je er voor me geweest en je onvoorwaardelijke vertrouwen heeft me veel steun gegeven. Daarnaast geniet ik zeer van jouw heerlijke nuchterheid en je humor, ik ben dan ook enorm gelukkig met jou.

CURRICULUM VITAE

Attje Sietske Hoekstra werd geboren op 7 maart 1986 te Makkum, Friesland. In 2004 verhuisde zij naar Groningen, waar zij de HBO opleiding Biologie en Medisch Laboratoriumonderzoek heeft gevolgd. Haar stage bij het Beatson Institute for Cancer Research in Glasgow onder supervisie van Professor Kevin Ryan heeft haar interesse in de genetica en de wetenschap doen versterken. Het onderzoek over het gen DRAM-1 welke via p53 autofagie kan moduleren leverde een co-auteurschap op. Na het behalen van haar Bachelor of Science in 2008, is zij begonnen met de Master opleiding Medisch Farmaceutische Wetenschappen te Groningen. In 2010 is ze verhuist naar Amsterdam om haar afstudeerstage naar de rol van vetweefsel in osteoarthritis op de afdeling Metabolic Health Research bij TNO in Leiden te doen. In 2011 heeft ze haar Master bul behaald en is ze begonnen met haar promotieonderzoek bij de Humane Genetica in het LUMC onder supervisie van Professor Peter Devilee en Dr. Jean-Pierre Bayley. Haar promotieonderzoek was gericht op paragangliomen als gevolg van *SDHx* mutaties en de onderliggende (genetische en moleculair biologische) mechanismes die verantwoordelijk zijn voor de tumorontwikkeling. Zij heeft haar werk op meerdere (inter)nationale congressen gepresenteerd, waaronder het International Symposium on Pheochromocytoma and Paraganglioma (ISP2014) in Kyoto, Japan. Momenteel werkt ze als Projectleider op de afdeling Product Development bij MRC-Holland te Amsterdam.

PUBLICATIONS

Loss of maternal chromosome 11 is a signature event in SDHAF2, SDHD, and VHL-related paragangliomas, but less significant in SDHB-related paragangliomas

Hoekstra AS, Hensen EF, Jordanova ES, Korpershoek E, van der Horst-Schrivers ANA, Corssmit EPM, Hes FJ, Jansen JC, Kunst HPM, Timmers HJLM, Bateman A, Eccles D, Bovée JVMG, Devilee P, Bayley JP. Submitted

IDH1 or -2 mutations do not predict outcome and do not cause loss of 5-hydroxymethylcytosine or altered histone modifications in central chondrosarcomas

Cleven AHG, Suijker J, Agrogiannis G, Briaire-de Bruijn IH, Frizzell N, Hoekstra AS, Wijers-Koster PM, Cleton-Jansen AM, Bovée JVMG. Submitted

Simple and rapid characterization of novel large germline deletions in SDHB, SDHC and SDHD-related paraganglioma

Hoekstra AS, van den Ende B, Julià XP, van Breemen L, Scheurwater K, Tops CM, Malinoc A, Devilee P, Neumann HP, Bayley JP. Clinical Genetics (2016)

Parent-of-origin tumorigenesis is mediated by an essential imprinted modifier in SDHD-linked paragangliomas: SLC22A18 and CDKN1C are candidate tumour modifiers

Hoekstra AS, Addie RD, Ras C, Seifar RM, Ruivenkamp CA, Briaire-de Bruijn IH, Hes FJ, Jansen JC, Corssmit EP, Corver WE, Morreau H, Bovée JV, Bayley JP, Devilee P. Human Molecular Genetics (2016)

Inactivation of SDH and FH cause loss of 5hmC and increased H3K9me3 in paraganglioma/pheochromocytoma and smooth muscle tumors

Hoekstra AS, de Graaff MA, Briaire-de Bruijn IH, Ras C, Seifar RM, van Minderhout I, Cornelisse CJ, Hogendoorn PC, Breuning MH, Suijker J, Korpershoek E, Kunst HP, Frizzell N, Devilee P, Bayley JP, Bovée JV. Oncotarget (2015) 17(36):38777-88

Models of parent-of-origin tumorigenesis in hereditary paraganglioma

Hoekstra AS, Devilee P, Bayley JP. Seminars in Cell and Developmental Biology (2015) 43:117-24

Paraganglioma and pheochromocytoma upon maternal transmission of SDHD mutations

Bayley JP, Oldenburg RA, Nuk J, Hoekstra AS, van der Meer CA, Korpershoek E, McGillivray B, Corssmit EP, Dinjens WN, de Krijger RR, Devilee P, Jansen JC, Hes FJ. *BMC Medical Genetics* (2014) 10:111

The role of complex II in disease

Hoekstra AS, Bayley JP. *Biochimica et Biophysica Acta* (2013) 1827(5):543-51

DRAM-1 encodes multiple isoforms that regulate autophagy

Mah LY, O'Prey J, Baudot AD, Hoekstra A, Ryan KM. *Autophagy* (2012) 8(1):18-28